

**METHODOLOGY FOR DESIGNING THE FUZZY RESOLVER FOR  
A RADIAL DISTRIBUTION SYSTEM FAULT LOCATOR**

A Dissertation

by

JUN LI

Submitted to the Office of Graduate Studies of  
Texas A&M University  
in partial fulfillment of the requirements for the degree of

DOCTOR OF PHILOSOPHY

December 2005

Major Subject: Electrical Engineering

**METHODOLOGY FOR DESIGNING THE FUZZY RESOLVER FOR  
A RADIAL DISTRIBUTION SYSTEM FAULT LOCATOR**

A Dissertation

by

JUN LI

Submitted to the Office of Graduate Studies of  
Texas A&M University  
in partial fulfillment of the requirements for the degree of

DOCTOR OF PHILOSOPHY

Approved by:

Co-Chairs of Committee,	Karen L. Butler-Purry B. Don Russell
Committee Members,	Andrew Chan Reza Langari
Head of Department,	Chanan Singh

December 2005

Major Subject: Electrical Engineering

## ABSTRACT

Methodology for Designing a Fuzzy Resolver for a Radial Distribution System Fault

Locator. (December 2005)

Jun Li, B.Eng.; M.Eng., Xi'an Jiaotong University

Chair of Advisory Committee: Dr. Karen L. Butler-Purry

Dr. B. Don Russell

The Power System Automation Lab at Texas A&M University developed a fault location scheme that can be used for radial distribution systems. When a fault occurs, the scheme executes three stages. In the first stage, all data measurements and system information is gathered and processed into suitable formats. In the second stage, three fault location methods are used to assign possibility values to each line section of a feeder. In the last stage, a fuzzy resolver is used to aggregate the outputs of the three fault location methods and assign a final possibility value to each line section of a feeder.

By aggregating the outputs of the three fault location methods, the fuzzy resolver aims to obtain a smaller subset of line sections as potential faulted sections than the individual fault location methods. Fuzzy aggregation operators are used to implement fuzzy resolvers.

This dissertation reports on a methodology that was developed utilizing fuzzy aggregation operators in the fuzzy resolver. Three fuzzy aggregation operators, the min, OWA, and uninorm, and two objective functions were used to design the fuzzy resolver. The methodologies to design fuzzy resolvers with respect to a single objective function and with respect to two objective functions were presented. A detailed illustration of the design process was presented. Performance studies of designed fuzzy resolvers were also performed.

In order to design and validate the fuzzy resolver methodology, data were needed. Due to the lack of real field data, simulating a distribution feeder was a feasible alternative to generate data. The IEEE 34 node test feeder was modeled. Time current

characteristics (TCC) based protective devices were added to this feeder. Faults were simulated on this feeder to generate data.

Based on the performance studies of designed fuzzy resolvers, the fuzzy resolver designed using the uninorm operator without weights is the first choice. For this fuzzy resolver, no optimal weights are needed. In addition, fuzzy resolvers using the min operator and OWA operator can be used to design fuzzy resolvers. For these two operators, the methodology for designing fuzzy resolvers with respect to two objective functions was the appropriate choice.

To my wife, Mei Wang  
for her love and encouragement.

## ACKNOWLEDGEMENTS

I am indeed grateful to my advisor, Dr. Karen L. Butler-Purry, for her patience, guidance and support throughout my research work. Dr. Butler, thank you for providing me the opportunity to work as a research assistant on this project. Thank you for all the effort you put into providing my assistantship throughout my Ph.D. study.

Thanks go to the members of my dissertation committee members, Dr. Reza Langari, Dr. B. Don Russell, and Dr. Andrew Chan, for spending your precious time to serve as my committee members. I especially thank Dr. Reza Langari for his help in solving problems in my research.

I cannot forget to thank Carl L. Benner, whose expertise and suggestions played an important role in my research.

I wish to thank Karthick Manivannan for his constant support. My thanks extend my fellow students within the Power System Automation Laboratory for their friendship and support in my research. I thank you for your friendship and support, and wish all of you have a happy life and a wonderful future.

Finally, but not least, I thank my wife for her constant love and encouragement. Without her love, I could not have finished my Ph.D. study. I also thank my mother and sisters. They always trusted me and encouraged me to finish my Ph.D. study. This dissertation is in memory of my beloved father, who passed away during my Ph.D. study. He gave me all his love and support.

## TABLE OF CONTENTS

	Page
ABSTRACT .....	iii
DEDICATION .....	v
ACKNOWLEDGEMENTS .....	vi
TABLE OF CONTENTS .....	vii
LIST OF FIGURES.....	ix
LIST OF TABLES .....	xi
CHAPTER	
I INTRODUCTION .....	1
1.1 Introduction... ..	1
1.2 Research Objectives and Dissertation Organization.....	2
II LITERATURE REVIEW .....	6
2.1 Introduction.....	6
2.2 Literature Review of Existing Fault Location Methods for Distribution Systems.....	7
2.3 Literature Review of Fuzzy Aggregation Operators.....	20
2.4 Chapter Summary .....	28
III PROBLEM FORMULATION .....	29
3.1 Introduction.....	29
3.2 Fault Location Scheme .....	33
3.3 Problem Formulation of the Fuzzy Resolver Methodology .....	48
3.4 Chapter Summary .....	66
IV SYSTEM MODELING AND SIMULATION.....	67
4.1 Introduction.....	67
4.2 Modeling the IEEE 34 Node Test Feeder with Protective Devices.....	68
4.3 Comparison of Steady State Results with IEEE Published Results.....	86
4.4 Determination of Fault Resistances .....	91
4.5 Simulated Fault Cases.....	93
4.6 Chapter Summary .....	96
V METHODOLOGY FOR DESIGNING A FUZZY RESOLVER .....	97
5.1 Introduction.....	97

CHAPTER	Page
5.2 Genetic Algorithms (GA) .....	98
5.3 Methodology for Designing a Fuzzy Resolver with Respect to a Single Objective Function .....	103
5.4 Methodology for Designing a Fuzzy Resolver with Respect to Two Objective Functions .....	122
5.5 Chapter Summary.....	149
<b>VI STUDIES AND RESULTS .....</b>	<b>152</b>
6.1 Introduction .....	152
6.2 Case Study.....	153
6.3 Fuzzy Fault Location Scheme.....	157
6.4 Performance Studies .....	158
6.5 Summary of Studies and Recommendations .....	173
6.6 Chapter Summary.....	177
<b>VII CONCLUSIONS AND FUTURE WORK .....</b>	<b>178</b>
7.1 Summaries.. .....	178
7.2 Conclusions.....	180
7.3 Future Work.....	182
<b>REFERENCES .....</b>	<b>184</b>
<b>APPENDIX A .....</b>	<b>194</b>
<b>VITA .....</b>	<b>202</b>



## LIST OF FIGURES

FIGURE	Page
2.1 Value Ranges of Four Fuzzy Aggregation Operators.....	28
3.1 Architecture of the Fault Location Scheme .....	33
3.2 One-line Diagram of a Simple Distribution Feeder.....	35
3.3 Fault Event Illustrating the Definition of Subevent.....	36
3.4 A Bolted Single Phase to Ground Fault at a Line Section.....	39
3.5 A Bolted Phase B to C Fault at a Line Section.....	40
3.6 A Simple Distribution Feeder with Protective Devices.....	42
3.7 Illustration of the Comparison between a TCC curve and an Operating Point .....	42
3.8 Architecture of the Operated Device Identification Method .....	44
3.9 Feeder with Outputs of Three Fault Location Methods.....	47
4.1 IEEE 34 Node Test Feeder .....	68
4.2 Three-phase T-line.....	72
4.3 Single-phase T-line .....	73
4.4 Exact Lumped Load Model .....	74
4.5 IEEE 34 Node Test Feeder with Added Protective Devices .....	77
4.6 Structure of a Protective Device .....	79
4.7 Structure of the Control Logic Block of Fuses .....	80
4.8 Output of the Comparator .....	81
4.9 Flowchart of the Control Signal Determination Block of Fuses .....	82
4.10 Illustration of the Comparison between Fault Duration and Operating Time	83
4.11 Structure of the Control Logic Block of Three-phase Reclosers.....	84
4.12 Flowchart of the Control Signal Determination Block of Three-phase Reclosers.....	85
4.13 Determination of Fault Resistances .....	92

FIGURE		Page
5.1	Single-point Crossover .....	101
5.2	Three-point Crossover .....	102
5.3	Uniform Crossover .....	103
5.4	Process for Obtaining Optimal Weights and Parameters.....	106
5.5	Stochastic Universal Sampling Approach .....	107
5.6	Representation of a Chromosome for the Min and Uninorm Operator .....	108
5.7	Representation of a Chromosome for the OWA Operator .....	109
5.8	Pareto-based Ranking (Goldberg's Ranking).....	124
5.9	Pareto-based Ranking (Fonseca and Fleming's Ranking).....	125
5.10	Pareto-based Tournament Selection .....	126
5.11	Pareto-based Method Proposed by Tamaki .....	127
6.1	Illustration of the $\alpha$ -level .....	154
6.2	Outputs of the Fault Location Methods .....	155
6.3	Outputs of Fuzzy Resolvers.....	156

## LIST OF TABLES

TABLE	Page
2.1 Equation to Calculate the Apparent Impedance .....	18
2.2 Properties of T-norms .....	21
2.3 Commonly Used T-norms .....	21
2.4 Properties of T-conorms .....	22
2.5 Commonly Used T-conorms.....	23
2.6 Properties of Mean Type Operators.....	24
3.1 Different Hypotheses Generated for $N_{S-E}=3$ .....	45
3.2 Summary of the Numerical Tests of Fuzzy Aggregation Operators .....	55
3.3 Description of the Symbols Used in Table 3.2 .....	55
4.1 Loads and Fault Currents for Selected Line Segments.....	78
4.2 Chosen Protective Devices .....	78
4.3 Comparison of Node Phase Voltages .....	87
4.4 Comparison of Line Segment Currents .....	88
4.5 Fault Resistance Levels at Line Segments.....	92
4.6 Percentage of Fault Cases Whose Actual Faulted Section Has the Largest Possibility Value .....	94
4.7 Percentage of Fault Cases Where at Least One Non-faulted Section Has Different Possibility Value from the Actual Faulted Section.....	95
4.8 Number of Non-distinguishable Sections .....	95
5.1 Optimal Weights of the Min Operator with Respect to the First Objective Function and Using the First Transformation Method.....	110
5.2 Optimal Weights of the Min Operator with Respect to the First Objective Function and Using the Second Transformation Method .....	111
5.3 Optimal Weights of the OWA Operator with Respect to the First Objective Function and Using the First Transformation Method.....	113

TABLE	Page
5.4	Optimal Weights of the OWA Operator with Respect to the First Objective Function and Using the Second Transformation Method ..... 113
5.5	Optimal Weights of the Uninorm Operator with Respect to the First Objective Function..... 115
5.6	Optimal Weights of the Min Operator with Respect to the Second Objective Function and Using the First Transformation Method..... 117
5.7	Optimal Weights of the Min Operator with Respect to the Second Objective Function and Using the Second Transformation Method ..... 117
5.8	Optimal Weights of the OWA Operator with Respect to the Second Objective Function and Using the First Transformation Method..... 118
5.9	Optimal Weights of the OWA Operator with Respect to the Second Objective Function and Using the Second Transformation Method ..... 119
5.10	Optimal Weights of the Uninorm Operator with Respect to the Second Objective Function..... 120
5.11	Objective Values Obtained Using the Min Operator without Weights ..... 131
5.12	Optimal Weights of the Min Operator with Respect to Two Objectives Functions and Using the First Transformation Method..... 132
5.13	Optimal Weights of the Min Operator with Respect to Two Objectives Functions and Using the Second Transformation Method ..... 134
5.14	Objective Values Obtained Using the OWA Operator without Weights .... 137
5.15	Optimal Weights of the OWA Operator with Respect to Two Objectives Functions and Using the First Transformation Method..... 139
5.16	Optimal Weights of the OWA Operator with Respect to Two Objectives Functions and Using the Second Transformation Method ..... 142
5.17	Objective Values Obtained Using the Uninorm Operator without Weights ..... 145
5.18	Optimal Weights of the Uninorm Operator with Respect to Two Objectives Functions..... 146

TABLE	Page
5.19	Summaries of Fuzzy Resolvers..... 151
6.1	Outputs of the Three Fault Location Methods..... 155
6.2	Outputs of Fuzzy Resolvers..... 157
6.3	Fuzzy Resolvers Used in Studies..... 160
6.4	Results of the Fuzzy Resolver Designed Using the Min Operator with Respect to Two Objective Functions..... 161
6.5	Results of the Fuzzy Resolver Designed Using the OWA Operator with Respect to Two Objective Functions..... 163
6.6	Results of the Fuzzy Resolver Designed Using the Uninorm Operator with Respect to Two Objective Functions..... 165
6.7	Results of the Fuzzy Resolver Designed Using the Min Operator with Respect to the First Objective Function..... 167
6.8	Results of the Fuzzy Resolver Designed Using the OWA Operator with Respect to the First Objective Function..... 168
6.9	Results of the Fuzzy Resolver Designed Using the uninorm Operator with Respect to the First Objective Function..... 169
6.10	Results of the Fuzzy Resolver Designed Using the Min Operator without Weights..... 170
6.11	Results of the Fuzzy Resolver Designed Using the OWA Operator without Weights..... 171
6.12	Results of the Fuzzy Resolver Designed Using the Uninorm Operator without Weights..... 172
6.13	Performance of Individual Fault Location methods and the Fuzzy Resolver Designed Using the Uninorm Operator without Weights ..... 175

# CHAPTER I

## INTRODUCTION

### 1.1 INTRODUCTION

Electrical power distribution systems connect customers to distribution substations through feeders. There is a large number of equipment in distribution systems. This equipment ages over time, which may lead to defects. Furthermore, most distribution systems are overhead systems, which are easily affected by adverse weather conditions, animals, and traffic accidents. These two characteristics make faults in distribution systems inevitable. However, with increasing reliance on electricity, customers want an acceptable and reliable power supply at economic costs. In other words, they want to reduce the outage time and operating cost. Whenever a portion of a feeder experiences a loss of power, it is important to keep the duration of the outage to a minimum by quickly locating the cause of the disturbance to restore service to affected customers. In order to locate faults quickly, automated fault location is needed.

The primitive fault location method for distribution systems is visual inspection, which is time consuming and needs a lot of manpower. With the advent of microprocessors and sophisticated data acquisition technology, it is possible to develop some computer programs that help system operators perform complicated computations and dramatically reduce the time to process huge amounts of data. Some fault location methods have been developed and implemented using computer programs so that automatic fault location becomes possible. Most fault location methods are based on one approach for locating faults. However, these approaches each have some shortcomings. Therefore, the accuracy is not high when system operators locate faults based on one approach. Besides the accuracy problem, many methods are designed for one specific system and not easily applied to other systems. Some methods use detection devices

---

This dissertation follows the style and format of *IEEE Transactions on Power Systems*.

installed in the system. Therefore, they cannot be used for systems where detection devices are not installed. Some other methods locate faults based on the status of protective devices and heavily rely on supervisory control and data acquisition (SCADA) systems, fault detectors, and communication channels. Due to economic constraints, the communication between protective devices and the substation are limited to some important substations. For many systems, measurements are only available at the substation, and the operation status of feeder protective devices is unknown. For such systems, these methods based on the status of protective devices are not feasible. Some utilities estimate the fault location by executing fault location programs. System operators review the results and take the necessary action. Many fault location methods are customized for a specific utility and estimate fault locations based on the available information in that utility. However, utilities may have different information available. Those methods specifically designed for a utility may not be able to generally apply to another utility. Development of a generic fault location method that can be applied to most utilities is necessary.

## **1.2 RESEARCH OBJECTIVES AND DISSERTATION ORGANIZATION**

The dissertation discusses research that focused on the development of a fuzzy resolver methodology used in a new fault location scheme. The objective of the new fault location scheme is to develop a generic fault location scheme that can be applied to most utilities to identify potential faulted line sections. The new scheme consists of three stages: the input stage, the fault location methods stage, and the output stage.

In order to be used for most utilities, the input data for this scheme should be available from most utilities. In this new fault location scheme, only the current and voltage measurements at the substation, feeder topological data, and protective device settings and locations are required. The input stage is used to process and format the data to a form useable by the fault location methods stage.

There are three independent fault location methods in the fault location methods stage. The fault distance method locates faults by calculating the fault distance. The phase selector method locates faults by identifying faulted phases and based on the presence of phases on each line section. The operated device identification method locates faults by identifying the operated protective device for a fault. Since there are uncertainties in the load component of the fault current, the fault resistance, the raw data, etc., fuzzy logic was utilized in the development of these methods. Each fault location method assigns possibility values to each line section of a distribution feeder. These possibility values represent how possible a line section is involved in a fault.

In the last stage, a fuzzy resolver is used to aggregate the outputs of the three fault location methods and produce one final aggregation possibility value for each line section. Fuzzy aggregation operators were used in the fuzzy resolver.

This dissertation discusses a methodology for designing fuzzy resolvers. In the methodology, fuzzy aggregation operators were used to design the fuzzy resolver. To choose fuzzy aggregation operators to design a fuzzy resolver, commonly used fuzzy aggregation operators were investigated, and the min, OWA, and uninorm operators were chosen as candidate operators based on the characteristics of the three fault location methods. To take account of the accuracy of the three fault location methods, weights (important factors) were assigned to the three methods. In order to incorporate these weights, transformation methods were used for each fuzzy aggregation operator to transform the outputs of the three fault location methods into effective values. After that, a fuzzy aggregation operator was used to aggregate these effective values to generate final possibility values for each line section of a feeder.

In the design process of a fuzzy resolver, the optimal weights of the three fault location methods and the optimal parameters of the OWA operator needed to be determined. In order to determine these weights and parameters, field data representing many distribution systems were needed. Since field data from real distribution feeders



were unavailable to this research, modeling a distribution feeder with protective devices and simulating fault cases on the feeder were feasible alternatives. The IEEE 34 node test feeder was modeled with the addition of protective devices. Load flow and short circuit analysis studies were implemented on this feeder using the software, WindMil [94], to determine the protective devices' settings. The author developed a methodology for modeling TCC-based protective devices using the MATLAB SimPowerSystems blockset. Faults were exhaustively simulated at all line sections to generate data. After generating data, the optimal parameters of the fuzzy resolver (the weights of the three fault location methods and the parameters of the OWA operator) needed to be determined. Genetic algorithm based methods were used to determine them. Two objective functions were used in the optimization process. The first objective function was to maximize the number of actual faulted sections whose possibility values are greater than or equal to a large possibility value  $p_1$ , which aimed to achieve the result that actual faulted sections had a large possibility value. The other objective function was to maximize the number of non-faulted sections whose possibility values are less than a small possibility value  $p_2$ , which aimed to achieve the result that actual faulted sections had a large possibility value. Optimal parameters were obtained with respect to the first objective function individually and the second objective function individually. Then, optimal parameters were obtained with respect to two objective functions.

This dissertation consists of seven chapters. In Chapter I, an introduction of this research work and an organization of the dissertation are presented. In Chapter II, the literature of distribution system fault location methods and fuzzy aggregation operators are reviewed. In Chapter III, the three fault location methods developed by other researchers in the research group are introduced. Fuzzy aggregation operators used in fuzzy resolvers are discussed. In Chapter IV, a methodology developed for modeling and simulating the benchmark distribution feeder with time-current characteristics (TCC) based protective devices is presented. In chapter V, methodologies developed to design

fuzzy resolvers with respect to a single objective function and with respect to two objective functions are discussed. The designed fuzzy resolvers are studied. In chapter VI, the performance of designed fuzzy resolvers is studied using the test cases. In Chapter VII, conclusions are drawn and some remarks about future work are presented.

## **CHAPTER II**

### **LITERATURE REVIEW**

#### **2.1 INTRODUCTION**

Over the years, many researchers have put considerable effort into the development of fault location methods for transmission systems. However, due to economic constraints, utilities do not pay as much attention nor expend as many resources for service reliability and quality of the power supply for distribution systems. Therefore, research on fault location methods for distribution systems was not active for many years. A primitive fault location method for distribution systems is visual inspection, which is time consuming and needs a lot of manpower. When a fault happens, system operators normally perform fault locations based on the customer's report. Upon receiving trouble calls from customers, system operators determine the outage area based on the feeder map and the protection scheme. Then repair crews are sent to patrol the outage area. The process is very time consuming so that the outage may last a very long time.

Distribution systems have some unique characteristics that make fault location methods for transmission systems not effective for distribution systems. First, distribution lines are much more complex topologies than transmission lines. Transmission lines generally are from point to point, or networks have a tee. Distribution lines have dozens or even hundreds of laterals, tees, load taps, etc. This difference in topology makes many techniques that were designed for transmission lines incapable of functioning on distribution lines. Impedance-based algorithms suffer from this because a distribution line has many points with the same impedance from the substation. The traveling wave-based algorithms are "confused" because a distribution line has many discontinuities, each of which causes a reflection. Second, distribution systems have many single-phase and two-phase laterals away from the main feeder, which makes the system unbalanced. Further, distribution lines are not fully transposed so that they have an asymmetrical nature. Therefore, many methods using symmetrical components cannot be used. In

addition, distribution systems involve non-homogenous lines, a large number of elements, dynamic loads, as well as topological changes because of network expansion. Hence, fault location methods specifically designed for distribution systems are needed.

With the advent of sensitive loads, customers require a high quality of service. In addition, due to the introduction of a competitive market into the power industry, service quality and reliability of distribution systems have recently caught the utilities' attention, and many researchers have begun to develop fault location methods for distribution systems.

In this chapter, the literature on fault location methods for distribution systems is reviewed and summarized, and the shortcomings of these methods are discussed. In order to overcome these shortcomings, researchers in the Power System Automation Lab at Texas A&M University developed a new fault location scheme that locates faults based on several fuzzy logic based methods. Fuzzy aggregation operators were used in the new scheme for aggregating these fault location methods' outputs. In this chapter, the commonly used fuzzy aggregation operators are also introduced.

## **2.2 LITERATURE REVIEW OF EXISTING FAULT LOCATION METHODS FOR DISTRIBUTION SYSTEMS**

Most fault location methods for distribution systems can be categorized into five groups: impedance and other fundamental frequency component based methods, high frequency components and traveling wave based methods, artificial intelligence and statistical analysis based methods, distributed device based methods, and hybrid methods. In the following sections, each of these is reviewed. After reviewing the research work on distribution system fault location, commercial products and applied fault location systems will also be reviewed.

### **2.2.1 Impedance and Other Fundamental Frequency Component Based Methods**

Many fault location methods that use the fundamental frequency component find the fault location by calculating the apparent impedance. In these methods, the fault types

and faulted phases are identified first. Then, the apparent impedance is calculated based on the selected voltage and selected current. For the distribution system fault location, load currents at different taps are sources of error if they are not considered. Girgis [1] gave equations to calculate all kinds of faults occurring at the main feeder and a single-phase lateral. In this paper, loads were considered as constant impedance loads. The dynamic nature of the loads was not considered, and multiphase taps were not considered either. Saha [2] presented a method that could include many intermediate load taps. The non-homogeneity of the feeder sections was also taken into account in this method, but he assumed the system was balanced. Santoso [3] presented a method similar to [1]. However, he used a different method to take account of the fault resistance. Das [4]-[6] developed a technique that took account of non-homogenous lines, load taps, and the dynamic nature of the loads. However, he still considered the line were fully transposed, and was only good for line-to-ground faults. This technique calculated the apparent impedance to find the faulted section first. Then an iterative method was used to solve an implicit equation in order to find the distance from the start node of the faulted section to the fault point.

Other methods also use the fundamental frequency component to locate faults. However, they are not based on the apparent impedance. Aggarwal [7],[8] presented a single-ended fault location technique, which was based on the concept of superimposed components of voltages and currents rather than total quantities. The method also treated all loads as constant impedance loads. The line was modeled using the lumped parameter model. This fault location technique located faults by finding "the point on the line that gives the minimum values of the healthy-phase fault path currents." It was highly insensitive to variations in source impedances and to the presence of taps with variable loads. However, it was only good to locate faults on the three phase main feeder. Choi [9] proposed a method for locating faults by solving a quadratic equation resulting from the direct circuit analysis. However, it assumed all load impedance was accurately known.

### 2.2.2 High Frequency Components and Traveling Wave Based Methods

Traveling wave based methods locate faults based on a fault generating high frequency signals. These methods have high accuracy, even for high impedance faults, and their accuracy does not rely on system condition. They are used for transmission systems because of their simple topologies. However, these techniques need high sample rate (above 20 MHz) and have some problems for low inception angle faults. The implementation of these methods is more expensive than the implementation of impedance based techniques. For distribution systems, there are a lot of load taps and discontinuities in a line that will reflect a traveling wave, which makes it difficult to apply traveling wave based methods to distribution systems. Thomas [10] tried to use the cross-correlation function between the incident wave and the reflected wave to locate faults in distribution systems. Both the double-ended method and the single-ended method were used. The double-ended method could provide an accurate result if the fault happened at the line where the fault recorders were installed, or at the main feeder. The single-ended method did not work well. The author did not present any idea to overcome the problem caused by multiple discontinuities in distribution systems. Bo [11] presented another method to locate faults. In order to distinguish the reflected wave from the fault point and that from the remote bus bar, a new fault locator unit was developed, which captured high frequency voltage signals between 1 and 10 MHz. Around this range, the bus capacitance dominated the bus impedance so that the reflected voltage signal from the remote bus had the opposite sign to the incident voltage, while the reflected voltage signal from the fault location had the same sign as the incident voltage. Then by identifying two successive waves that had the same polarity, the fault distance could be determined. Bo found the effects of tapped-off loads were significant, and caused problems in identifying the fault location, but he did not solve the problem completely.

There are many other methods that use high frequency components, but they do not use traveling wave theory. Johns, El-Hami, and Tang [12]-[14] developed a device that

could identify the fault direction based on the voltage magnitude difference between the device's terminal voltages. However, this method needed to insert some equipment into to distribution feeders. It could not be done only using the terminal measurements. Magnago [15] proposed a new method based on the high frequency signals measured at the substation. Based on the knowledge that different fault locations have different attenuation factors resulting from different number of junctions between the substation and the fault location, the high frequency signals were decomposed using the wavelet, and the wavelet coefficients carried some information that could be used to identify different fault laterals. However, in order to use this method, simulations need to be done for each distribution system so that users know the wavelet coefficients of different fault laterals, and can identify the faulted lateral based on these coefficients. Utilities cannot afford to implement a solution on a distribution feeder if there has to be significant configuration and/or modeling of each specific feeder. Further, distribution line topology also changes frequently (e.g., load diverted from one feeder to another during maintenance; addition/removal of individual customers, etc.). Even if a utility could enter feeder-specific topology information during initial setup, it never would be able to keep it up-to-date.

### **2.2.3 Artificial Intelligence (AI) and Statistical Analysis Based Methods**

With the development of computers, many artificial intelligent methods such as expert systems, neural networks, etc., emerged. These methods provide a way to capture the experience of operators or engineers, and can help people to do much laborious work. By using these methods, the time factor is substantially reduced and human mistakes are avoided. Hence, many researchers used AI based methods in distribution system fault locations.

In the old days, people's expertise was needed to process alarm messages to identify the fault location after faults happened. With computer programs that simulate the behavior of human experts in solving a complex problem, expert systems have received

considerable attention for developing fault location methods. Many researchers [16]-[22] used rule-based expert systems. In these methods, the trouble calls, the protective devices' status, supervisory control and data acquisition (SCADA) system, and/or automatic meter reading (AMR) systems were needed. In addition, the protection scheme should be known. Kumano [23] proposed a rule based expert system that also used the protective devices' status. This method was different from other methods due to its consideration of sequential information. Ypsilantis [24] developed a rule-based fault diagnostic system that used feeder topological information and real time data from SCADA systems. The system used two types of rules. A set of core rules using breaker trips and bus status was normally enough to cover a majority of faults. In the cases where the core rules failed, exception rules were generated by interaction with system operators. These exception rules used breaker trip information and the islands formed in the faulted network. Rule-based expert systems have a powerful capability to mimic human experience. However, a number of rules are needed to describe various devices. The tasks of knowledge-acquisition and maintenance of knowledge base are often laborious and tedious, and the development of an expert system is often a costly and lengthy process. Hence, the portability of expert systems is very important. Instead of representing the operator's expertise as complicated rules, Teo [25] presented a special knowledge based system that captured the postfault network state, and recorded it as a pattern. When linking to a distribution network simulator, the diagnostic system was trained. When a new fault happened, a matching mechanism was used to compare the network state with records to identify the fault location. If no one matched, the system would consider it as a new fault and prompt the user to enter the faulted element.

Yang [26]-[27] proposed neural network based methods to locate distribution system faults. The system in [26] had a similar profile to an expert system, but a different design of the inference engine. Neural networks were used as the knowledge base, instead of heuristic rules. The status of protective devices was needed in this method. In [27], a



distributed neural nets diagnosis system was constructed by the training database that associated the protective scheme with the individual sections. By using the distributed processing technique, the burden of communication between the control center and substations was alleviated. In order to implement an on-line fault section estimation system, Bi [28],[29] employed a multi-way graph partitioning method based on weighted minimum degree reordering to partition a large-scale power network into some sub-networks. Then a Radial Basis Function Neural Network and its companion fuzzy system were used to implement sub-network fault section estimation systems based on information on the status of protective devices available from SCADA systems. The speed of the distributed fault section estimation system made it possible to use it as an on-line system. Al-shaher [30] developed a fault location method for multi-ring distribution systems using neural network. The feeder fault voltage, circuit breaker status, real power of feeders during the normal condition, and real power of feeders during short circuit, etc, were used to train the neural network. Martins [31] proposed a method for locating faults for parallel double-circuit distribution lines. The Clarke-Concordia transformation was used to transform line currents into  $\alpha\beta 0$  current components. Based on these components, a data sample correlation matrix was constructed. The eigenvalues of the correlation matrix had a non-linear relationship with the fault distance. A neural network was used to extract the unknown relationship. In [32] and [33], a neural network was used to identify the faulted section based on pattern recognition. Some measurements uniquely defined a fault pattern, and a neural network was used to recognize the pattern to locate a fault.

Shahrestain [34] used pattern recognition techniques to identify power system faults. During different faults, the network exhibited different patterns, which consisted of the status of buses, lines, feeders, and protective devices. With identifying a fault's pattern and comparing the pattern with the knowledge base, the fault location was decided.

Most of methods mentioned above estimated the faulted section(s) based on the status of protective devices, which were obtained from SCADA systems. However, there are uncertainties in these data due to the malfunction or wrong alarm of relays and circuit breakers, errors during the data acquisition and transmission, and time inaccuracy. Fuzzy set theory provides a convenient means to model uncertainties and inexactness, and several researchers [35]-[38] developed distribution system fault location methods based on it. In [35]-[36], fuzzy set theory was used to enhance expert system computation. In [37], sagittal diagrams were used to represent fuzzy relations for power systems. The expert system diagnosed faulted sections by the operation relations, instead of heuristic rules. Zhong [38] used fuzzy sets to represent fault currents measured by sensors, fault currents calculated by short circuit analysis, and operator's experience. As the result, a priority list of possible faulted sections was provided.

Wen [39] proposed a method that constructed a probabilistic causality matrix to represent the probabilistic relationship between faulted sections and protective device action. After the construction, the parsimonious set covering theory was applied to make the faulted section estimation as an integer-programming problem. Finally, a refined genetic algorithm (RGA) was adopted to solve the problem. Based on the "natural selection, best survival" theory, the RGA found the most reasonable hypothesis or hypotheses based on the evaluation result of each hypothesis evaluated by set covering theory. Besides GA, another evolutionary algorithm has also been used. In [40], Huang proposed a method that located faults based on an immune-based optimization approach. In this method, each section of the power system model was treated as an antibody. The fittest antibody became the solution.

Huang [41] and Lo [42],[43] proposed a new Petri Nets knowledge representation scheme, which was based on status of related protective devices and the heuristic rules used by system operators. The inference of the faulted section was through simple matrix operations.

The statistical hypotheses testing method [44] was also used. The method needed the time of outage measurements obtained from customer ends. In [45], a Bayesian network was used to identify the faulted device by prioritizing all possible faulted equipment according to the fault statistics, the feeder prefault and fault environment, and the patrols' knowledge. Bayesian network was used to combine expert knowledge and historical data. Thukaram's [46] method estimated the voltage magnitude and phase angle at all load buses through state estimation. In order to implement the state estimation, the method needed to know power flows and power injections. From estimated values, the abnormal data or a protective device operation was noticed. Then, the fault detector compared the abnormal data with the normal data. A threshold was used to detect the fault path.

Chen [47] used a cause-effect network to represent causality between faults and the actions of protective devices. The cause-effect network's features of high-speed inference and ease of implementation made it feasible to implement an on-line fault section estimation system. Based on the actions of protective devices, the network could quickly find faulted section candidates. The Group Method of Data Handling (GMDH) networks was also used to identify the possible faulted sections using the time-stamped information of protective devices [48].

#### **2.2.4 Distributed Device Based Methods**

Besides the methods in the above four categories, there are some methods using different techniques. Wang [49] presented a mathematical approach that located faults based on installed voltage sensors' information and the network's topological structure. The relation of the voltage sensors with sections was formulated as a matrix. The other matrix was constructed based on the topological relation between sections and nodes in an electric network. Through some matrix operations, all faulted sections could be found. In [50], fault-sensing transmitters were installed in a cable distribution system. These transmitters transmitted the coded signal to the control center. Operators located faults based on these signals.

### **2.2.5 Hybrid Methods**

Almost all of the above methods locate faults based on one algorithm, such as the fault distance calculation or operated protective device's status analysis, to locate faults. Some have investigated the use of hybrid methods that locate faults based on more than one algorithm to achieve a more accurate estimation of the faulted section. Zhu [51] proposed a hybrid method that computed the fault distance using measurements available at the substation. Based only on the fault distance calculation, the method determined multiple potential fault locations. To identify the actual fault location, a fault diagnosis procedure was applied to rank the list of multiple potential fault locations. By doing a circuit simulation, the operation of a particular combination of protective devices and the load change pattern during different fault scenarios could be obtained. Then by matching the fault situation to these scenarios, the actual faulted section could be determined. However, this diagnosis procedure modeled the circuit and simulated different fault scenarios, which were time-consuming tasks, and the modeling process needed to be done again for another system. Järventausta [35] used the fault distance calculation, fault detector information, and geographical information of the distribution system to locate faults. Zhong [38] presented a method to locate faults based on fault current measurements, fault currents calculated from short circuit analysis, and system operators' experience. Lee [52] calculated the fault distance first to provide some fault location candidates. Then, by current pattern matching and interrupted load analysis, the candidate pool was reduced.

### **2.2.6 Commercial Products for Distribution System Fault Location**

In addition to research work on distribution system fault location, some companies have developed commercial products for distribution system fault location, and some utilities have applied systems to implement distribution system fault location. In the following sections, these products and systems are reviewed.

### **2.2.6.1 Signature System**

The Signature System Company developed a Radial Fault Locator Answer Module [53] that can identify a fault, determine its type, and calculate the distance from the monitoring point to the fault. This computes the apparent sequence impedance at the monitoring point and estimates the fault distance from the monitoring point. According to their literature, its typical error of estimated distance is 10-15%.

### **2.2.6.2 ABB**

ABB developed the RES 505 terminal that includes a fault location function [54]. It achieves optimum accuracy by using a measuring principle. This principle eliminates measuring errors caused by the infeed of fault current from the remote end, load current prior to the fault, and magnitude of fault resistance.

ABB also developed a fault analysis and evaluation tool called PSM 505 [55]. The tool applies an algorithm that calculates the loop impedance of the faulted line. In this algorithm, parallel lines are considered. This tool utilizes one-terminal fault location algorithm and two-terminal fault location algorithm. According to their literature, the one-terminal fault location algorithm can achieve an accuracy that is typically better than 3.5% of the distance to the fault, while the accuracy of the two-terminal fault location algorithm is 1% of the line length.

### **2.2.6.3 Phase to Phase BV**

Phase to Phase BV is a company in the Netherlands that develops software for network calculations. This company developed a fault location system for distribution systems [56]. The measurements recorded by digital protection equipment are used to calculate the impedance from the substation to the fault location. The calculated result is fed into a network model where a fault analysis is performed to find the exact location. Simulations are implemented on the network model. In the simulation process the calculated short circuit currents, voltages, and reactances are compared with the

measured values. The best match reveals the location of the fault. This approach requires a detailed circuit model.

#### 2.2.6.4 Schweitzer Engineering Laboratories (SEL)

SEL developed the SEL-221-16 distance relay with fault locator [57]. It can provide high-speed and time-delayed protection for transmission, subtransmission, and distribution lines. Analog inputs from current and voltage transformers are delivered to the protective relaying element to locate a fault. The relay uses two fault location methods: the simple reactance method when prefault data are not available [58],[59], or the Takagi method where prefault data are available [58]-[60].

The simple reactance method calculates the apparent impedance using (2.1), where  $V_{select}$  and  $I_{select}$  are the selected voltage and current, respectively. For different types of faults, the apparent impedance is calculated as Table 2.1, where  $k=(Z_0-Z_1)/Z_1$ ,  $Z_0$  is the zero sequence line impedance,  $Z_1$  is the positive sequence line impedance,  $I_a$ ,  $I_b$ , and  $I_c$  are phase currents for phase A, B and C, respectively,  $I_0$  is the zero sequence current,  $V_a$ ,  $V_b$ , and  $V_c$  are phase voltages for phase A, B and C, respectively. The fault distance is calculated using (2.2), where  $m$  is the per unit distance to the fault,  $\text{Im}(\cdot)$  is the imaginary part.

$$Z_{app} = \frac{V_{select}}{I_{select}} \quad (2.1)$$

$$m = \frac{\text{Im}(Z_{app})}{\text{Im}(Z_1)} \quad (2.2)$$

When the prefault data are available, it is possible to improve the result accuracy using the Takagi method. This method improves upon the simple reactance method by reducing the effect of load flow and minimizing the effect of fault resistance.

When the fault is a phase A to ground fault, the fault distance is calculated using (2.3) and (2.4), where  $\text{Im}(\cdot)$  is the imaginary part,  $V_k$  is the phase  $k$  voltage,  $I_k$  is the phase  $k$  fault current,  $I_{kpre}$  is the phase  $k$  prefault current,  $Z_{kj}$  is the mutual impedance between

phase  $k$  and  $j$ ,  $I_{ksup}^*$  is the complex conjugate of  $I_{ksup}$ . For other single phase to ground fault, the distance is calculated using similar equations.

TABLE 2.1 EQUATION TO CALCULATE THE APPARENT IMPEDANCE

Fault Type	Apparent Impedance Equation ( $Z_{app}=\$ )
AG	$V_a/(I_a + kI_0)$
BG	$V_b/(I_b + kI_0)$
CG	$V_c/(I_c + kI_0)$
AB or ABG	$(V_a - V_b)/(I_a - I_b)$
BC or BCG	$(V_b - V_c)/(I_b - I_c)$
CA or CAG	$(V_c - V_a)/(I_c - I_a)$
ABC	$(V_a - V_b)/(I_a - I_b)$ or $(V_b - V_c)/(I_b - I_c)$ or $(V_c - V_a)/(I_c - I_a)$

$$m = \frac{\text{Im}(V_a I_{a\text{sup}}^*)}{\text{Im}((Z_{aa} I_a + Z_{ab} I_b + Z_{ac} I_c) I_{a\text{sup}}^*)} \quad (2.3)$$

$$I_{a\text{sup}} = I_a - I_{a\text{pre}} \quad (2.4)$$

When the fault is a phase B to C fault, the fault distance is calculated using (2.5)-(2.9), where  $\text{Im}(\cdot)$  is the imaginary part,  $V_k$  is the phase  $k$  voltage,  $I_k$  is the phase  $k$  fault current,  $I_{k\text{pre}}$  is the phase  $k$  prefault current,  $Z_{kj}$  is the mutual impedance between phase  $k$  and  $j$ ,  $I_{kjsup}^*$  is the complex conjugate of  $I_{kjsup}$ . For other phase to phase faults, the distance is calculated using similar equations.

$$m = \frac{\text{Im}(V_{bc} I_{bc\text{sup}}^*)}{\text{Im}(((Z_{bb} - Z_{bc})I_b - (Z_{cc} - Z_{bc})I_c + (Z_{ab} - Z_{ac})I_a)I_{bc\text{sup}}^*)} \quad (2.5)$$

$$I_{bc\text{sup}} = I_{bc} - I_{bc\text{pre}} \quad (2.6)$$

$$I_{bc} = I_b - I_c \quad (2.7)$$

$$I_{bc\text{pre}} = I_{b\text{pre}} - I_{c\text{pre}} \quad (2.8)$$

$$V_{bc} = V_b - V_c \quad (2.9)$$

For phase to phase to ground faults and three phase faults, the fault distance calculation is the same as for phase to phase faults.

#### **2.2.6.5 General Electric**

The F60 Feeder Management Relay developed by General Electric is a microprocessor-based relay that was designed for feeder protection [61]. This relay has a fault location function. The single-ended impedance-based method is used in this relay. According to the literature, the relay accuracy is  $\pm 1.5\%$ , and the maximum accuracy is achieved if the fault resistance is zero or fault currents from all line terminals are in phase.

#### **2.2.6.6 Carolina Power and Light**

Carolina Power and Light developed a system to locate faults on distribution feeders [62]. The system locates in substations and finds the fault location based on feeder monitoring system (FMS) and short circuit data match. When a fault occurs, the RMS fault current is obtained from a FMS, and this RMS current is compared with fault currents that are calculated at one-mile increments from the substation using the short circuit analysis to locate the fault.



### **2.2.7 Shortcomings of Existing Fault Location Methods**

Almost all existing methods need SCADA systems, digital fault detectors, AMR systems, or other specific equipment installed in a system. Therefore, these methods need telecommunication channels and are subject to telecommunication channel's failure and data transmission error. In addition, most methods locate faults according to one algorithm. Since each algorithm has its own limitation, their accuracy is not good.

The objective of this research is to develop a fault location method that can be used in various distribution systems. However, most of the above mentioned methods need SCADA and AMR systems, and these systems may not be available in some distribution systems, which makes the portability of these methods poor. To achieve the research's goal, a fault location method that is based on several fault location algorithms and that only needs substation measurements and some topological information is desirable.

## **2.3 LITERATURE REVIEW OF FUZZY AGGREGATION OPERATORS**

Fuzzy aggregation operators are used in the fuzzy resolver methodology developed by the author. In the following sections, commonly used fuzzy aggregation operators are reviewed.

### **2.3.1 Fuzzy Intersections (T-norms)**

Fuzzy intersections are usually referred to as triangle norms (t-norms). For each candidate,  $x$ , in a candidate set, these operators calculate the membership value of the candidate in the intersection set of set A and set B based on the candidate's membership value in A and B [63].

A fuzzy intersection between two arguments  $a$  and  $b$  is expressed as  $i(a,b)$ . T-norms must satisfy the following requirements as shown in Table 2.2.

TABLE 2.2 PROPERTIES OF T-NORMS

Boundary condition:	$i(a,1)=a$ . The intersection of any membership value with 1 is equal to the value itself.
Monotonicity:	$b \leq d$ implies $i(a,b) \leq i(a,d)$ . If $b \leq d$ , the intersection of any value with $b$ is not larger than the intersection of the value with $d$ .
Commutativity:	$i(a,b)=i(b,a)$ . The order of the input arguments does not affect the result.
Associativity:	$i(a,i(b,d))=i(i(a,b),d)$ . When three arguments are intersected together, the sequence of the intersection does not matter.

Based on the four requirements, several t-norms can be achieved. The most commonly used t-norms are shown in Table 2.3.

TABLE 2.3 COMMONLY USED T-NORMS

Standard intersection:	$i(a,b)=\min(a,b)$
Algebraic product:	$i(a,b)=ab$
Bounded difference:	$i(a,b)=\max(0,a+b-1)$
Drastic intersection:	$i(a,b)= \begin{cases} a & \text{when } b = 1 \\ b & \text{when } a = 1 \\ 0 & \text{otherwise} \end{cases}$

For these operators, the lowest possibility value confines the aggregation possibility value. One criterion's low value makes the final result low no matter how high the other

criterion's values are. In other words, high possibility values do not compensate low possibility values.

Though t-norms are defined on two arguments, their satisfaction of the associativity condition ensures these operators are easy to extend for n arguments. Based on the requirements that t-norms satisfy, it is easy to prove that the standard intersection is the largest t-norm:  $i(s_1, \dots, s_q) \leq \min(s_1, \dots, s_q)$ , where  $s_i$  is a possibility value [63].

### 2.3.2 Fuzzy Unions (T-conorms)

Fuzzy unions are often called triangle conorms (t-conorms). For each candidate, x, in a candidate set, these operators yield the membership value of the candidate in the union set of set A and set B based on the candidate's membership value in A and B [63].

The operator  $u(a,b)$  represents the union of the membership value a and b. T-conorms also must satisfy four requirements as shown in Table 2.4.

TABLE 2.4 PROPERTIES OF T-CONORM

Boundary condition:	$u(a,0)=a$ . The union of any value with 0 equals to the value itself.
Monotonicity:	$b \leq d$ implies $u(a,b) \leq u(a,d)$ . If $b \leq d$ , the union of any value a with b is not larger than the union of the value with d.
Commutativity:	$u(a,b)=u(b,a)$ .
Associativity:	$u(a,u(b,d))=u(u(a,b),d)$ .

Several t-conorms can satisfy the above requirements. Among them, the following t-conorms shown in Table 2.5 are commonly used:

TABLE 2.5 COMMONLY USED T-CONORMS

Standard union:	$u(a,b)=\max(a,b)$
Algebraic sum:	$u(a,b)=a+b-ab$
Bounded sum:	$u(a,b)=\min(1,a+b)$
Drastic union:	$u(a,b)= \begin{cases} a & \text{when } b = 0 \\ b & \text{when } a = 0 \\ 1 & \text{otherwise} \end{cases}$

In contrast to t-norm operators, the highest possibility value confines the aggregation possibility value. A high possibility value from one criterion will make the final result high no matter how low the other criteria's values are. Hence, t-conorms also do not provide compensation between criteria.

As associative operators, these t-conorms can easily be extended to n arguments, and it is easy to prove that the standard union is the smallest t-conorm:  $u(s_1, \dots, s_q) \geq \max(s_1, \dots, s_q)$  [63].

### 2.3.3 Fuzzy Averaging Operators (Mean type operators)

Fuzzy averaging operators are also known as mean type operators. Unlike t-norms and t-conorms, these operators cannot be explained using set theory.

Mean type operators have the properties as shown in Table 2.6 [64].

TABLE 2.6 PROPERTIES OF MEAN TYPE OPERATORS

Idempotency:	$M(a, a, \dots, a) = a$ . When the operators aggregate several equal values, the aggregation value must equal to the value.
Monotonicity:	$a_i \leq b_i$ implies $M(a_1, a_2, \dots, a_n) \leq M(b_1, b_2, \dots, b_n)$ . If there are two sets of ordered values $a$ and $b$ , where $a_1 \leq a_2 \leq \dots \leq a_n$ , $b_1 \leq b_2 \leq \dots \leq b_n$ , and $a_i \leq b_i$ , the aggregation value of the set of values $a$ is not larger than the aggregation value of the set of values $b$ .
Commutativity:	$M(a_1, a_2, \dots, a_n) = M(a_n, \dots, a_2, a_1)$ . This property ensures the order of the input arguments does not affect the final aggregation value.

The three commonly used mean type operators are listed below. The first one is the simple mean operator. Its mathematical form is (2.10).

$$A(a_1, a_2, \dots, a_n) = \frac{1}{n} \sum_{i=1}^n a_i \quad (2.10)$$

The second one is the median operator. It is defined as the  $(n/2)^{\text{th}}$  largest element of a set  $(a_1, \dots, a_n)$  if  $n$  is even, and as the  $((n+1)/2)^{\text{th}}$  largest element if  $n$  is odd [64].

The last one is the ordered weighted averaging operator (OWA) [65], and it is a parameterized operator.

$$A(a_1, a_2, \dots, a_n) = W_1 b_1 + W_2 b_2 + \dots + W_n b_n = \bar{W} \bullet \bar{B} \quad (2.11)$$

where  $b_i$  is the  $i^{\text{th}}$  largest element in  $a_1, a_2, \dots, a_n$ ,  $w_i$  is the  $i^{\text{th}}$  weight,  $\sum_{i=1}^n W_i = 1$ .

$\bar{W} = [W_1, W_2, \dots, W_n]$ , and  $\bar{B} = [b_1, b_2, \dots, b_n]^T$ . By adjusting the weights, the OWA operator can move from the min operator to the max operator. The Orness of the weights is used to represent how close the operator is to the max operator. The definition of Orness is given in (2.12).

$$Orness(w_1, w_2, \dots, w_n) = \frac{1}{n-1} \sum_{i=1}^n (n-i)W_i \quad (2.12)$$

Mean type operators demonstrate the compromise (neutral) attitude of decision makers, who are neither pessimistic nor optimistic. Therefore, neither the minimum value nor the maximum value decides the final result. The aggregation value ranges between the minimum value and the maximum value. Different from t-norms and t-conorms, these operators provide compensation between different criteria. One criterion's value does not solely affect the aggregation result.

Based on the monotonic and idempotent properties, the mean type operators range in values between the minimum value and the maximum value:  $\min(s_1, \dots, s_q) \leq A(s_1, \dots, s_q) \leq \max(s_1, \dots, s_q)$  [64].

#### 2.3.4 Full Reinforcement Operators

Full reinforcement operators are hybrid operators that can be used to represent hybrid behaviors of decision makers [66]. For these operators, there is a fixed element,  $g$  (called identity). The possibility values above  $g$  cause an increase in the aggregation value while those below  $g$  cause a decrease in the aggregation value. These operators perform like t-norms when all individual possibility values are less than the identity; they perform like t-conorms when all individual values are larger than the identity. Hence, in these operators, the behavior of the decision maker is not fixed. Sometimes, the decision maker uses a t-conorm operator; sometimes he uses a t-norm operator.

All full reinforcement operators belong to fixed identity monotonic identity commutative aggregation (FIMICA) operators [66]. As the name suggests, these operators have the following properties: monotonicity, commutativity, and having a fixed identity. While all these operators have the characteristics that a collection of high values (larger than  $g$ ) reinforces each other to make the aggregation value more affirmative than any of the individual values and a group of low values (less than  $g$ ) makes the aggregation value more disaffirmative than any of the individual values, the difference

among these operators is how they aggregate a group of values when some values are high and others are low (called the mixture situation hereafter).

The commonly used full reinforcement operators are listed below [66]. Here,  $a_i$  is the aggregated possibility values.

- Additive family of FIMICA

$$R(a_1, a_2, \dots, a_n) = f\left(\sum_{i=1}^n (a_i - g)\right) \quad (2.13)$$

where  $f$  is a monotonic increasing function.

- Product family of FIMICA

$$R(a_1, a_2, \dots, a_n) = f\left(\prod_{i=1}^n \frac{a_i}{g}\right) \quad (2.14)$$

where  $f$  is a monotonic increasing function

- Uninorm

Type I:

$$R(x, y) = \begin{cases} g \times i\left(\frac{x}{g}, \frac{y}{g}\right) & \text{if } 0 \leq x \leq y \leq g \\ g + (1-g) \times u\left(\frac{x-g}{1-g}, \frac{y-g}{1-g}\right) & \text{if } g \leq x \leq y \leq 1 \\ \min(x, y) & \text{if } \min(x, y) \leq g \leq \max(x, y) \end{cases} \quad (2.15)$$

Type II:

$$R(x, y) = \begin{cases} g \times i\left(\frac{x}{g}, \frac{y}{g}\right) & \text{if } 0 \leq x \leq y \leq g \\ g + (1-g) \times u\left(\frac{x-g}{1-g}, \frac{y-g}{1-g}\right) & \text{if } g \leq x \leq y \leq 1 \\ \max(x, y) & \text{if } \min(x, y) \leq g \leq \max(x, y) \end{cases} \quad (2.16)$$

where,  $i(\cdot)$  and  $u(\cdot)$  are a t-norm operator and a t-conorm operator, respectively.

- FIMICA created from fuzzy models

These operators are based on the following two rules [66]:

Rule 1: If the aggregated possibility values are all low, then use a t-norm operator.

Rule 2: If the aggregated possibility values are all high, then use a t-conorm operator.

Using the algebraic product as the t-norm operator, the algebraic sum as the t-conorm operator, and the center of area (COA) as the defuzzification technique, the triple  $\Pi$  operator, R, emerges [66].

$$R(a_1, a_2, \dots, a_n) = \frac{\prod_{j=1}^n a_j}{\prod_{j=1}^n a_j + \prod_{j=1}^n \bar{a}_j} \quad (2.17)$$

where  $\bar{a}_i = 1 - a_i$ .

Using the min operator as the t-norm operator, the max operator as the t-conorm operator, and the mean of maximum (MOM) as the defuzzification technique, another operator is derived [66].

$$R(a_1, a_2, \dots, a_n) = \begin{cases} \min_i(a_i) & \text{if } \min_i(\bar{a}_i) > \min_i(a_i) \\ \max_i(a_i) & \text{if } \min_i(\bar{a}_i) < \min_i(a_i) \\ \frac{1}{2}(\min_i(a_i) + \max_i(a_i)) & \text{if } \min_i(\bar{a}_i) = \min_i(a_i) \end{cases} \quad (2.18)$$

In summary, aggregation operators have different value ranges. The value ranges of different operators that aggregate a set of values  $A=(a_1, a_2, \dots, a_n)$  are shown in Figure 2.1.



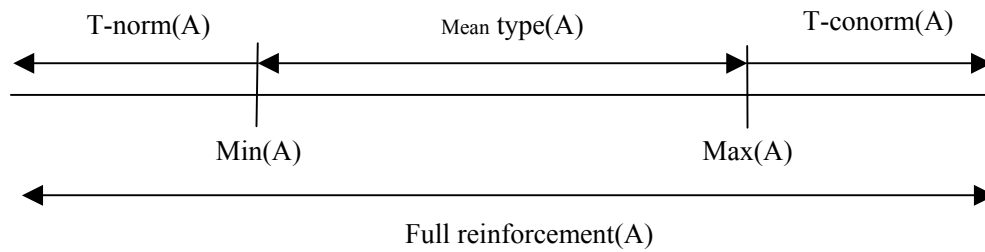


Figure 2.1 Value ranges of four fuzzy aggregation operators

## 2.4 CHAPTER SUMMARY

In this chapter, the fault location problem for distribution systems was introduced. Existing distribution fault location methods were reviewed. In addition, the shortcomings of existing fault location methods were pointed out. In this dissertation, the author will discuss a methodology developed to implement fuzzy resolvers. Commonly used fuzzy aggregation operators used in fuzzy resolvers were also introduced.

Chapter III introduces a new fault location scheme developed by other researchers in the Power System Automation Lab at Texas A&M University. Three fault location methods used in this scheme are discussed. The problem of the fuzzy resolver that is studied in this dissertation is formulated.

## CHAPTER III

### PROBLEM FORMULATION

#### 3.1 INTRODUCTION

Electrical power distribution systems connect customers to distribution substations through feeders. Most feeders are radial, which means that the electricity flows only through one path from the source to each customer [67]. A feeder may consist of a three-phase primary feeder, laterals (three-phase, two-phase or single-phase), loads, transformers, shunt capacitor banks, and protective devices.

There are a large number of apparatus in distribution systems. These apparatus age over time, which may lead to defects. Furthermore, most distribution systems are overhead systems, which are easily affected by changing weather conditions, animals, and traffic accidents. These two characteristics make faults in distribution systems inevitable. However, with increasing reliance on electricity, customers want an acceptable and reliable power supply at economic costs. In order to reduce the operating cost and the outage time and improve the quality of the power supply, fast and accurate location of faults is necessary.

Most fault location methods reviewed in the last chapter are based on one algorithm for locating faults. However, all algorithms have some shortcomings. The accuracy of the methods that calculate the fault distance from the fault related data is impacted by some characteristics of distribution systems, such as unbalance, non-homogenous feeder conductors, load types, and fault resistance. The sampling rate, voltage inception angle, and load taps or discontinuities in a feeder heavily influence the accuracy of traveling wave-based methods. Therefore, the accuracy may not be high if system operators locate faults based on one algorithm.

Beside the accuracy problem, many methods are designed for one specific system and are not easily applied to other systems. Some high frequency component based methods need to install detection devices in the system. Therefore, they cannot be used for systems

where detection devices are not installed. Some AI-based methods usually locate faults based on the status of protective devices and heavily rely on supervisory control and data acquisition (SCADA) systems, fault detectors, and communication channels. Due to economic constraints, the communication between protective devices and the substation are limited to some important substations. For many systems, measurements are only available at the substation and the operation status of feeder protective devices is unknown. For such systems, these methods are not feasible. Many expert system-based methods locate faults by using information obtained from SCADA systems, the network map and the dispatcher's past experience. Therefore, these methods are customized to one system and difficult to apply to different distribution systems.

In order to overcome the problems mentioned above, a new fault location scheme for radial distribution systems has been developed in the Power System Automation Lab at Texas A&M University. In order to improve the accuracy of the fault location method, the researchers developed a new fault location scheme that consists of three fuzzy fault location methods [69][70]. These methods decide the potential fault locations based on different algorithms. The final result is to be obtained by combining all three methods' outputs. Therefore, its accuracy is better than those methods using only one algorithm. In addition, this new scheme locates faults only based on the current and voltage measurements at the substation, feeder topological data, and protective device settings and locations. Hence, the new scheme can be used for almost all distribution systems.

The methods in the new scheme locate faults using some heuristic rules and analytical expressions. These heuristic rules represent human being's decision-making process. In a decision-making process, people always use some vague knowledge, which is expressed using natural language. For example, people say that a large current increment at a phase means that the phase is involved in a fault. This rule gives a qualitative, not quantitative, judgment. However, various people have different viewpoints about what "large" may be. Some may think a 30% increment is a large increment, while others may think a 50%

increment is a large increment. There is no sharp boundary between “large” and “small.” In order to deal with such situations, fuzzy logic is used in the new fault location scheme.

Another reason for adopting a fuzzy logic technique is that there are uncertainties in the measurements and some parameters used in the fault location methods. These uncertainties can be modeled by fuzzy membership functions. These uncertainties are mainly introduced by the dynamic nature of loads, feeder parameters, protective device operations, and data processing. In the following paragraphs, the author will briefly discuss uncertainties in distribution system fault locations.

### **3.1.1 Uncertainties in Distribution System Fault Locations**

The dynamic nature of loads introduces uncertainty in determining the load component in the fault current. The determination of loads plays a significant role in impedance-based methods. Because the customer load information is usually unknown, loads are always assumed to distribute evenly, and their time-varying nature is ignored.

In impedance-based fault location methods, fault resistances have a big impact on the accuracy of results, and are usually unknown. Besides fault resistances, the uncertainty in line parameters also reduces the accuracy of these methods.

Many AI-based methods use protective device’s information to locate faults. There may be errors in the transmission of the protective device operation data. The operated protective device may be mistakenly identified due to a protective device malfunction. The ambient temperature and prefault load influence the operation of protective devices. For example, the clearing time of fuses changes based on the ambient temperature and prefault load.

The raw data are processed to acquire the required data for fault location methods. The processing of data also leads to some uncertainties. For example, some fault location methods need the information about the fault current magnitude and the fault time duration. This information is then used to determine the fault location. The uncertainties

introduced in the process to obtain this information will reflect in the results of these methods.

In order to consider the uncertainties, fuzzy logic was used. In the following section, the author will introduce some fundamentals of fuzzy logic.

### 3.1.2 Fundamentals of Fuzzy Logic

Fuzzy logic refers to all of the technologies employing fuzzy set theory. Fuzzy set theory provides a way to represent uncertainties, and is used to deal with the fuzziness of the world. Before the advent of fuzzy set theory, the classical crisp set was used in the decision-making process. There is a sharp boundary in the crisp set. An element either belongs to a set or not, nothing in between. For the crisp set, the membership of an element  $x$  in a set  $A$  is represented mathematically with the indicator function (3.1).

$$\mu_A(x) = \begin{cases} 1, & \text{if } x \in A \\ 0, & \text{if } x \notin A \end{cases} \quad (3.1)$$

Human beings reason very effectively with fuzzy definitions. In order to capture imprecise and vague information, Zadeh [68] extended the notion of binary membership to accommodate various “degrees of membership” on the interval  $[0,1]$ , which allow a gradual transition from 0 to 1. The degree of membership is called the possibility. Zadeh defines a fuzzy set as:

$$F = \{(x, \mu_F(x)) | x \in X\} \quad (3.2)$$

where  $\mu_F$  is the membership function of  $x$  in  $F$ , and  $X$  is the universe of objectives with elements  $x$ .

Same as the crisp set, fuzzy sets have some set operations, such as the intersection, union, and complement. In addition to these basic operations, there are many other operations that can be applied to performing mathematical operations on fuzzy sets. Many of these operations are not uniquely defined; it is up to the fuzzy set practitioner to

choose appropriate operators that best reflect expert reasoning in the specific human decision-making process.

In the following sections, the fault location scheme is introduced, and three developed fault location methods are presented. In the new fault location scheme, there is a fuzzy resolver to aggregate three fault location methods' outputs. This dissertation is to develop a methodology for designing the fuzzy resolver. The author will formulate the problem of the fuzzy resolver methodology.

## 3.2 FAULT LOCATION SCHEME

### 3.2.1 Overall Scheme

The fault location scheme locates faults for radial distribution systems using the current and voltage measurements at the substation, feeder topological data, and protective device information. The architecture of the scheme is illustrated in Figure 3.1. The boxes shown with dotted lines have not been implemented yet.

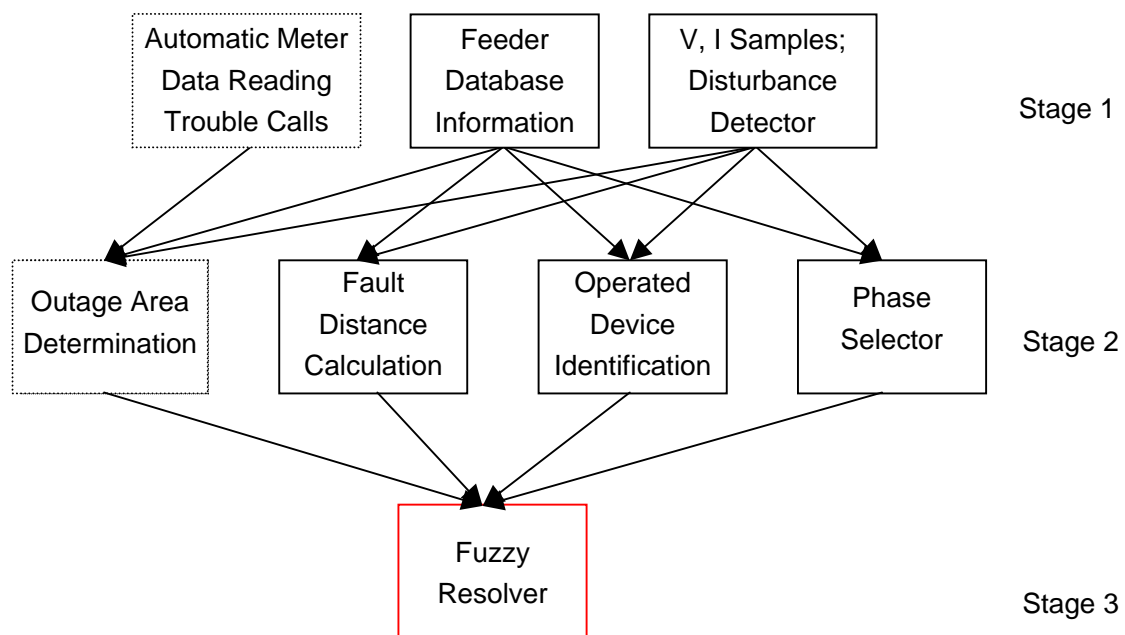


Figure 3.1 Architecture of the fault location scheme

The fault location scheme consists of three stages and is designed to locate faults on a radial distribution feeder with single- and multi-phase laterals. All needed information is gathered and processed into suitable formats in stage 1. The information includes feeder database information, voltage and current samples, and information from disturbance detectors. There are three fault location methods in stage 2. They locate faults based on different algorithms. These methods were implemented in a modular manner and independent of each other. Each of these methods computes possibility values – between 0 and 1 – for all line sections of a feeder to indicate the possibility of each line section being involved in a fault. Because the automatic meter reading data and trouble call information are not easily available from many utilities, the outage area determination method has not been implemented. Andoh, a graduate student, developed the fault distance calculation and phase selector methods [69]. Manivannan, another graduate student, developed the operated device identification method [70]. The fuzzy resolver, in stage 3, combines all three methods' outputs together to produce a final possibility value for each line section of a feeder. In the following sections, all three fault location methods and the function of the fuzzy resolver are introduced.

### **3.2.2 Phase Selector Method**

The phase selector method locates potential faulted sections by analyzing the current measured at the substation, that is,  $I_{abc}$  in Figure 3.2. Based on the knowledge that the faulted phases' currents increase when a fault happens, the faulted phases can be identified by observing the current magnitudes' variations during a fault [69].

Upon the detection of a fault event, the method extracts subevents. The definition of a subevent is shown in Figure 3.3. The start of a subevent within a fault event is the instance when any phase's current is larger than a preset percentage of its normal value; the end of a subevent is the instance when the currents of all phases drop below a preset percentage of their normal values for the first time.

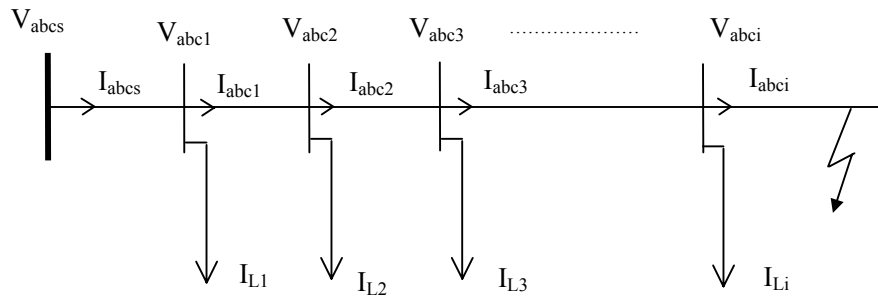


Figure 3.2 One-line diagram of a simple distribution feeder

For each subevent, phase possibility values of all phases are calculated. There are three factors influencing the phase possibility value that represents the degree to which a phase is involved in a fault. The first factor is the level of the current increment of each phase from its normal value. The second factor is the relative current increment of a phase with respect to the current increment of other phases. The reason to consider the relative current increment is that the current increment of a phase may be due to the mutual coupling between different phases, i.e., the currents of healthy phases may increase due to their mutual coupling with the faulted phase(s). When a feeder is reclosed after clearing a fault, the inrush currents may be several times those of the normal load currents. However, the current increase is due to a reclose transient, not a fault. The reclose transient is the third factor influencing the phase possibility value. A reclose transient can be distinguished from a fault by calculating the second harmonic component of currents. Usually the inrush currents include a large second harmonic component, while the fault currents do not.



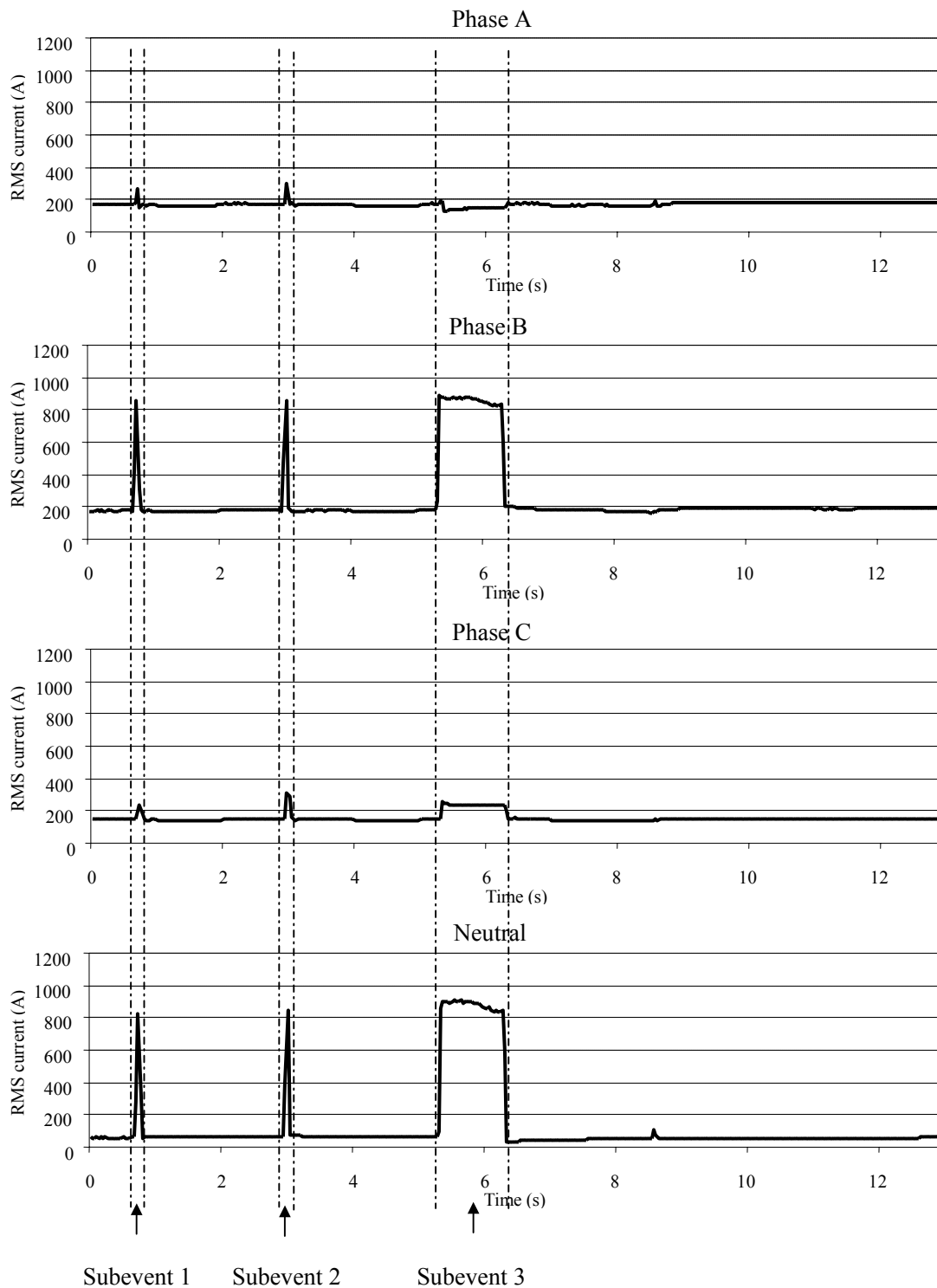


Figure 3.3 Fault event illustrating the definition of subevent

In order to take account of these three factors, three membership functions were defined in this method. There are the significant increase membership function, the relative current change membership function, and the reclose transient current membership function. If a phase is involved in a fault, it should have a large significant current increase membership value, a large relative current change membership value, and a small reclose transient change membership value.

For each subevent, three membership values were calculated using these three membership functions, and the phase possibility value of each phase was calculated using (3.3) based on the three membership values.

$$\pi_{sub-event k, phase j} = \mu_1 \wedge \mu_2 \wedge (1 - \mu_3) \quad (3.3)$$

where  $\mu_1$  is the significant current increase membership value,  $\mu_2$  is the relative current change membership value,  $\mu_3$  is the reclose transient membership value, and  $\wedge$  is the minimum operator.

For a fault event, the phase possibility value of each phase was calculated based on the inference rule: if a phase is involved in any one of the subevents, it is involved in the fault event. Based on this inference rule, the possibility value of each phase for the fault event was calculated using (3.4).

$$\pi_{event, phase j} = \pi_{subevent 1, phase j} \vee \pi_{subevent 2, phase j} \vee \dots \vee \pi_{subevent n, phase j} \quad (3.4)$$

where  $\vee$  is the fuzzy maximum operator,  $n$  is the total number of subevents in a fault event.

Based on possibility values of all phases, for each line section, the present phase possibility value and non-present phase possibility value were calculated using (3.5) and (3.6).

$$\pi_{section k}^P = \vee \pi_{event, phase j} \quad \forall \text{ phases present at section } k \quad (3.5)$$

$$\pi_{section k}^{NP} = \wedge (1 - \pi_{event, phase j}) \quad \forall \text{ phases present at section } k \quad (3.6)$$

where  $\forall$  means “for all”.

With these two possibility values, each line section's possibility value was calculated using (3.7).

$$\pi_{\text{section } k} = \wedge \left\{ \pi_{\text{section } k}^P, \pi_{\text{section } k}^{NP} \right\} \quad (3.7)$$

### 3.2.3 Fault Distance Method

The objective of the fault distance method is to exclude some line sections from the set of potential faulted sections based on the fault distance calculation so that a smaller set of potential faulted sections is obtained [69].

A simple distribution feeder shown in (3.3) is used to explain how the method works. The method assumes that the substation voltage and current measurements,  $V_{\text{abcs}}$  and  $i_{\text{abcs}}$ , are available, load currents,  $I_{L_i}$ , are available or are computed from load flow programs, and the impedance matrix of each line segment,  $Z_{\text{abci}}$ , is given. From the substation measurements, the subevents are extracted in the same way as discussed in 3.2.2. The phasors of these measurements,  $V_{\text{abcs}}$  and  $I_{\text{abcs}}$ , are calculated from the longest duration subevent. For each line section  $i$ , the voltage and current phasors at the sending-end,  $V_{\text{abci}}$  and  $I_{\text{abci}}$ , are calculated using (3.8) and (3.9), respectively.

$$[V_{\text{abci}}] = [V_{\text{abcs}}] - [Z_{\text{abcs}}][I_{\text{abcs}}] - \sum_{j=1}^{i-1} [Z_{\text{abcej}}][I_{\text{abcej}}] \quad (3.8)$$

where  $V_{\text{abcs}}$  is the voltage phasor value at the substation, and  $Z_{\text{abcej}}$  is the impedance matrix of the line segment  $j$ .  $I_{\text{abcej}}$  is the current phasor value on line segment  $j$ .

$$[I_{\text{abcej}}] = [I_{\text{abcs}}] - \sum_{k=1}^{j-1} [I_{Lk}] \quad (3.9)$$

where  $I_{\text{abcs}}$  is the current vector at the substation, and  $I_{Lk}$  is the current injection of the load connected to node  $k$ .

After calculating the sending-end voltage and current phasors, the fault distance calculation is performed on a section-by-section basis. In the following paragraphs, the

fault distance calculations for bolted single phase-to-ground faults and for bolted phase-to-phase faults are illustrated.

A bolted single phase to ground fault on phase A at a line section is shown in Figure 3.4, where  $I_f$  represents the fault current and  $Z_{abc}$  is the impedance matrix of the line section.  $V_a$ ,  $V_b$ , and  $V_c$  are the sending-end voltages, which are calculated according to (3.8);  $I_a$ ,  $I_b$ , and  $I_c$  are the sending-end currents, which are calculated according to (3.9). For the faulted phase, the relationship in (3.10) exists. All values except the fault distance in (3.10) are known. For each line section, the fault distance can be calculated using (3.11) hence.

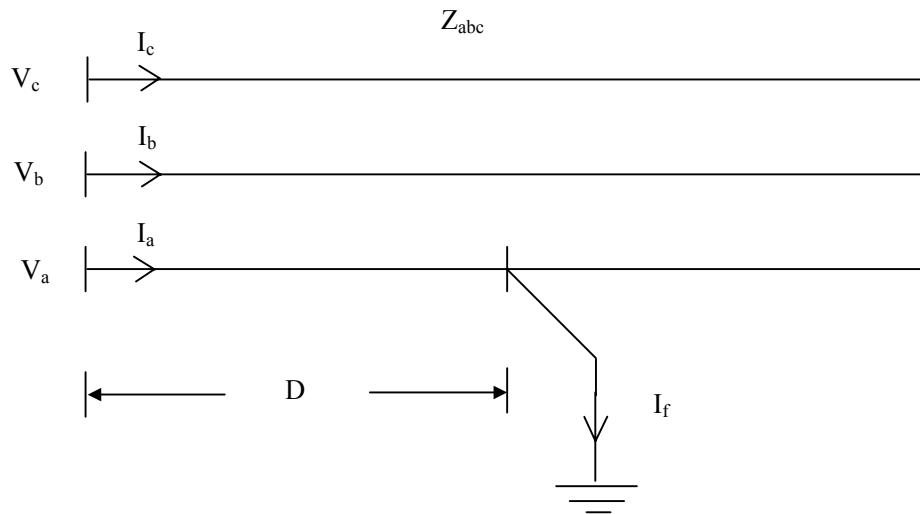


Figure 3.4 A bolted single phase to ground fault at a line section

$$V_a = D(z_{aa}I_a + z_{ab}I_b + z_{ac}I_c) \quad (3.10)$$

$$D = \frac{V_a}{z_{aa}I_a + z_{ab}I_b + z_{ac}I_c} \quad (3.11)$$

A bolted phase-to-phase fault between phases B and C at a line section is shown in Figure 3.5. It can be seen from Figure 3.5 that  $V_b' = V_c'$ , where  $V_b'$  is the phase B voltage at the fault point, and  $V_c'$  is the phase C voltage at the fault point. The relationships in (3.12) and (3.13) exist. By subtracting (3.13) from (3.12), the voltages at the fault point are eliminated and the relationship in (3.14) is obtained. All values except the fault distance in (3.14) are known. For each line section, the fault distance can be calculated using (3.15) for each line section.

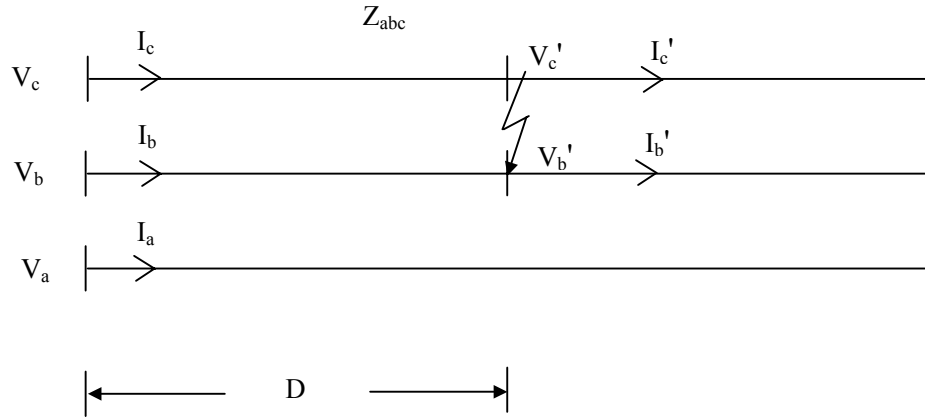


Figure 3.5 A bolted phase b to c fault at a line section

$$V_b = V_b' + D(z_{ba}I_a + z_{bb}I_b + z_{bc}I_c) \quad (3.12)$$

$$V_c = V_c' + D(z_{ca}I_a + z_{cb}I_b + z_{cc}I_c) \quad (3.13)$$

$$V_c - V_b = D(I_a(z_{ca} - z_{ba}) + I_b(z_{cb} - z_{bb}) + I_c(z_{cc} - z_{bc})) \quad (3.14)$$

$$D = \frac{V_c - V_b}{I_a(z_{ca} - z_{ba}) + I_b(z_{cb} - z_{bb}) + I_c(z_{cc} - z_{bc})} \quad (3.15)$$

After calculating the fault distance for a line section, the fault distance is compared with the line section's length. If the distance is larger than the line section's length, the fault is not on this line section; otherwise, the line section is a feasible faulted section.

After finding all feasible faulted sections, the line section's possibility value is assigned. This fault location method assumes that all faults are bolted, which means the fault resistance is equal to zero. Usually the fault resistance is non-zero and the value of the fault resistance is unknown. By assuming all faults are bolted, the calculated fault distance is the maximum possible distance [69], and the actual faulted section may be between the substation and the found feasible faulted section. Therefore, all sections between the substation and the found feasible faulted section are assigned a possibility value 1. The sections between the found feasible faulted section and the ends of a feeder are assigned a possibility value 0. This process is shown as (3.16).

$$\pi_{sectionk} = \begin{cases} 0 & k \text{ is downstream of a feasible faulted section} \\ 1 & k \text{ is upstream of a feasible faulted section} \end{cases} \quad (3.16)$$

### 3.2.4 Operated Device Identification Method

The objective of this method is to identify the operated protective device based on protective device's time current characteristics (TCC) curves[70]. In Figure 3.6, a simple distribution feeder with protective devices is shown. The phasor-differenced values of the current measurements at the substation,  $I_s$ , are used in this method [70]. The phasor-differenced values are approximations of the instantaneous current after the removal of the load components. When a fault is detected, subevents of the fault are extracted based on the definition shown in Figure 3.3. Then, the time durations and RMS currents of all phases of all subevents are obtained.

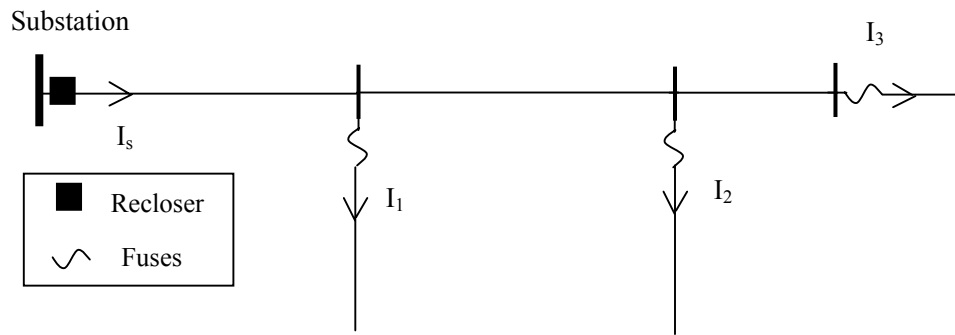


Figure 3.6 A simple distribution feeder with protective devices

For each subevent, the time duration and RMS current of a phase form a pair. Each pair corresponds to a point, called operating point, in the time-current plane such as point A shown in Figure 3.7. The method compares the point to various protective devices' time-current characteristic (TCC) curves to get the distances between the operating point and various TCC curves. The time intervals between subevents are compared with protective device's time settings if protective devices are reclosing devices. If a protective device recloses a fault, the time interval should be larger than or equal to its time settings. The architecture of this method is shown in Figure 3.8.

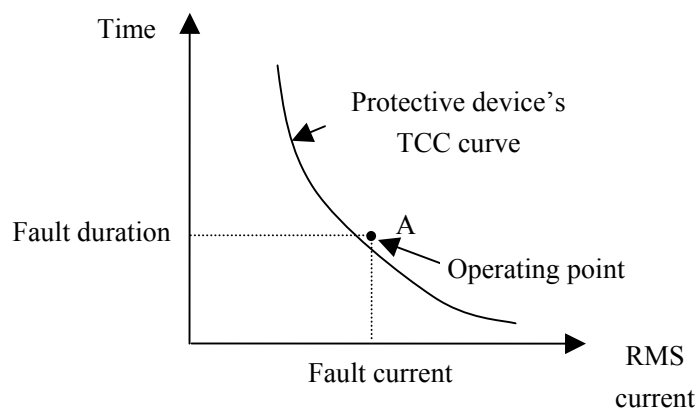


Figure 3.7 Illustration of the comparison between a TCC curve and an operating point

After extracting subevents, the number of subevents ( $N_{S-E}$ ) in an event could be determined. The total number of combinations of the operating sequence of a device can be found using (3.17), where  $N_{S-E}$  is the number of subevents,  $N_{H\_Comb}$  is the number of hypotheses combinations.

$$N_{H\_Comb} = 2^{N_{S-E}} \quad (3.17)$$

A hypothesis is defined as a particular operation sequence of a device's operations. The hypotheses generated for an event that has three subevents are shown in Table 3.1. A value of '1' under the subevent column shows that a device operates, and a value of '0' implies that a device does not operate. For example, the hypothesis (0 0 1) means that a device does not operate on the first and second subevents and operates on the third subevent.

After generating hypotheses, four possibility values are calculated for each hypothesis. They are the device operation possibility  $\pi_{Op}$ , event downstream possibility  $\pi_{Dwn}$ , time-satisfaction possibility  $\pi_{Time}$ , and event self-cleared possibility  $\pi_{Self}$ . The device operation possibility represents the possibility that a protective device operates in an event, and this possibility value is calculated in block 1 of Figure 3.8. The event downstream possibility is the possibility that a protective device allows an event to be downstream of it based on its operation characteristics, and this possibility value is calculated in block 2 of Figure 3.8. The time-satisfaction possibility is the possibility that a protective device allows an event to happen downstream of it based on its time settings, and this possibility value is calculated in block 3 of Figure 3.8. The event self-cleared possibility represents the possibility that the event is a temporary fault and cleared by itself without the operation of the protective device, and this possibility value is calculated in block 4 of Figure 3.8. The calculation of this possibility requires characterization of arcing phenomena and a detailed study of the behavior of temporary



faults, which was not included by Manivannan. Therefore, the event self-cleared possibility is always set to be 1.

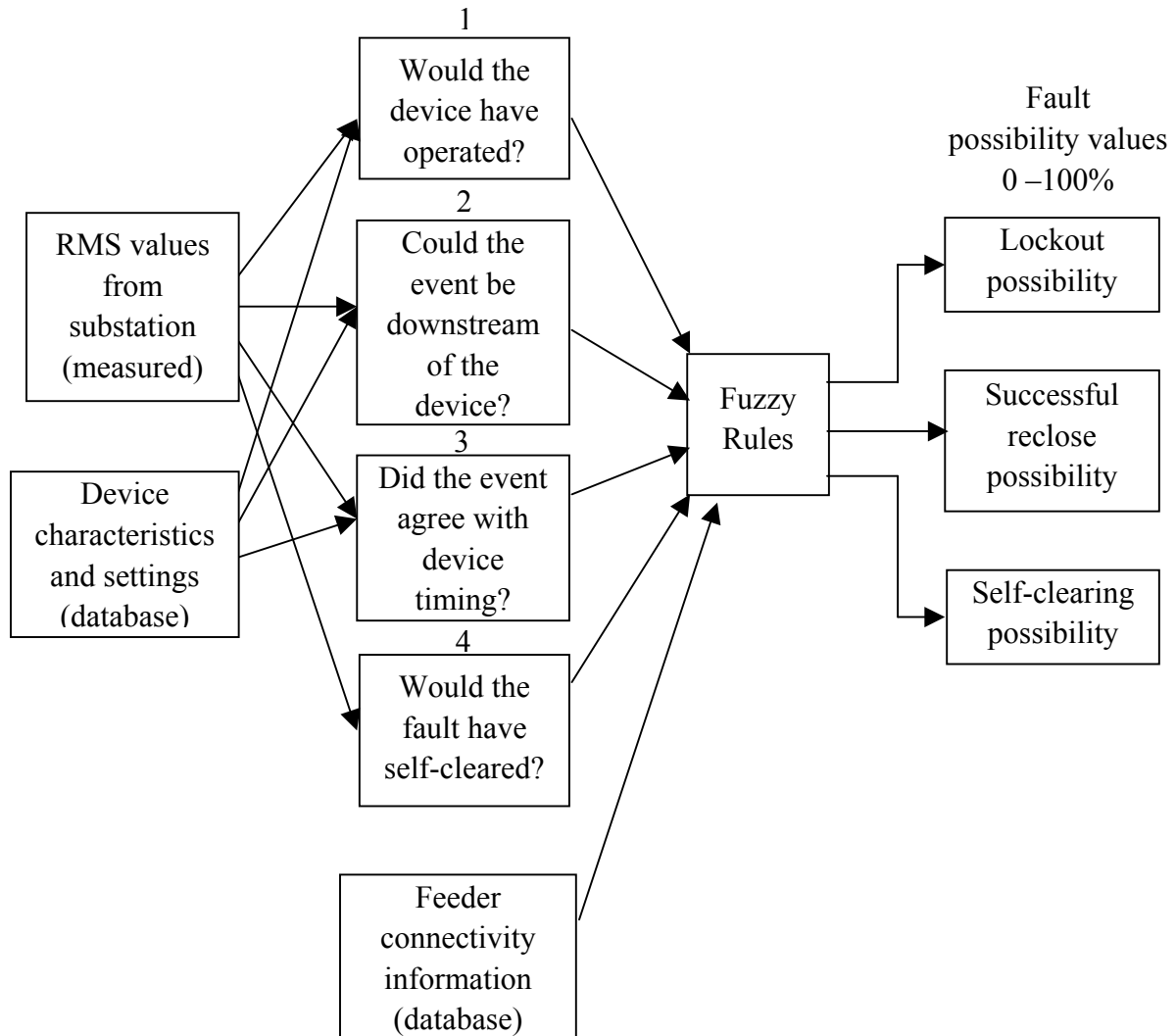


Figure 3.8 Architecture of the operated device identification method

The calculation of the above four possibility values is only based on the distances between the operating point and various TCC curves and the protective device's time settings. During the calculation, each protective device is considered alone, and the

coordination between protective devices is not considered. In the next step, some fuzzy rules are used to re-evaluate these four possibility values with consideration of the coordination between protective devices. The coordination information is available from the feeder connectivity information database.

Based on these re-evaluated possibility values, the device lockout possibility, device successful reclose possibility, and event self-clearing possibility are calculated using some fuzzy rules. The device lockout possibility value represents the possibility that a section is involved in a permanent fault, and the device protecting this section locks out to isolate the fault. The rule to calculate this possibility is that “The event was downstream of the device AND the device operated AND the event satisfied the time settings of the device AND the number of device operations was equal to  $N_{Max-op}$  AND the device operated on the final sub-event  $N_{S-E}$ ,” and the possibility is calculated using (3.18).

TABLE 3.1 DIFFERENT HYPOTHESES GENERATED FOR  $N_{S-E}=3$

	Subevent		
	1	2	3
Hypotheses	0	0	0
	0	0	1
	0	1	0
	0	1	1
	1	0	0
	1	0	1
	1	1	0
	1	1	1

The device’s successful reclose possibility represents the possibility that a section is involved in a temporary fault, and the device protecting the section has a successful

reclose to clear the fault. The rule to calculate this possibility is that “The event was downstream of the device AND the device operated AND the event satisfied the time settings AND the number of device operations was equal to  $N_{Max-op}$  AND the device operated on the final sub-event  $N_{S-E}$ .” This possibility is calculated using (3.19).

The event self-clearing possibility is the possibility that a section is involved in a temporary fault and the fault is gone without the device protecting the section operating. The possibility is calculated using the rule, “The event was downstream of the device AND the device operated AND the event satisfied the time settings AND the number of device operations was less than  $N_{Max-op}$  AND the device did not operate on the final sub-event  $N_{S-E}$  AND the fault self cleared on the last sub-event.” It is calculated using (3.20).

$$\pi_{Lock}(n_D, n_H) = \pi_{Op} \wedge \pi_{Dwn} \wedge \pi_{Time} \wedge (N_{Max\_Op} == N_{Op}) \wedge (n_H(N_{S-E}) == 1) \quad (3.18)$$

$$\pi_{Reclose}(n_D, n_H) = \pi_{Op} \wedge \pi_{Dwn} \wedge \pi_{Time} \wedge (N_{Max\_Op} > N_{Op}) \wedge (n_H(N_{S-E}) == 1) \quad (3.19)$$

$$\pi_{Self}(n_D, n_H) = \pi_{Op} \wedge \pi_{Dwn} \wedge \pi_{Time} \wedge (N_{Max\_Op} > N_{Op}) \wedge (n_H(N_{S-E}) \neq 1) \quad (3.20)$$

where  $n_D$  is a protective device,  $n_H$  is a hypothesis of the protective device’s operation sequence,  $\pi_{Op}$  is the operation possibility,  $\pi_{Dwn}$  is the downstream possibility,  $\pi_{Time}$  is the time-satisfaction possibility,  $N_{Max\_Op}$  is the maximum number of times that the device is set to operate,  $N_{Op}$  is the number of times the device operated according to the hypothesis  $n_H$ .  $N_{S-E}$  is the number of subevents,  $\wedge$  is the minimum operator.

After calculating these three possibility values, the possibility value of a protective device is calculated using (3.21) and (3.22).

$$\pi_{Fault}(n_D, n_H) = \pi_{Lock}(n_D, n_H) \vee \pi_{Reclose}(n_D, n_H) \vee \pi_{Self}(n_D, n_H) \quad (3.21)$$

$$\pi_{Fault}(n_D) = \max_{i=1}^{N_H} (\pi_{Fault}(n_D, n_H)) \quad (3.22)$$

where  $\pi_{Lock}(n_D, n_H)$ ,  $\pi_{Reclose}(n_D, n_H)$ , and  $\pi_{Self}(n_D, n_H)$  are calculated using (3.18)-(3.20),  $N_H$  is the total number of hypotheses,  $\vee$  is the maximum operator.

Based on the protective device's possibility, line section's possibility values are assigned using (3.23), where  $n_D$  is the primary protective device of line section  $k$ . The details of this method are given in [70].

$$\pi_{section k} = \pi_{Fault}(n_D) \quad (3.23)$$

### 3.2.5 New Fuzzy Resolver

For a fault, each of these three fault location methods assigns possibility values for all line sections of a feeder. Therefore, each line section of the feeder gets three possibility values as shown in Figure 3.9,  $A_{ODIM}$ ,  $A_{PS}$ , and  $A_{FD}$ , where  $A_{ODIM}$  is the output of the operated device identification method,  $A_{PS}$  is the output of the phase selector method, and  $A_{FD}$  is the output of the fault distance method. The new developed fuzzy resolver will combine all three possibility values into one final possibility value. The sections with high possibility values are potential faulted sections.

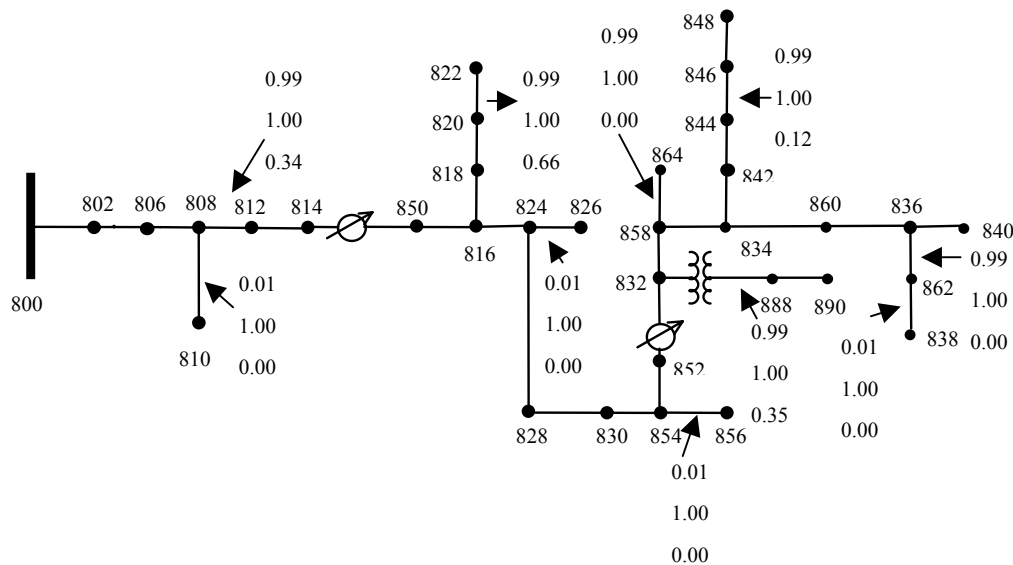


Figure 3.9 Feeder with Outputs of Three Fault Location Methods

### **3.3 PROBLEM FORMULATION OF THE FUZZY RESOLVER METHODOLOGY**

In order to design a fuzzy resolver, data representing many distribution systems are needed to generalize the parameters of the fuzzy resolver. Hence, data from several distribution feeders that can provide enough information to apply all three fault location methods is needed. These fault location methods need some information, such as the feeder's topological data, the protective device's placements and settings, and measurements at the substation. However, not all of this information was available to the author from the utilities. Therefore, no real data were used to design the fuzzy resolver. In this dissertation work, one distribution feeder was modeled to generate data. These data were not enough to generalize the parameters of the fuzzy resolver. Therefore, only the fuzzy resolver methodology is developed in this dissertation.

In the fuzzy resolver methodology, the performance of commonly used fuzzy aggregation operators were studied first. Then the candidate fuzzy aggregation operators used to design the fuzzy resolver were chosen based on the characteristics of the fault location problem. To take account of different accuracy of the three fault location methods, weights were assigned to all methods. In order to determine optimal weights, two objectives were proposed. After that, an optimization method was selected. Weights of the three fault location methods were optimized based on two objective functions and using some training cases. The optimal weights were obtained with respect to a single objective function first. Then they were obtained with respect to two objective functions. The performance of these fuzzy resolvers was compared in terms of these two objective functions. After that, the performance of some good fuzzy resolvers were studied using the test cases.

### 3.3.1 Fuzzy Aggregation Problem

In the new fault location scheme, there are three fault location methods. Each method uses a criterion. Based on each criterion, a line section is assigned a possibility value to indicate the possibility that the line section is involved in a fault. In order to improve the accuracy of the result, the fuzzy resolver combines all three methods' output values to produce final possibility values for all sections. The methodology for designing the fuzzy resolver is to solve a fuzzy aggregation problem. Fuzzy aggregation operators are needed in the fuzzy resolver methodology.

For each fault case, each method assigns a possibility value  $A_j(x) \in [0, 1]$  for each line section  $x$  to indicate the degree to which  $x$  may be involved in the fault. In the proposed methodology, the fuzzy resolver formulates the overall decision function  $D$  from the individual possibility values. For any alternative  $x$ ,  $D(x) \in [0, 1]$  indicates the degree to which  $x$  satisfies three criteria.

$$D(x) = F(A_{ODIM}(x), A_{PS}(x), A_{FD}(x)) \quad (3.24)$$

The structure  $F$  should satisfy the following properties:

Monotonicity property: with the individual possibility increasing, the overall possibility should increase; if  $A_j(x) \geq A_j(y)$  for all  $j$ , then  $D(x) \geq D(y)$ .

Symmetry property:  $F$  should be symmetric with respect to individual possibilities if three methods are equally important. In other words, the ordering of the individual possibility is irrelevant.  $F(A_{ODIM}(x), A_{PS}(x), A_{FD}(x)) = F(A_{PS}(x), A_{ODIM}(x), A_{FD}(x))$ .

All fuzzy aggregation operators introduced in Chapter II satisfy these two properties and can be used as the overall decision function  $D$ . Usually when people choose the aggregation operators, they make a choice based on their attitude to the problem. Pessimistic people use fuzzy intersections to aggregate possibility values to ensure all criteria are satisfied, while optimistic people use fuzzy unions to aggregate in order to satisfy at least one of the criteria. However, various possibility values may have different

accuracy levels due to the decision-making process, and this characteristic should be considered.

In the decision-making process of each fault location method, the decision maker assigns a low possibility value to a line section when the decision maker is sure that the fault is not on the line section based on a criterion. In contrast, when the decision maker is uncertain that the fault is not on the line section, the decision maker assigns a high possibility value to the line section. By doing this, the actual fault location is not eliminated from the potential fault locations. Hence, high possibility values just mean the fault may be on the line section but is not necessarily on the line section. Therefore, high possibility values are less accurate than low possibility values. When choosing fuzzy aggregation operators for the fuzzy resolver, this characteristic should be considered. In the following paragraphs, the author will investigate commonly used aggregation operators introduced in Chapter II and choose appropriate aggregation operators for the fuzzy resolver.

### ***3.3.1.1 Study of Fuzzy Aggregation Operators***

All commonly used operators mentioned in Chapter II were investigated [92]. In the study, three arbitrary possibility values that might be assigned by three fault location approaches were aggregated using various aggregation operators. The aggregated possibility values and the aggregation results obtained using different operators are listed in Table 3.2. The description of the symbols used in Table 3.2 is explained in Table 3.3. From the numerical tests, various characteristics of the different operators were observed.

T-norm operators (min, algebraic product) emphasize low possibility values. One low possibility value makes the final result low regardless of the other values. The min operator does not distinguish between situations such as  $(0.1, 0.2, 1)$  and  $(0.1, 0.8, 1)$ . For both situations, the min operator assigns 0.1 as the final result. However, these two situations are different because under the first situation two criteria assign a low possibility to the candidate, while for the second situation only one criterion assigns a

low possibility value to the candidate. Intuitively, the second case should yield an aggregation possibility value larger than in the first case. Although the algebraic product gives different values for these two situations, it does not really distinguish between the situations. For these two situations, it assigns 0.02 and 0.08 as the final values for (0.1,0.2,1) and (0.1,0.8,1), respectively. These two results are less than the minimum value of the input possibility values. Hence, high possibility values have no substantial effect on the final value and high possibility values do not compensate low possibility values. Based on the property  $i(s_1, \dots, s_q) \leq \min(s_1, \dots, s_q)$  [63], it is known that all t-norm operators assign the aggregation possibility value equal to or less than the minimum value. Therefore, all of them lack the compensation property and cannot distinguish between situations such as these two either. In addition, the algebraic product sometimes gives a low possibility value when all criteria give high possibility values. For example, it assigns 0.343 for (0.7,0.7,0.7).

T-conorm operators (max, algebraic sum) emphasize high possibility values. If one criterion gives a high possibility value, the final value is high and largely unaffected by other values. Similar to t-norms, t-conorms have the property  $u(s_1, \dots, s_q) \geq \max(s_1, \dots, s_q)$  [63], so that they cannot assign the aggregation possibility value less than the maximum value of the input possibility values. Hence, they also lack the compensation property and cannot distinguish between cases such as (0.1,0.2,1) and (0.1,0.8,1). In both cases, they assign the final value as 1.

OWA operators can be a max-type operator or a min-type operator based on their parameters [65]. In the numerical study, the Orness of OWA1 is larger than 0.5 and is equal to 0.6965, which means OWA1 is closer to the max operator than to the min operator. It can be seen that its final results tends to high possibility values. OWA2 is closer to the min operator; its Orness is equal to 0.0775. The test results confirm the emphasis on low possibility values. As seen in Table 3.2, an advantage of OWA over



t-norms and t-conorms is that OWA operators can discern cases  $(0.1,0.2,1)$  and  $(0.1,0.8,1)$  due to their compensation property.

The additive family of FIMICA assigns a large possibility value even when one criterion gives a low possibility value, such as  $(0.9,0.9,0.2)$ . In the case  $(0.7,0.7,0.6)$ , all possibility values are larger than the identity  $g$  (choosing  $g=0.5$ ). Hence, as a full reinforcement operator, this family assigns an aggregation possibility value larger than  $0.7$ . For situations such as  $(0.9,0.9,0.2)$  and  $(0.7,0.7,0.6)$ , the summation of  $(a_i/g)$  with  $g=0.5$  are equal, so that the operator should assign the same value to these two situations. Since a value larger than  $0.7$  is assigned to  $(0.7,0.7,0.6)$ , the operator also assigns a possibility value larger than  $0.7$  to  $(0.9,0.9,0.2)$ . Due to the choice of the function  $f_1$ , FIMICA1 assigns  $1.0$  as the final results for both situations. The product family of FIMICA has a similar feature as the additive family, i.e., it assigns a large value when one criterion assigns a low possibility value. Since the product of  $(a_i/g)$  is the same in both situations, the operator cannot distinguish between the situations  $(0.9,0.9,0.2)$  and  $(0.55,0.55,0.536)$ . For  $(0.55,0.55,0.536)$ , all input possibility values are larger than  $g=0.5$ . Hence, the family assigns a final value that is larger than  $0.536$  for the situation. Due to the same product of the two situations, the values assigned to these two situations are equal. Hence, it also assigns a value larger than  $0.536$  to  $(0.9,0.9,0.2)$ . Due to the formula of the function  $f_2$ , FIMICA2 assigns  $0.648$  as the final result for  $(0.9,0.9,0.2)$ . The triple  $\Pi$  operator sometimes assigns a possibility value even though one of its inputs is a low possibility value. For the case  $(0.8,0.8,0.3)$ , this operator assigns  $0.873$  as the final value, which is larger than both input values  $0.8$  and  $0.3$ . Sometimes, another FIMICA operator from fuzzy model theory (FM2) assigns a large value when one criterion assigns a low possibility value. One example of this situation is  $(0.2,0.6,0.9)$ . In this case, because  $\Delta=\min(1-0.2,1-0.6,1-0.9)=0.1$ ,  $\Omega=\min(0.2,0.6,0.9)=0.2$  and  $\Delta<\Omega$ , FM2 gives  $\max(0.2,0.6,0.9)=0.9$  as the final result.

The type II uninorm assigns a large value as the final value even when one or two of the input values are small. For example, for the case (0.2,0.6,0.9), the type II uninorm assigns 0.9 as the aggregation possibility value.

### ***3.3.1.2 Choosing Fuzzy Aggregation Operators for the Fuzzy Resolver***

In the new fault location scheme, three methods are used to assign possibility values to each line section of a radial distribution system. With the assumption that each method is equally accurate, operators are chosen only based on the characteristics of the fault location methods, which means that low possibility values are more accurate than high possibility values.

When t-norms aggregate several possibility values, they emphasize low possibility values. Hence, t-norms may be used for the aggregation in the new fault location scheme described earlier. Among all t-norms, the min operator is the best choice because all other t-norm operators produce an aggregation possibility value lower than the minimum value of the aggregated possibility values [63], which is not desirable. In addition, the algebraic product may assign a low possibility value when all individual possibility values are high, which means that when all criteria suggest it is possible that a fault occurred on a candidate, the aggregation result shows that it is quite possible that the fault did not occur on the candidate. Obviously, this is not reasonable, so the product operator does not fit our problem. Other commonly used t-norms have the same problem because their values are less than the value of the algebraic product [63]. This is not reasonable and they do not fit the fault location method either. The min operator is the only appropriate t-norm for the fault location method.

T-conorms stress high possibility values and do not provide compensation between different criteria. Based on these two features, t-conorms are not effective for the new fault location scheme.

There are several mean type operators that range between the min operator and the max operator. For this fault location scheme, the mean type operators close to the min

operator are more effective. In the commonly used mean type operators, both the simple mean operator and the median operator tend to be in the middle of the range. The OWA operator, with an appropriate set of weights, can stress low possibility values. Therefore, the OWA operator is a good choice for the fault location scheme.

There are two types of uninorm operators, and they use different aggregation operators under the mixture situation. The type I uninorm (uninorm1) uses the min operator while uninorm2 uses the max operator. Hence, uninorm1 emphasizes low possibility values and it is effective for the new fault location scheme. Due to its emphasis on high possibility values, uninorm2 is not a good operator for the problem.

As stated earlier, both the additive family and the product family of FIMICA sometimes assign a high possibility value as the aggregation possibility value when one criterion assigns a low possibility value. Since low possibility values are more accurate than high possibility values, the final result should not be too high. Therefore, these two operators are not good aggregation operators for the fault location scheme. Neither are the triple  $\Pi$  operator or FM2.

TABLE 3.2 SUMMARY OF THE NUMERICAL TESTS OF FUZZY AGGREGATION OPERATORS

			T-NORMS		T-CONORMS		OWA		FIMICA					
			A1	A2	A3	Min	ALGEBRAIC PRODUCT	MAX	ALGEBRAIC SUM	OWA1	OWA2	UNINORM 1	UNINORM 2	FIMICA1
0.1	0.2	1	0.1	0.02	1	1.000	0.643	0.123	0.100	1.000	0.300	0.080	1.000	1.000
0.1	0.8	1	0.1	0.08	1	1.000	0.787	0.203	0.100	1.000	0.900	0.320	1.000	1.000
0.7	0.7	0.7	0.7	0.343	0.7	0.973	0.700	0.700	0.973	0.973	1.000	1.000	0.927	0.700
0.7	0.7	0.6	0.6	0.294	0.7	0.964	0.682	0.614	0.964	0.964	1.000	1.000	0.891	0.700
0.9	0.9	0.2	0.2	0.162	0.9	0.992	0.771	0.301	0.200	0.900	1.000	0.648	0.953	0.900
0.55	0.55	0.536	0.54	0.162	0.55	0.906	0.547	0.538	0.906	0.906	0.636	0.648	0.633	0.550
0.8	0.8	0.3	0.3	0.192	0.8	0.972	0.708	0.372	0.300	0.800	0.900	0.768	0.873	0.800
0.2	0.6	0.9	0.2	0.108	0.9	0.968	0.700	0.261	0.200	0.900	0.700	0.432	0.771	0.900

TABLE 3.3 DESCRIPTION OF THE SYMBOLS USED IN TABLE 3.2

SYMBOL	DESCRIPTION
A1,A2,A3	Three input possibility values, which represent the possibility values of a candidate assigned by three criteria
Min	The minimum value of $(a_1, a_2, a_3)$
algebraic product	$a_1 \times a_2 \times a_3$
Max	The maximum value of $(a_1, a_2, a_3)$
algebraic sum	$(a_1 + a_2 - a_1 \times a_2) + a_3 - (a_1 + a_2 - a_1 \times a_2) \times a_3$

TABLE 3.3 CONTINUED

SYMBOL	DESCRIPTION
OWA1	An OWA operator close to the max operator, where $w_1=0.577$ , $w_2=0.239$ , $w_3=0.184$ . $Orness(OWA1)=1/2 \times (2 \times 0.577 + 1 \times 0.239 + 0 \times 0.184) = 0.6965$ .
OWA2	An OWA operator close to the min operator, where $w_1=0.011$ , $w_2=0.133$ , $w_3=0.856$ . $Orness(OWA2)=1/2 \times (2 \times 0.011 + 1 \times 0.133 + 0 \times 0.856) = 0.0775$
Uninorm1	Type I uninorm operator
Uninorm2	Type II uninorm operator
FIMICA1	<p>A member of the additive family of FIMICA. In order to keep the characteristics that when the satisfaction degrees to two criteria equal to <math>g</math>, the final result equals to the satisfaction degree to the other criterion. The defined the function, <math>f_1(\cdot)</math>, as:</p> $f_1(a_1, a_2, a_3) = \begin{cases} 0 & \Sigma \leq 0 \\ \Sigma & 0 < \Sigma < 1 \\ 1 & \Sigma \geq 1 \end{cases}$ <p>where <math>\Sigma = ((a_1 - g) + (a_2 - g) + (a_3 - g) + g)</math></p>
FIMICA2	<p>A member of the product family of FIMICA. Similar to FIMICA1, the function, <math>f_2(\cdot)</math>, was defined as:</p> $f_2(a_1, a_2, a_3) = \begin{cases} 0 & \Pi \leq 0 \\ \Pi & 0 < \Pi < 1 \\ 1 & \Pi \geq 1 \end{cases}$ <p>where. <math>\Pi = (a_1 / g) \times (a_2 / g) \times (a_3 / g)</math></p>
Triple $\Pi$ operator	$M_1(a_1, a_2, a_3) = \frac{a_1 \times a_2 \times a_3}{a_1 \times a_2 \times a_3 + (1 - a_1)(1 - a_2)(1 - a_3)}$

TABLE 3.3 CONTINUED

SYMBOL	DESCRIPTION
FM2	$M_2(a_1, a_2, a_3) = \begin{cases} \min(a_1, a_2, a_3) & \Delta > \Omega \\ \max(a_1, a_2, a_3) & \Delta < \Omega \\ \frac{1}{2}(\min(a_1, a_2, a_3) + \max(a_1, a_2, a_3)) & \Delta = \Omega \end{cases}$ <p style="text-align: center;">where <math>\Delta = \min(1 - a_1, 1 - a_2, 1 - a_3)</math>, <math>\Omega = \min(a_1, a_2, a_3)</math></p>

By investigating the commonly used aggregation operators, it was determined that the OWA operator that is close to the min operator is one of the best choices for the new fault location method. T-norms are also a good choice. Full reinforcement operators utilize the mutual reinforcement between the results of different criteria. Of the various full reinforcement operators, uninorm1 is a good operator for the fault location scheme.

In summary, the min operator, the OWA operator and the uninorm1 operator were investigated. As shown in (2.11), the OWA operator uses parameters.

### 3.3.2 Importance of Three Fault Location Methods

In the previous section, the author chose fuzzy aggregation operators with the assumption that the three fault location methods are equally important. However, the three fault location methods use different algorithms, and their accuracy levels may be different. In order to take into account the different importance of various methods, weights are assigned to all methods.

Fuzzy aggregation operators provide a way to associate the concept of weights or importance factors with the method's outputs, and they can be used to aggregate weighted bags. A weighted bag [64] is a bag whose elements are tuples  $(w_i, a_i)$ . For each tuple,  $w_i$  is the weight associated with an argument, and  $a_i$  is the value of the argument and represents the output of a fault location method. The process of aggregating weighted bags consists of two steps. The first step is a transformation step that converts a weighted bag into a single value called the effective value. The second step is to aggregate these effective values using fuzzy aggregation operators. In the following subsections, the author will discuss the factors influencing the accuracy of different methods and introduce the methods for incorporating weights in the chosen fuzzy aggregation operators.

### ***3.3.2.1 Factors Influencing the Accuracy of Three Fault Location Methods***

In order to locate faults, the fault distance method calculates the fault distance by using the current and voltage phasors at the sending end of each line section. The fault distance method does not know the fault resistance and assumes that the fault resistance is zero. This assumption does not usually reflect the actual situation. The results of this method have some errors when the fault resistance is not equal to zero. In addition, there are errors and uncertainties in line parameters and in the process of estimating phasors. In the process of getting line currents, load currents during a fault are assumed to be the same as prefault load currents. However, prefault load currents can only approximate load currents during a fault, and there are some differences between them. All these errors and uncertainties affect the accuracy of the distance calculation of this method.

The phase selector method determines the faulted phases based on the current increase. However, the fault resistance heavily affects the current increment during a fault. In addition, healthy phases' currents may also increase during a fault due to the mutual couplings between various phases, and some current increase is due to the load change. All these factors make it difficult to determine the threshold of the current increment that indicates a fault. If the threshold is too low, the current increase due to the load change or the mutual coupling may be considered as a fault; if the threshold is too high, the current increase due to a high impedance fault may be considered as a normal case.

The operated device identification method compares the current waveform measured at the substation with various protective devices' TCC curves and settings to find out the operated protective device. In order to get the correct result, the currents through various protective devices need to be estimated. There are errors in the process of estimating these currents and of matching the current waveform with the protective devices' TCC curves. In addition, there are errors in the measured data. These errors affect the accuracy of this method. Therefore, different factors impact the accuracy levels of various fault location methods. The three methods may have different accuracy levels. In order to



consider the different accuracy levels, the fuzzy resolver assigns weights to all three methods.

### 3.3.2.2 Fuzzy Resolver Considering Weights of Three Fault Location Methods

When weights are associated with each fault location method, the fuzzy resolver evaluates the overall decision function  $D$  from the individual weighted bags [66]. The overall decision function  $D$  given in (3.24) becomes (3.25), where  $\langle A_j(x), w_j \rangle$  is a weighted bag,  $A_j(x)$  is the output of the  $j^{\text{th}}$  fault location method,  $w_j$  is the weight assigned to the method.  $A_j(x) \in [0, 1]$ ,  $w_j \in [0, 1]$ .

$$D(x) = F(\langle A_{ODIM}(x), w_{ODIM} \rangle, \langle A_{PS}(x), w_{PS} \rangle, \langle A_{FD}(x), w_{FD} \rangle) \quad (3.25)$$

Fuzzy aggregation operators used as the overall decision function  $D$  first transform the weighted bag  $\langle A_j(x), w_j \rangle$  to an effective value  $B_j(x) \in [0, 1]$ . Then, they aggregate these effective values using (3.26).

$$D(x) = F(B_{ODIM}(x), B_{PS}(x), B_{FD}(x)) \quad (3.26)$$

The overall decision function should have the monotonicity property and symmetry property with respect to individual effective values  $B_j(x)$ , rather than individual possibility values  $A_j(x)$ .

The methods for transforming a weight bag to an effective value for the chosen aggregation operators are discussed in the following sections.

#### 3.3.2.2.1 Including Importance of Fault Location Methods in the Min Operator

For the min operator, low possibility values play a more significant role in the aggregation result than high possibility values. If a fault location method has low accuracy (importance), its output plays a trivial role in the final decision. Therefore, its output should become a large effective value. If a method has high accuracy (importance), its output plays a significant role in the final decision. Therefore, its output should be transformed into a small effective value. In [71], two commonly used methods for

including the importance of the fault location methods in the min operator were introduced. The first method is shown in (3.27), and the second method is shown in (3.28).

$$a' = (1 - w) + aw \quad (3.27)$$

$$a' = a^w \quad (3.28)$$

where  $a$  is the output of a fault location method,  $w$  is the weight to represent the accuracy (importance) of the method.

These two transformation methods are similar. When the accuracy of a fault location method is 0, which means the fault location method gives no useful information in its output, the two transformation methods transform its output,  $a$ , to 1. The transformed value, 1, does not affect the aggregation result of the min operator at all. When the accuracy of a fault location method is 1, which means the method is 100% sure that its output is correct, the two transformation methods will keep the method's output,  $a$ , as the effective value. The difference between these two methods is that when the output of a fault location method is 0, the first method transforms the value to  $1-w$  while the second one keeps the value as 0.

### 3.3.2.2.2 *Including Importance of Fault Location Methods in the OWA Operator*

The OWA operator has different aggregation behavior based on its parameters  $\bar{W}$ , as given in (2.11), which is a set of parameters associated with the OWA operator and different from the importance factor  $w$ . It can behave as a max-type operator, or a min-type operator. Based on the fuzzy modeling concept and the transformation methods used for the max operator and the min operator, Yager proposed a transformation method for the OWA operator [71]. The method is shown as (3.29).

$$a' = (1 - w)(1 - \alpha) + wa \quad (3.29)$$

where  $a$  is the output of a fault location method,  $w$  is the weight to represent the accuracy

(importance) of the method,  $\alpha$  is the degree of “Orness” of the OWA operator.

Yager suggested another possible transformation method for the OWA operator [65]. This is shown as (3.30).

$$a' = \max(w, 1 - \alpha) \times a^{\max(w, \alpha)} \quad (3.30)$$

### 3.3.2.2.3 *Including Importance of Fault Location Methods in the Uninorm Operator*

In [66], Yager presented a transformation method for the uninorm operator. The method is shown as (3.31).

$$a' = wa + (1 - w)g \quad (3.31)$$

where  $a$  is the output of a fault location method,  $w$  is the weight to represent the accuracy (importance) of the method,  $g$  is the identity of the uninorm operator.

### 3.3.2.2.4 *Observations and Summary*

These transformation methods have two common properties. The first one is that they monotonically increase with respect to the output of a fault location method,  $a$ . This property guarantees that a larger output  $a$  will cause a larger effective value  $a'$ . The second property is that when the weight,  $w$ , is equal to 1, the effective value,  $a'$ , is equal to  $a$ .

To consider the different accuracy of three fault location methods, weights are assigned to these methods. However, these weights cannot be assigned arbitrarily, and the optimal weights need to be decided. In addition, one of the chosen aggregation operators, the OWA operator, has parameters  $W$ , which decides the behavior of the OWA operator. These parameters cannot be decided arbitrarily either.

In the fuzzy resolver design methodology, to determine the optimal weights of three fault location methods and the optimal parameters of the OWA operator, an optimization technique is needed. The optimal weights and parameters are selected which maximize

two objective functions. For this work, the training data set is used to illustrate the process for determining the optimal weights.

The objective of the first function is to maximize the number of fault cases whose actual faulted section has a possibility value equal or larger than a preset value. It is shown as (3.32) and (3.33).

$$\max_m \sum_{i=1}^N F_1(P_{fi}(W_m)) \quad (3.32)$$

$$F_1(P_{fi}(W_m)) = \begin{cases} 1, & \text{if } P_{fi}(W_m) \geq p_1 \\ 0, & \text{if } P_{fi}(W_m) < p_1 \end{cases} \quad (3.33)$$

where N is the number of total fault cases in the training set,  $P_{fi}$  is the actual faulted section's possibility value of the  $i^{\text{th}}$  fault case.  $p_1$  is a preset possibility value,  $W_m$  is the  $m^{\text{th}}$  set of weights  $\langle W_{ODIM}, W_{PS}, W_{FD} \rangle$ .

The objective of the second function is to maximize the number of non-faulted line sections whose possibility value is less than another preset value. In order to determine these optimal values, optimization methods are needed.

$$\max_n \sum_{k=1}^N F_2(P_{nfk}(W_n)) \quad (3.34)$$

$$F_2(P_{nfk}(W_n)) = \begin{cases} 0, & \text{if } P_{nfk}(W_n) \geq p_2 \\ 1, & \text{if } P_{nfk}(W_n) < p_2 \end{cases} \quad (3.35)$$

where S is the number of total non-faulted line sections in the training set,  $P_{nfk}$  is the  $k^{\text{th}}$  non-faulted section's possibility value.  $p_2$  is a preset possibility value,  $W_n$  is the  $n^{\text{th}}$  set of weights  $\langle W_{ODIM}, W_{PS}, W_{FD} \rangle$ .

### 3.3.3 Choice of Optimization Method

Optimization methods fall into three classes: calculus-based methods, enumerative methods, and guided random search methods. Calculus-based methods find optimal solutions to a problem based on the gradient of objective functions. All calculus-based methods can be divided into two groups: indirect methods and direct methods. Since the

gradient of objective functions at local extrema equals to zero, indirect methods find local extrema by solving a set of nonlinear equations resulting from setting the gradient of objective functions equal to zero. Direct methods choose a starting point and calculate the gradient of objective functions at the point. The gradient is used to guide the search to a new point. Then the methods calculate the gradient of objective functions at the new point that guides the search to another new point. The process keeps going until the gradient of the new point approaches zero. The success of the methods is heavily dependent on both the choice of the starting point and the convexity of objective functions. If objective functions are not convex and the choice of the starting point is not appropriate, the methods may not find the optimal solution. Usually, calculus-based methods are suitable for objective functions that are differentiable and only have one extremum [72],[73].

Enumerative methods search every point around the search space, one point at a time. These methods are easily implemented. The optimal solutions are obtained by comparing the objective function's values at all these points. However, these methods are good only when the search space is small. A significant computation burden may hinder the application of these techniques. For many applications, the search space is too large to use these methods.

Guided random search methods are stochastic search methods. Genetic algorithms consist of the major part of these methods. Genetic algorithms model the natural evolution process such as selection, mutation, and competition to find optimal solutions [74]-[76]. Compared with calculus-based techniques, genetic algorithms do not need objective functions to be differentiable. Hence, their application range is much broader. Further, genetic algorithms are global optimization methods and can be used to solve objective functions with more than one extremum.

The proposed objective functions shown in (3.32) and (3.34) are not differentiable. Hence, the calculus-based methods are not appropriate. The search space for the

importance factors is too large to use enumerative methods. Genetic algorithms fit the application due to their flexibility for expressing objective functions and ability to solve non-differentiable objective functions. Hence, genetic algorithms are used to determine the optimal weights and parameters.

### **3.3.4 Simulation Data**

In order to design a fuzzy resolver, data representing many distribution systems are needed to generalize the parameters/weights of the fuzzy resolver. Hence, data from several distribution feeders that can provide enough information to apply all three fault location methods are needed. These fault location methods use information, such as the feeder's topological data, the protective devices' placements and settings, and measurements at the substation. However, not all of this information was available to this dissertation author from the utilities. Therefore, no real data were used to design the fuzzy resolver. Simulated data was a feasible alternative, and a distribution feeder was modeled. Transient fault cases were then simulated on the feeder to generate the necessary data. Then, the three fault location methods were executed for the simulated fault cases to determine possibility values for all line sections. Lastly, the outputs of three methods were used in investigating the fuzzy resolver design methodology.

The IEEE Power Engineering Society Distribution Subcommittee published several distribution feeders with their configurations, parameters, and power flow results [77]. These feeders and their results provide a benchmark to which network power flow program developers can compare their results and verify the correctness of their programs. Of all these feeders, the IEEE 34 node test feeder was chosen as the modeled feeder because it is an actual feeder, and its size is moderate. The published feeders do not include the protective devices. However, a distribution feeder with correctly coordinated protective devices is needed for simulating realistic data. The appropriate protective devices and their settings were chosen using the load flow and short circuit analysis studies. In addition, the protective devices were modeled and incorporated into the

feeder's model. After modeling the IEEE 34 node test feeder, fault cases were simulated on this feeder. For each three-phase line section, ten types of faults were simulated. For each single-phase line section, only the phase to ground fault was simulated. For each type of fault at each line section, three fault resistance levels were used.

### **3.4 CHAPTER SUMMARY**

In this chapter, the new fault location scheme and three fault location methods were introduced. To develop a fuzzy resolver methodology, fuzzy aggregation operators were investigated, and three fuzzy aggregation operators were chosen to implement the fuzzy resolver methodology. The three fault location methods may have different accuracy. Weights were assigned to all fault location methods to take account of their different accuracy levels. The fuzzy resolver methodology has to determine the optimal weights and parameters. In addition, the OWA operator has parameters, and these parameters also need to be optimized. In order to optimize weights and parameters, two objective functions were proposed, and optimization methods to obtain these optimal values were chosen. To develop the fuzzy resolver methodology, field data for several feeders that can provide enough information so that all three fault location methods can be applied were needed. Since the needed information was not available from the utilities, field data cannot be used, and a distribution feeder needs to be modeled to generate the data. One of the published feeders was chosen.

## **CHAPTER IV**

### **SYSTEM MODELING AND SIMULATION**

#### **4.1 INTRODUCTION**

In the new fault location scheme developed in the Power System Automation Lab, there are three fault location methods. Each locates a fault and assigns a possibility value to each line section of a distribution feeder. A fuzzy resolver is developed to aggregate the three methods' outputs and assign a final possibility value for each line section. In order to design the fuzzy resolver, field data representing many distribution feeders are needed to generalize the parameters/weights of the fuzzy resolver. The fault location methods use data such as all line parameters, feeder's topological data, protective device placements and setting, etc. Since this information was not available to the author from the utilities, field data were not used to design the fuzzy resolver. A feasible choice was to model a feeder with coordinated protective devices and simulated various fault cases. The author modeled one of the IEEE distribution test feeders using SIMULINK and SimPowerSystems of MATLAB [78],[79]. Also appropriate time current characteristic (TCC) based protective devices were added to the model.

Commonly used protective devices in distribution systems are fuses, reclosers, and circuit breakers [80]. Fuses are devices that will blow (i.e., open) within a specific time after a fault happens. In order to restore the power supply, repair crews need to replace the blown fuse. Reclosers and circuit breakers have the capability to trip and reclose a circuit during a fault. After a fault happens, they will trip to interrupt the fault. After several seconds, they can reclose and try to restore the power supply. If it is temporary, the fault is gone during outage time, and the power supply is restored when the protective device recloses. By using protective devices with the reclosing capability, outage time is reduced and the reliability of distribution systems is improved. However, reclosers and circuit breakers are more expensive than fuses.



## 4.2 MODELING THE IEEE 34 NODE TEST FEEDER WITH PROTECTIVE DEVICES

### 4.2.1 34 Node Test Feeder Model

The IEEE Power System Society distribution subcommittee published several distribution test feeders with their configurations, parameters, and power flow results [77]. These feeders and their results provide a benchmark to which network power flow program developers can compare their results and verify the correctness of their programs. The IEEE 34 node test feeder was modeled for this work because it is based on a real feeder, and its size is moderate. The configurations and parameters of these published feeders were downloaded from the website at <http://ewh.ieee.org/soc/pes/dsacom/testfeeders.html>. A figure of this feeder is shown as Figure 4.1; the feeder parameters that were used in this work are listed in Appendix A.

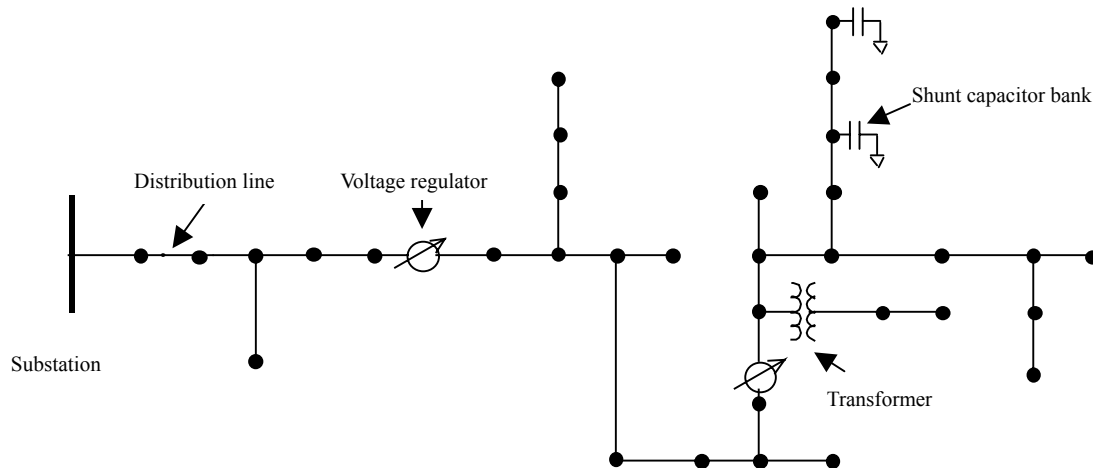


Figure 4.1 IEEE 34 node test feeder

## 4.2.2 Component Models

The feeder was modeled using SIMULINK and SimPowerSystems of MATLAB [78],[79]. The voltage level of the substation is 24.9 kV, and the capacity of the substation transformer is 2500 kVA. In the IEEE 34 node test feeder, there are 32 line segments, five different overhead line configurations, two transformers, two shunt capacitor banks, two voltage regulators, six spot loads, and nineteen distributed loads. The models developed for these components are described in the following sections.

### 4.2.2.1 Shunt Capacitor Models

The three-phase parallel RLC model was used to model the shunt capacitors given in Appendix A.6. The values of these capacitors were calculated as (4.1), where  $Q$  is each phase's rated kVar,  $\omega=120\pi$ , and  $U$  is the rated phase to ground voltage. The  $Q$  values used are given in Appendix A.6.

$$C = Q/(\omega U^2) \quad (4.1)$$

### 4.2.2.2 Transformer Models

There were two transformers in this feeder. One was at the substation, and the other was within the feeder. The one at the substation was modeled as the internal impedance of an infinite voltage source. The source's internal voltage was equal to 1.05 multiple of the substation transformer's secondary side voltage, which is given in Appendix A.3 and equal to 24.9 kV. The internal impedance of the source was set equal to the transformer's impedance, which was  $0.01+j0.08$  pu. The 3-phase infinite voltage source model was used to model the feeder source. The in-line transformer within the feeder was a two winding transformer. The three-phase two winding transformer model was used to model it. The primary side voltage and secondary side voltage are given in Appendix A.3. One half of the transformer impedance,  $0.95+j2.04$  pu, was put at the primary side, and the other half was put at the secondary side.

### 4.2.2.3 Voltage Regulator Models

There were two regulators in the feeder, which are used to step up voltages. However, SimPowerSystems does not have a regulator component model in its library. Therefore, the regulators were implemented using three single-phase wye connected linear transformers. The primary side voltages were set equal to the regulator's input voltages, while the secondary side voltages were set equal to the regulator's output voltages. The input and output voltages of the regulators were utilized from Kersting's load flow result at <http://ewh.ieee.org/soc/pes/dsacom/testfeeders.html> and given in Appendix A.9. Other parameters were chosen so that the series impedance of these single-phase transformers was close to zero, while the magnetization resistance and reactance were very large. To achieve this purpose, the power of these transformers was set to 100kVA; the series resistance and reactance of these single-phase transformers were set to  $10^{-6}$ pu; the magnetization resistance and reactance were set to 5000pu.

### 4.2.2.4 Line Models

Since the feeder has short line segments, the lumped pi model was used to model all line segments.

#### 4.2.2.4.1 Three-phase Line Models

For three-phase lines, the three-phase transmission line pi section was used to model most of the lines. For this model, the positive sequence and zero sequence of line segments were needed. The sequence transformation mentioned as shown in (4.2)-(4.4) [81] was used to obtain the positive and zero sequence impedances and shunt capacitance. The line impedances and shunt capacitances are given in Appendix A.8. The obtained positive and zero sequence impedances and shunt capacitance were used as the parameters of the three-phase transmission line pi section. When a line is connected to a protective device, the three-phase transmission line pi section cannot be used to model it due to numerical oscillation. The reason is that when the protective device is closed, there

are two capacitors in parallel through a small resistance (typically 0.01 ohm) if the three-phase transmission line pi section was used to model lines connecting the protective device, so the two states (capacitors' voltages) are almost the same. If they are exactly the same, it is impossible to formulate state equations in SimPowerSystems. For the situation where a low resistance connects two pi models, it is possible to formulate state equations but this situation will lead to numerical oscillations in the currents passing through the protective device. For this situation, the author developed a different model, the three-phase T-line. A figure of the three-phase T-line model is shown as Figure 4.2. This model uses the same parameters as the three-phase transmission line pi section, which is the sequence impedance and shunt capacitance of a line segment.

$$Z_{seq} = A^{-1}ZA \quad (4.2)$$

$$A = \begin{bmatrix} 1 & 1 & 1 \\ 1 & \alpha^2 & \alpha \\ 1 & \alpha & \alpha^2 \end{bmatrix} \quad (4.3)$$

$$\alpha = e^{j2\pi/3} \quad (4.4)$$

An example is used to illustrate how parameters for a T-line model as shown in Figure 4.2 were calculated. For a line section with the length of  $l$  miles, its per mile sequence impedance is  $[z_1, z_0]$ , and its per mile sequence admittance is  $[y_1, y_0]$ , where 1 represents the positive sequence and 0 represents the zero sequence. The parameters in Figure 4.2 are calculated using (4.5)-(4.15), where  $\text{imag}(\cdot)$  is the imaginary part of a number,  $\sinh(\cdot)$  is a hyperbolic sine function,  $\tanh(\cdot)$  is hyperbolic tangent function, and  $\omega=120\pi$ .

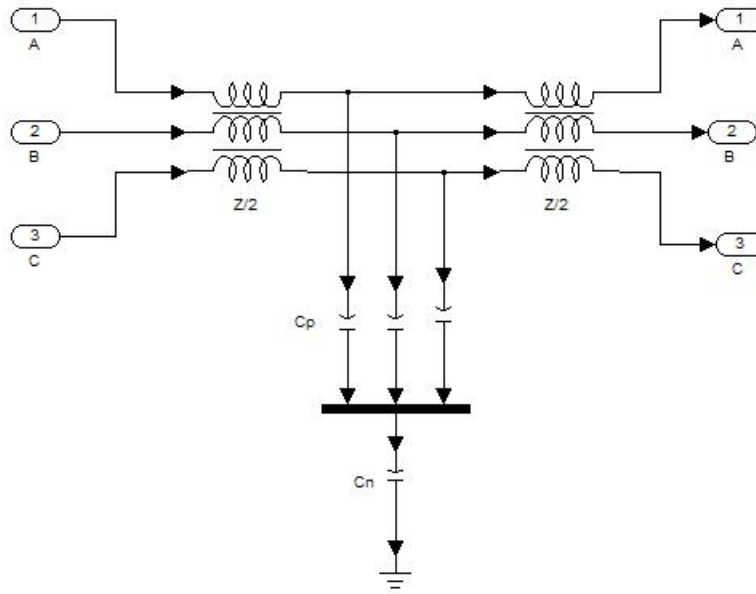


Figure 4.2 Three-phase T-line

$$z_{ser1} = \sinh(\sqrt{z_1 y_1} l) \times \sqrt{\frac{z_1}{y_1}} \quad (4.5)$$

$$y_{sh1} = \frac{\tanh\left(\frac{1}{2} \times \sqrt{z_1 y_1} l\right)}{\sqrt{\frac{z_1}{y_1}}} \quad (4.6)$$

$$z_{ser0} = \sinh(\sqrt{z_0 y_0} l) \times \sqrt{\frac{z_0}{y_0}} \quad (4.7)$$

$$y_{sh0} = \frac{\tanh\left(\frac{1}{2} \times \sqrt{z_0 y_0} l\right)}{\sqrt{\frac{z_0}{y_0}}} \quad (4.8)$$

$$Z_s = (2 \times z_{ser1} + z_{ser0}) / 3 \quad (4.9)$$

$$Z_m = (z_{ser0} - z_{ser1}) / 3 \quad (4.10)$$

$$Z = [Z_s \ Z_m] \quad (4.11)$$

$$C_1 = \text{imag}(y_{sh1}) / \omega \quad (4.12)$$

$$C_0 = \text{imag}(y_{sh0}) / \omega \quad (4.13)$$

$$C_p = C_1 \quad (4.14)$$

$$C_n = 3 \times C_1 \times C_0 / (C_1 - C_0) \quad (4.15)$$

#### 4.2.2.4.2 Single-phase Line Models

The pi section model was used to implement single-phase lines. In order to overcome the numerical oscillation problem mentioned in 4.2.2.1, the author developed the single-phase T-line model for a line that connects a protective device. The inside of the single-phase T-line model is shown as Figure 4.3. Its parameters are the same as the pi section model, and these parameters are given in Appendix A.8. For a line section with the length of  $l$  miles, its per mile impedance is  $z$ , and its per mile admittance is  $y$ .  $Z$  in Figure 4.3 is computed by  $zl$ , and  $C$  in Figure 4.3 is computed by  $y/\omega$ , where  $\omega=120\pi$ .

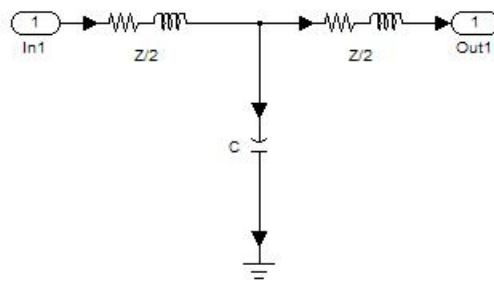
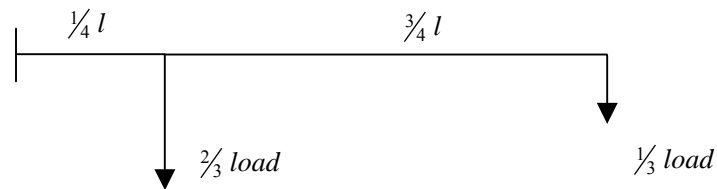


Figure 4.3 Single-phase T-line

#### 4.2.2.5 Load Models

There were two kinds of loads in the feeder model. One was the spot load, and the other was the distributed load. Spot loads were put at the nodes where loads were connected. Distributed loads were modeled using the exact lumped load model shown in Figure 4.4 [67]. That is,  $2/3$  of a distributed load was put at  $1/4$  the length of the line, and the other  $1/3$  of the distributed load was put at the end of the line. This exact lumped line model will give correct computation results for the voltage drop and the power loss down the line [67]. The series RLC load model in SimPowerSystems was used as the building block to model all loads. This model uses the voltage magnitude, active power, and reactive power as the parameters.

For both spot loads and distributed loads, there were three types: constant impedance loads, constant power loads, and constant current loads. In the following sections, the author will discuss the parameter calculations used for constant impedance loads, constant power loads, and constant current loads, respectively.



$l$ =length of a line

Figure 4.4 Exact lumped load model

##### 4.2.2.5.1 Constant Impedance Loads

The series RLC load model in SimPowerSystems was used to model constant impedance loads. For constant impedance loads, the nominal voltage was set as the

system rated voltage. For wye connected loads, the rated line to ground voltage was  $24.9 \text{ kV}/\sqrt{3}=14.38 \text{ kV}$  for loads connected upstream of the primary side of the in-line transformer, and  $4.16 \text{ kV}/\sqrt{3}=2.4 \text{ kV}$  for loads connected downstream of the secondary side of the in-line transformer. For delta connected loads, the rated phase to phase voltage was  $24.9 \text{ kV}$  for loads connected upstream of the primary side of the in-line transformer and  $4.16 \text{ kV}$  for loads connected downstream of the secondary side of the in-line transformer. The power values are given in Appendix A.4 and Appendix A.5.

#### 4.2.2.5.2 *Constant Power Loads*

In SimPowerSystems, there is no constant power load model. Therefore, this type of load was also developed using the series RLC load. Since this model was a constant impedance model, its parameters were modified for constant power loads. The power values of constant power loads specified in the IEEE 34 node test feeder are under the system rated voltage. Since the constant impedance load model was used to model a constant power load, to keep the power value as the specified value under the steady state condition, the voltage should be equal to the steady state voltage values of the nodes where the constant power load was connected. For example, there was a constant power load connected at node 860 in the IEEE 34 node test feeder, and the three-phase load was wye connected. For each phase, the active power and reactive power were given as 20 kW and 16 kVar, respectively. Using Kersting's load flow results [93], it was found that the phase A voltage at node 860 was 1.0305 pu. When calculating phase A load values for a wye connected three phase load, the voltage was modified to  $1.0305 \times 24.9/\sqrt{3}=14.8145 \text{ kV}$ , rather than  $1.0 \times 24.9/\sqrt{3}=14.38 \text{ kV}$ . The active power and reactive power were still set as 20 kW and 16 kVar.

This modeling method does not really implement a constant power load. It only guaranteed the load's power was equal to the specified values given in Appendix A.4 and Appendix A.5 under steady state.



#### 4.2.2.5.3 *Constant Current Loads*

The constant current load was also developed using the series RLC load with modified parameters. The voltage was modified as the constant power load; that is, the steady state voltage values gotten from Kersting's load flow results were used as the input voltage for constant current loads. In addition, the power value of a constant current load also needs to be modified in order to keep currents as the specified value under steady state. Since the current magnitude should be kept at the specified value, the power value was set proportional to the voltage. An example is used to demonstrate how these parameters were modified. A constant current load connected at node 840 was wye connected. The steady state voltage value of phase A was 1.0303. When calculating the voltage value in the load model, the phase A nominal voltage was  $1.0303 \times 24.9 / \sqrt{3} = 14.8116$  kV. The active power and reactive power of the load were 9 kW and 7 kVar, respectively. To keep currents as the specified values under steady state condition, the active power was modified to  $9 \times 1.0303 = 9.2727$  kW, and the reactive power was modified to  $7 \times 1.0303 = 7.2121$  kVar.

This modeling method does not really implement constant current loads. It only guaranteed the load's current was set equal to the specified value given in Appendix A.4 and Appendix A.5 under steady state.

#### 4.2.2.6 *Protective Device Selection*

It is very common to install a fuse at each lateral while a recloser or a circuit breaker with reclosing relays is put at the main feeder in order to reduce the number and duration of service interruptions due to temporary faults [78]. Based on the protection scheme discussed in [78], the author put a recloser at the substation to protect the main feeder, and put fuses at all laterals. The protection scheme is shown as Figure 4.5.

Load flow and short circuit analysis studies were implemented using software named WindMil [94] to select the appropriate ratings and settings for the protective devices. The calculated maximum load currents, minimum fault currents that are obtained when a

single phase fault with  $40 \Omega$  fault resistance occurs, and maximum fault currents of selected line segments are shown in Table 4.1. Based on these load currents and fault currents, protective devices were chosen [95]. For fuses, their rating must be equal to or greater than the maximum load [83]. The chosen protective devices are listed in Table 4.2.

After the chosen protective devices were put into the feeder model, coordination studies were performed using WindMil to ensure that these chosen protective devices were coordinated correctly. Coordination between different protective devices is necessary to reduce the outage area during faults in a distribution feeder.

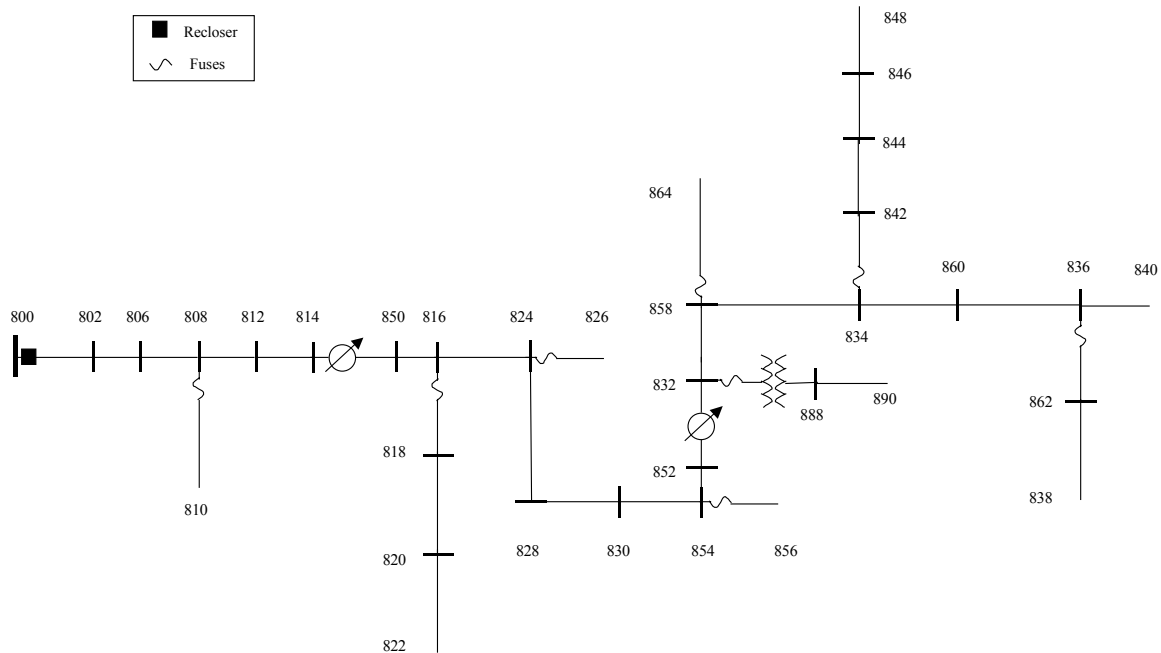


Figure 4.5 IEEE 34 node test feeder with added protective devices

#### 4.2.2.7 Protective Device Models

There is only one switch model in SimPowerSystems (i.e., the circuit breaker model) and it operates at a specified time or is controlled by an external signal. However, in the author's protective device scheme, the feeder was protected by several correctly coordinated protective devices that operate according to their TCC curves. The control logic was implemented for these protective devices to compute their operational status based on their TCC curves. The settings for the devices are given in Appendix A.10.

TABLE 4.1 LOADS AND FAULT CURRENTS FOR SELECTED LINE SEGMENTS

Start Node	End Node	Max. Load Current (A)	Min. Fault Current (A)	Max. Fault Current (A)
800	802	51.80	48	719
808	810	1.22	229	527
816	822	12.91	119	335
824	826	3.10	161	313
854	856	0.31	129	273
832	888	11.71	48	223
858	864	0.14	123	218
834	842	16.37	118	212
836	862	2.08	117	207

TABLE 4.2 CHOSEN PROTECTIVE DEVICES

Start Node	End Node	Type	Rating
800	802	Recloser	50H
808	810	Fuse	2T
816	822	Fuse	15T
824	826	Fuse	5QA
854	856	Fuse	1T
832	888	Fuse	12T
858	864	Fuse	1T
834	842	Fuse	20K
836	862	Fuse	3T

The structure of the protective device model is shown as Figure 4.6. The control logic determines the open time of a protective device according to its TCC curve and sends the open signal to the switch that opens the circuit. If the protective device is a reclosing device, the operation logic also sends the reclosing signal to the switch when the reclosing time is reached. This protective device model was connected in series within the feeder model. In the figure,  $I_{in}$  is a current flowing in the model. To simulate TCC-based protective devices, the control logic to determine the control signal status is the key element. In the feeder model, fuses and three-phase reclosers were used as protective devices. In the following sections, the author will introduce the control logic developed for fuses and reclosers, respectively.

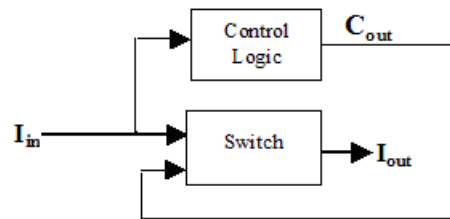


Figure 4.6 Structure of a protective device

#### 4.2.2.7.1 Control Logic of Fuses

The structure of the control logic developed for fuses is shown in Figure 4.7. It consists of six blocks: filter, A/D converter, magnitude/angle computation, comparator, RMS calculation, and control signal determination. For each type of protective device, all blocks are the same except the control signal determination block.

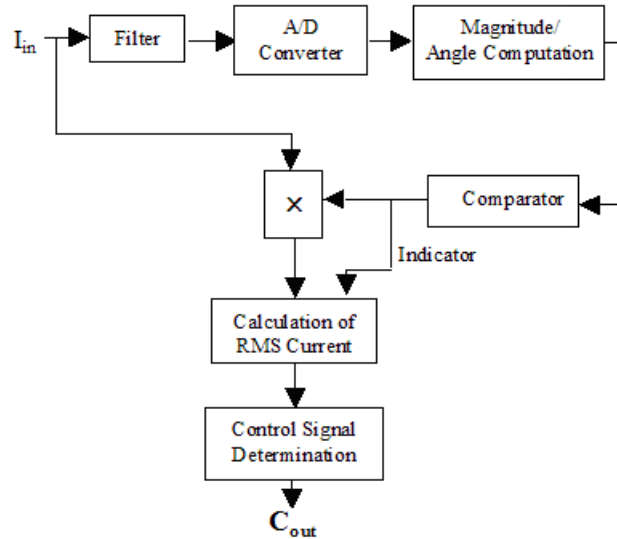


Figure 4.7 Structure of the control logic block of fuses

Current signals first go through an anti-alias filter to avoid aliasing. The cutoff frequency of the filter was specified as less than half of the sample rate of the A/D converter. Then the A/D converter digitizes the filtered signals at the user-specified sampling rate.

After that, the magnitude/angle computation block performs a DFT (Discrete Fourier Transform) on the digital signal. It estimates the fundamental frequency (60Hz) component's magnitude and phase angle of the current. The input to the comparator block is the fundamental frequency component's magnitude. This block compares the magnitude with the pickup value of a protective device. If the magnitude is larger than the pickup value, the block outputs a value of one; otherwise, it outputs a value of zero. For example, in the situation where a fuse is the primary protective device and a recloser is its secondary device, if a fault is located downstream of the fuse, the recloser will trip once (this number is specified according to the setting of the recloser) and then the fuse will burn. In such a situation, the block outputs a rectangle waveform as shown in Figure 4.8. This output has two functions. First, it is multiplied by the input current signal so that

if the fundamental frequency component's magnitude of the current is larger than the protective device's pickup value, it is passed to the RMS calculation block. Otherwise, a value of zero is passed to the RMS calculation block. Second, the output itself is one of the inputs of the RMS calculation block serving as an indicator.

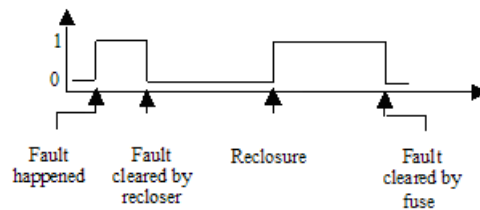


Figure 4.8 Output of the comparator

As shown in Figure 4.7, the RMS calculation block has two inputs: one is the product of the current signal (SIMULINK signal) and the output of the comparator, and the other is the comparator's output. The second input is the indicator that informs the block when it should reset the calculation. If a fault happens, the block will find a step up change in the indicator and at every time step calculate the fault RMS current value and the time duration, which is from the fault occurrence time to the present time. If a protective device clears the fault, the block will notice the step down change in the indicator and continuously calculate the RMS current value (zero) and the time duration, which is from the fault clearing time to the present time. The time is the protective device's open time and is used to determine when the device needs to reclose if the device is a reclosing device. The outputs of this block are the RMS current value and the time duration.

The control signal determination block is implemented by S-functions (a powerful mechanism provided by SIMULINK), which is “a computer language description of a SIMULINK block” [82]. It is used to simulate the control logic determination process of

fuses. This block has two inputs: one is the RMS current value and the other one is the time duration during which the RMS current value is calculated.

The flowchart of the block is shown in Figure 4.9. The control signal status is checked first. If the control signal status is zero, it means that the block did not send an open signal to the switch box at a previous time step, and the program will call the open decision function, which determines if the switch should open by comparing the fault time duration with the operating time of a specific fuse's TCC curve at the fault current. The comparison method is shown in Figure 4.10. If the fault duration is larger than the operating time, the open decision function will set the control signal status to one to inform the switch to open. Otherwise the function will set the control signal status to zero, and the switch remains closed. Then the simulation time increases one time step, and another loop begins. If the control signal status is one, it means this determination block has already sent an open signal to the switch at a previous time step. Since fuses are non-reclosing devices, no action is required. The simulation time increases one time step, and another loop begins.

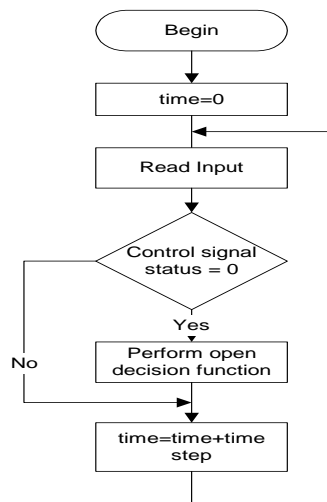


Figure 4.9 Flowchart of the control signal determination block of fuses

The above paragraphs described how to model a single-phase fuse. For a three-phase line, three single-phase fuses were used to protect it.

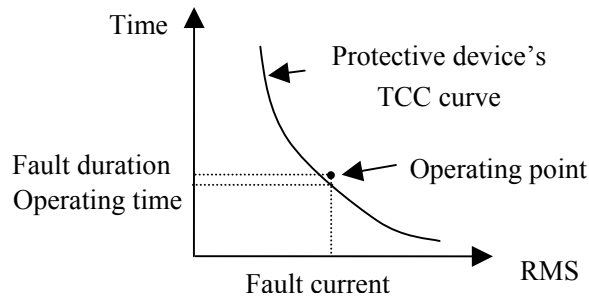


Figure 4.10 Illustration of the comparison between fault duration and operating time

#### 4.2.2.7.2 Control Logic of Three-phase Reclosers

The structure of the control logic of three-phase reclosers is shown in Figure 4.11. The first five blocks--filter, A/D converter, magnitude/angle computation, comparator, and RMS calculation--are the same as the control logic of fuses. The only different block is the control signal determination block. In the following paragraph, the control signal determination block of three-phase reclosers is discussed.

The block has six inputs. They are the RMS current values for three phases and the time durations during which the RMS current values are calculated. The flowchart of the block is shown in Figure 4.12. First the program checks if the control signal status is zero. If the control signal status is zero, it means that the logic did not send a signal to open the switch at a previous step. Then the open decision function is called to determine if the switch should open according to the RMS current values, time durations, and the recloser's TCC curve. The open decision function is very similar to the open decision



function of fuses. However, this function checks the RMS currents and time durations of all three phases. If any of these time durations is larger than the recloser's operating time, the open decision function will set the control signal status to one to instruct the switch to open. Otherwise the function will set the control signal status to zero, and the switch will remain closed. If the control signal status is one, the circuit open status will be checked. The control signal status and circuit open status are different. The control signal status determines if the open decision function sent an open signal to the switch to open it at a previous time step. Since the switch model in SimPowerSystems opens at the zero crossing point of the current, the control signal status equal to one does not mean that the switch has already opened. The circuit open status is used to determine if the switch opened, and it will not be set to one until the RMS currents through the switch is equal to zero.

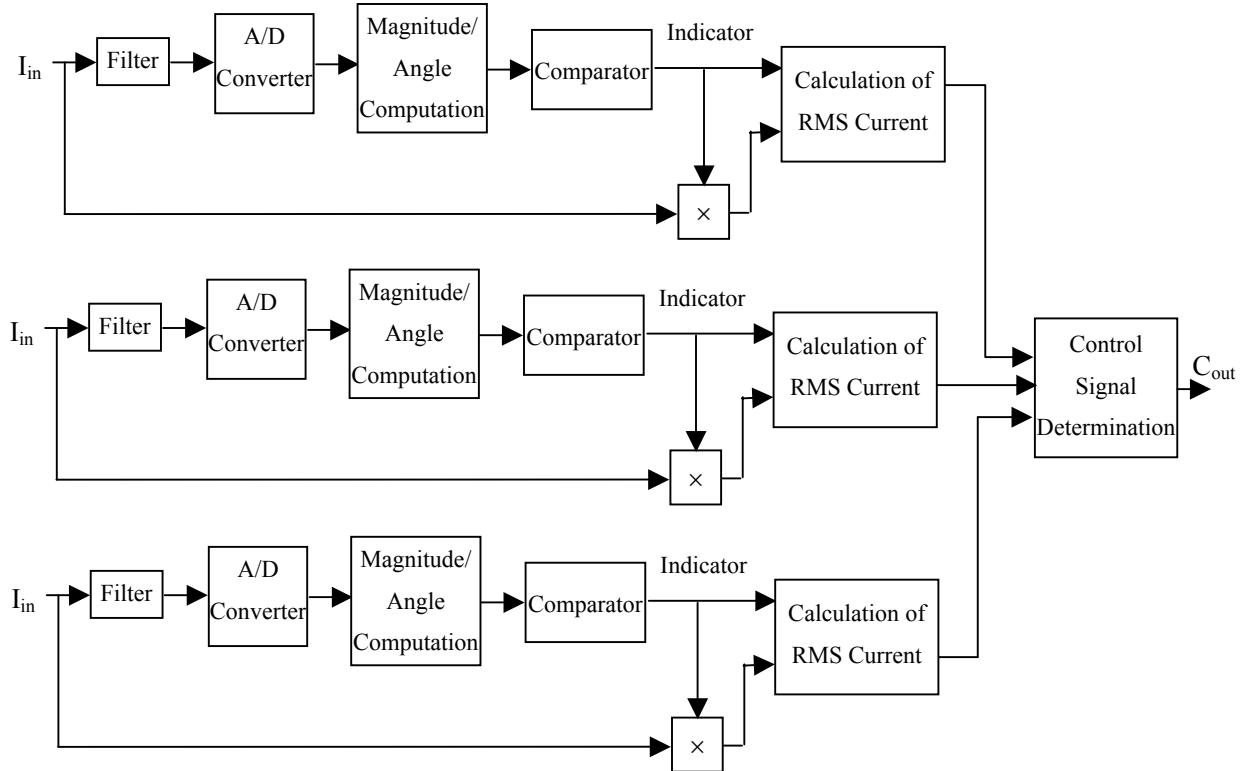


Figure 4.11 Structure of the control logic block of three-phase reclosers

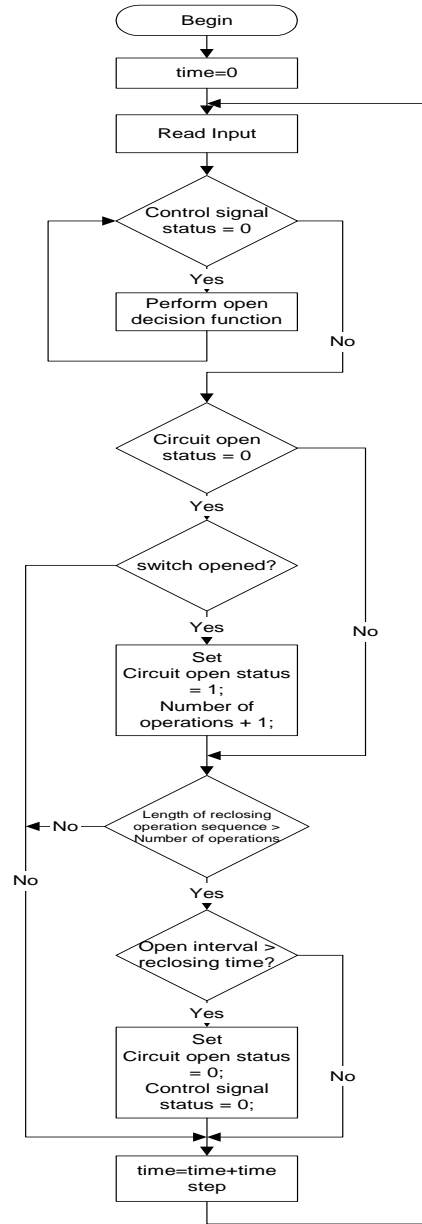


Figure 4.12 Flowchart of the control signal determination block of three-phase reclosers

If the circuit open status is equal to zero, the program will check the RMS currents through the switch to see if the switch opened. If the switch did not open, the simulation time increases one time step, and a new loop begins. If the switch opened, the circuit open status will be set to one, and the number of operations will increase by one. The number of operations is used to determine if a recloser has finished its operation sequence.

If the circuit open status is equal to one, the program checks if the number of operations is larger than the number of a recloser's operation sequence. If yes, it means that the recloser has already finished its operation sequence and locked out. There is nothing to do, and the simulation time increases one time step. Otherwise, the program compares the open time, which is obtained from the RMS calculation block, with the recloser's settings to see if the open time is larger than the time setting. If no, the simulation time increases one time step, and a new loop begins. If yes, the control signal status and circuit open status are set to zero, and the switch closes immediately once the control signal status is set to zero.

### **4.2.3 Feeder Model**

After developing models for all components, the IEEE 34 node test feeder was developed by connecting the component's models mentioned before. Each line segment was split at its midpoint to simulate faults at the middle point of line segments. A three-phase fault model (SimPowerSystems built-in module) was inserted in the feeder model to model faults on the feeder.

According to [78], a substation feeder recloser is typically set with an operating sequence of one fast and two delay tripping operations. The author set the recloser's operation curves as [FSS], where F represents the recloser's instantaneous curve, and S represents the recloser's time delay curve. The reclosing time was set as 1 second based on [84]. All protective device's settings are given in Appendix A.10.

## **4.3 COMPARISON OF STEADY STATE SIMULATED RESULTS WITH IEEE PUBLISHED RESULTS**

The steady state result of the simulated feeder model was compared with the IEEE published results [93]. The comparison results of node voltages are listed in Table 4.3, and the comparison results of line currents are listed in Table 4.4. From Table 4.3, it is found that all voltage errors were less than 1% except phase B voltage at node 890, which is 1.5%. From Table 4.4, it is found that most current errors were less than 2.5%.

TABLE 4.3 COMPARISON OF NODE PHASE VOLTAGES

	V(pu/degree)						V(pu/degree, IEEE)						Error (%)		
	A		B		C		A		B		C		A	B	C
	Mag.	Ang.	Mag.	Ang.	Mag.	Ang.	Mag.	Ang.	Mag.	Ang.	Mag.	Ang.			
800	1.0497	0.00	1.0497	-120.00	1.0497	120.00	1.0500	0.00	1.0500	-120.00	1.0500	120.00	0.032	0.032	0.032
802	1.0476	-0.05	1.0483	-120.06	1.0483	119.95	1.0475	-0.05	1.0484	-120.07	1.0484	119.95	0.007	0.012	0.012
806	1.0462	-0.09	1.0469	-120.11	1.0476	119.92	1.0457	-0.08	1.0474	-120.11	1.0474	119.92	0.047	0.049	0.017
808	1.0149	-0.8	1.0274	-120.91	1.0274	119.31	1.0136	-0.75	1.0296	-120.95	1.0289	119.30	0.127	0.213	0.058
810			1.0274	-120.91					1.0294	-120.95				0.194	
812	0.9780	-1.67	1.0058	-121.84	1.0079	118.61	0.9763	-1.57	1.0100	-121.92	1.0069	118.59	0.247	0.412	0.102
814	0.9495	-2.4	0.9885	-122.59	0.9912	118.04	0.9467	-2.26	0.9945	-122.7	0.9893	118.01	0.296	0.608	0.195
850	1.0204	-2.4	1.0198	-122.59	1.0218	118.04	1.0176	-2.26	1.0255	-122.7	1.0203	118.01	0.348	0.560	0.151
816	1.0204	-2.41	1.0198	-122.6	1.0218	118.03	1.0172	-2.26	1.0253	-122.71	1.0200	118.01	0.319	0.609	0.180
818	1.0198	-2.41					1.0163	-2.27					0.340		
820	0.9961	-2.47					0.9962	-2.32					0.010		
822	0.9926	-2.47					0.9895	-2.33					0.386		
824	1.0114	-2.53	1.0093	-122.81	1.0135	117.79	1.0082	-2.37	1.0158	-122.94	1.0116	117.76	0.387	0.638	0.187
826			1.0093	-122.81					1.0156	-122.94				0.618	
828	1.0107	-2.54	1.0086	-122.83	1.0128	117.77	1.0074	-2.38	1.0151	-122.95	1.0109	117.75	0.398	0.638	0.188
830	0.9933	-2.82	0.9912	-123.25	0.9961	117.27	0.9894	-2.63	0.9982	-123.39	0.9938	117.25	0.396	0.698	0.232
854	0.9926	-2.83	0.9905	-123.26	0.9954	117.26	0.989	-2.64	0.9978	-123.40	0.9934	117.24	0.437	0.728	0.202
852	0.9627	-3.35	0.9592	-124.02	0.9662	116.36	0.9581	-3.11	0.9680	-124.18	0.9637	116.33	0.554	0.905	0.259
832	1.0413	-3.35	1.0253	-124.02	1.0385	116.36	1.0359	-3.11	1.0345	-124.18	1.036	116.33	0.523	0.888	0.245
858	1.0392	-3.41	1.0225	-124.11	1.0364	116.25	1.0336	-3.17	1.0322	-124.28	1.0338	116.22	0.545	0.936	0.256
834	1.0364	-3.48	1.0198	-124.22	1.0344	116.12	1.0309	-3.24	1.0295	-124.39	1.0313	116.09	0.538	0.947	0.297
842	1.0364	-3.49	1.0198	-124.23	1.0344	116.12	1.0309	-3.25	1.0294	-124.39	1.0313	116.09	0.538	0.937	0.297
844	1.0364	-3.51	1.0198	-124.25	1.0337	116.09	1.0307	-3.27	1.0291	-124.42	1.0311	116.06	0.558	0.908	0.249
846	1.0364	-3.55	1.0198	-124.30	1.0344	116.04	1.0309	-3.32	1.0291	-124.46	1.0313	116.01	0.538	0.908	0.297

TABLE 4.3 CONTINUED

	V(pu/degree)						V(pu/degree, IEEE)						Error (%)		
	A		B		C		A		B		C		A	B	C
	Mag.	Ang.	Mag.	Ang.	Mag.	Ang.	Mag.	Ang.	Mag.	Ang.	Mag.	Ang.			
848	1.0364	-3.56	1.0198	-124.31	1.0344	116.03	1.0310	-3.32	1.0291	-124.47	1.0314	116.00	0.528	0.908	0.287
860	1.0358	-3.48	1.0198	-124.22	1.0337	116.12	1.0305	-3.24	1.0291	-124.39	1.0310	116.09	0.577	0.908	0.259
836	1.0358	-3.48	1.0191	-124.22	1.0337	116.12	1.0303	-3.23	1.0287	-124.39	1.0308	116.09	0.529	0.937	0.278
840	1.0358	-3.48	1.0191	-124.22	1.0337	116.12	1.0303	-3.23	1.0287	-124.39	1.0308	116.09	0.529	0.937	0.278
862	1.0358	-3.48	1.0191	-124.22	1.0337	116.13	1.0303	-3.23	1.0287	-124.39	1.0308	116.09	0.529	0.937	0.278
838			1.0191	-124.22					1.0285	-124.39				0.918	
864	1.0392	-3.41					1.0336	-3.17					0.545		
888	1.0047	-4.87	0.9893	-125.56	1.0030	114.82	0.9996	-4.64	0.9983	-125.73	1.0000	114.82	0.507	0.905	0.301
890	0.9239	-5.64	0.9097	-126.37	0.9235	114.00	0.9167	-5.19	0.9235	-126.78	0.9177	113.98	0.831	1.490	0.630
856			0.9905	-123.27					0.9977	-123.41				0.718	

TABLE 4.4 COMPARISON OF LINE SEGMENT CURRENTS

From	To	Current (A/degree)						Current (A/degree, IEEE)						Error (%)		
		A		B		C		A		B		C		A	B	C
		Mag.	Ang.	Mag.	Ang.	Mag.	Ang.	Mag.	Ang.	Mag.	Ang.	Mag.	Ang.			
800	802	52.10	-13.18	43.77	-127.67	41.37	118.01	51.56	-12.74	44.57	-127.70	40.92	117.37	1.047	1.795	1.100
802	806	52.11	-13.23	43.78	-127.73	41.38	117.95	51.58	-12.80	44.57	-127.76	40.93	117.31	1.028	1.772	1.100
806	808	52.12	-13.26	41.68	-126.78	39.70	119.16	51.59	-12.83	42.47	-126.83	39.24	118.52	1.027	1.860	1.172
808	812	52.24	-13.85	40.59	-127.04	39.70	118.35	51.76	-13.47	41.30	-127.10	39.28	117.76	0.927	1.719	1.069
808	810			1.21	-144.57					1.22	-144.62				0.574	
812	814	52.38	-14.53	40.66	-127.93	39.71	117.43	51.95	-14.18	41.29	-127.99	39.33	116.90	0.828	1.526	0.966
814	850	52.49	-15.04	40.71	-128.63	39.72	116.72	52.10	-14.73	41.29	-128.69	39.37	116.23	0.749	1.405	0.889

TABLE 4.4 CONTINUED

From	To	Current (A/degree)						Current (A/degree, IEEE)						Error (%)		
		A		B		C		A		B		C		A	B	C
		Mag.	Ang.	Mag.	Ang.	Mag.	Ang.	Mag.	Ang.	Mag.	Ang.	Mag.	Ang.			
850	816	48.81	-15.03	39.46	-128.61	38.50	116.74	48.47	-14.73	40.04	-128.69	38.17	116.23	0.701	1.449	0.865
816	818	13.01	-26.83					13.02	-26.69					0.077		
816	824	36.18	-10.82	39.47	-128.62	38.50	116.73	35.83	-10.42	40.04	-128.70	38.17	116.23	0.977	1.424	0.865
818	820	13.02	-26.91					13.03	-26.77					0.077		
820	822	10.59	-29.13					10.62	-28.98					0.282		
824	826			3.08	-148.79					3.10	-148.92				0.774	
824	828	36.20	-11.08	36.40	-127.29	38.37	116.73	35.87	-10.70	36.93	-127.39	38.05	116.25	0.920	1.435	0.841
828	830	36.20	-11.11	36.40	-127.31	38.09	116.91	35.87	-10.72	36.93	-127.41	37.77	116.42	0.920	1.435	0.847
830	854	34.52	-10.34	35.71	-127.37	36.78	116.72	34.22	-9.97	36.19	-127.47	36.49	116.26	0.877	1.326	0.795
854	852	34.52	-10.35	35.44	-127.62	36.78	116.71	34.23	-9.99	35.93	-127.72	36.49	116.25	0.847	1.364	0.795
854	856			0.30	-98.55					0.31	-98.70				1.677	
852	832	34.60	-11.31	35.49	-128.55	36.79	115.81	34.35	-11.00	35.90	-128.66	36.52	115.41	0.728	1.142	0.739
832	Xfrm	11.77	-32.64	11.64	-152.91	11.66	87.77	11.68	-32.29	11.70	-152.73	11.61	87.39	0.771	0.513	0.431
832	858	21.45	0.24	23.09	-116.51	24.54	128.74	21.31	0.47	23.40	-116.89	24.34	128.36	0.657	1.325	0.822
858	834	20.86	0.80	22.84	-116.01	24.21	128.86	20.73	1.01	23.13	-116.39	24.02	128.48	0.627	1.254	0.791
858	864	0.14	-23.05					0.14	-22.82					2.643		
834	860	11.22	-43.21	8.90	-154.38	10.67	100.24	11.16	-43.05	9.09	-154.82	10.60	99.34	0.538	2.101	0.660
834	842	14.83	34.42	16.14	-95.50	15.17	151.12	14.75	34.68	16.30	-95.63	15.12	151.05	0.542	0.982	0.331
842	844	14.83	34.41	16.13	-95.51	15.17	151.11	14.74	34.67	16.30	-95.64	15.12	151.03	0.611	1.043	0.331
844	846	9.88	78.61	9.29	-63.73	9.44	-170.61	9.83	78.88	9.40	-63.87	9.40	-170.67	0.539	1.128	0.426
846	848	9.82	78.56	9.30	-52.42	9.82	-161.87	9.76	78.80	9.40	-52.54	9.78	-161.93	0.645	1.074	0.409
860	836	4.18	-30.33	5.79	-154.00	3.61	92.76	4.16	-30.19	5.96	-154.63	3.60	90.25	0.505	2.819	0.250
836	840	1.50	-20.34	2.19	-149.92	1.71	72.94	1.50	-20.01	2.33	-151.97	1.75	68.00	0.133	5.966	2.514
836	862			2.07	-149.22					2.09	-149.38				0.957	

TABLE 4.4 CONTINUED

		Current (A/degree)						Current (A/degree, IEEE)						Error (%)		
From	To	A		B		C		A		B		C		A	B	C
		Mag.	Ang.	Mag.	Ang.	Mag.	Ang.	Mag.	Ang.	Mag.	Ang.	Mag.	Ang.			
862	838			2.07	-149.34					2.09	-149.50				0.861	
888	890	70.27	-32.59	69.50	-152.86	69.60	87.82	69.90	-32.29	70.04	-152.73	69.50	87.39	0.529	0.771	0.144

#### 4.4 DETERMINATION OF FAULT RESISTANCES

For a three-phase line segment, ten types of faults were simulated. They are phase A to ground, phase B to ground, phase C to ground, phase A to B, phase B to C, phase C to A, phase A to B to ground, phase B to C to ground, phase C to A to ground, and 3 phase faults. For a single-phase line segment, only phase to ground faults were simulated.

Three different fault resistances were used in the simulation process. For each type of fault at each line segment, three fault resistances were used: low resistance, middle resistance, and high resistance. The low resistance was chosen as  $10^{-6} \Omega$ . The middle resistance and high resistance varied with line segments. To determine the middle resistance and high resistance, for each type of fault, some fault cases with different fault resistance were simulated for a short time at line segments. Then, the fault cases whose fault currents were between 35-65% of that of the low resistance fault were considered as middle resistance faults; the fault cases whose fault currents were between 5-15% of that of the low resistance fault were considered as high resistance faults. A curve showing the different resistances for a particular line segment is illustrated in Figure 4.13. The fault resistance levels used for each line segment are shown in Table 4.5.



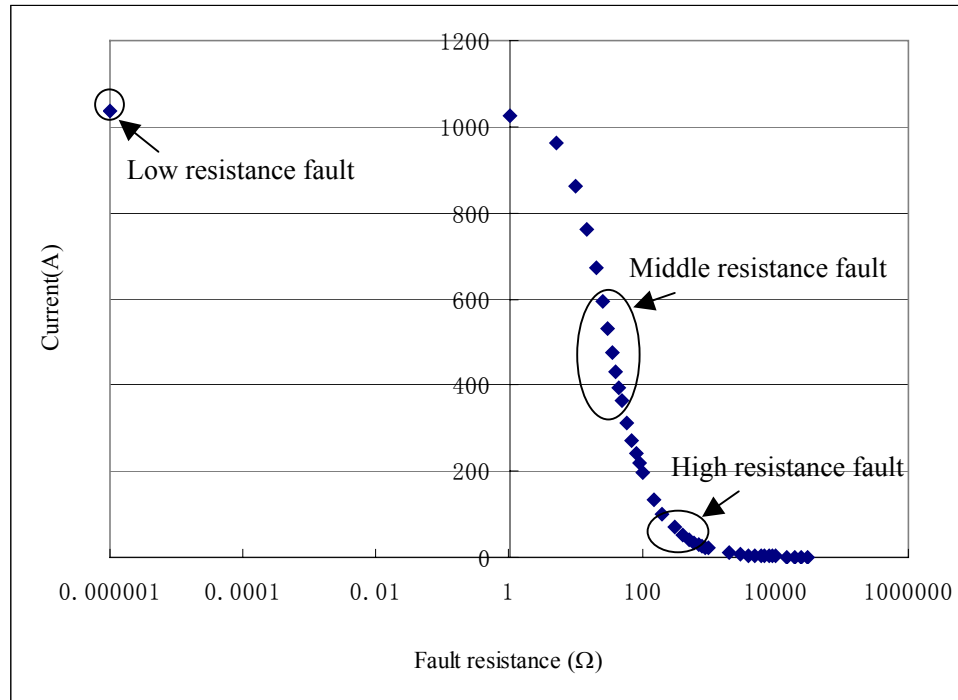


Figure 4.13 Determination of fault resistances

TABLE 4.5 FAULT RESISTANCE LEVELS AT LINE SEGMENTS

From	To	Low ( $\Omega$ )	Middle ( $\Omega$ )	High ( $\Omega$ )
800	802	$10^{-6}$	40	200
802	806	$10^{-6}$	40	200
806	808	$10^{-6}$	40	200
808	810	$10^{-6}$	50	300
808	812	$10^{-6}$	50	300
812	814	$10^{-6}$	50	400
814	850	$10^{-6}$	50	400
816	818	$10^{-6}$	80	500
816	824	$10^{-6}$	60	500
818	820	$10^{-6}$	90	600
820	822	$10^{-6}$	110	800
824	826	$10^{-6}$	80	500
824	828	$10^{-6}$	70	500
828	830	$10^{-6}$	70	500
830	854	$10^{-6}$	70	500

TABLE 4.5 CONTINUED

From	To	Low ( $\Omega$ )	Middle ( $\Omega$ )	High ( $\Omega$ )
832	858	$10^{-6}$	90	650
834	860	$10^{-6}$	90	650
834	842	$10^{-6}$	90	750
836	840	$10^{-6}$	90	650
836	862	$10^{-6}$	95	850
842	844	$10^{-6}$	90	750
844	846	$10^{-6}$	90	750
846	848	$10^{-6}$	90	750
850	816	$10^{-6}$	60	500
852	832	$10^{-6}$	70	500
854	856	$10^{-6}$	80	600
854	852	$10^{-6}$	70	500
858	864	$10^{-6}$	120	900
858	834	$10^{-6}$	90	650
860	836	$10^{-6}$	90	650
862	838	$10^{-6}$	90	900
888	890	$10^{-6*}$	5*	40*

\* The resistance is at the secondary side of the in-line transformer.

#### 4.5 SIMULATED FAULT CASES

After modeling the IEEE 34 node test feeder, 508 fault cases were simulated on the feeder. These 508 fault cases represent different fault types at different line sections, and include low impedance, middle impedance, and high impedance faults. Of 508 fault cases, 172 cases were randomly selected as the training cases. The training cases were used to obtain the optimal weights and parameters in the fuzzy resolver methodology. The remaining 336 cases were used as the test cases, which were used to study the performance of some designed fuzzy resolvers.

##### 4.5.1 Performance of Three Fault Location Methods on Simulated Fault Cases

After simulating these fault cases, the three fault location methods were used to assign possibility values for all fault cases. Based on these possibility values, the performance of the three fault location methods on the simulated fault cases was observed.

First, we want to know if a fault location method assigns the largest possibility value to the actual faulted section. Table 4.6 shows the percentage of fault cases whose actual faulted section is assigned the largest possibility value with using different fault location methods for different categories of fault resistances.

TABLE 4.6 PERCENTAGE OF FAULT CASES WHOSE ACTUAL FAULTED SECTION HAS THE LARGEST POSSIBILITY VALUE

	Low Resistance	Middle Resistance	High Resistance
Phase Selector	100%	100%	100%
Fault Distance	100%	100%	100%
ODIM	100%	100%	100%

Due to the limitation of fault location methods, some fault location methods gave all line sections an identical possibility value for some fault cases. For these specific cases, the actual faulted section obtained the largest possibility value but the fault location method did not provide any useful information to reduce the number of potential faulted line sections and it treated all line sections as potential faulted sections. Therefore, we also want to know the percentage of the 508 fault cases where at least one non-faulted section has a different possibility value from the actual faulted section. The percentage of fault cases where all sections do not have identical possibility values for different categories of fault resistances is shown as Table 4.7.

Even though the fault location methods did not give all line sections the identical possibility value, each fault location method might identify several line sections as potential faulted sections. However, only one section was the actual faulted section and the other sections were non-faulted (healthy) sections that had been assigned the same possibility value as the actual faulted section. When the three fault location methods were considered together, the number of non-faulted sections that have the same possibility

values as the actual faulted sections may reduce. For example, there were three sections: the first one was the actual faulted section; the others were non-faulted sections. The fault distance method assigned them possibility values [1 1 0]. The phase selector method and operated device identification method assigned them possibility values [0.95 0.4 0.95] and [0.92 0.92 0.6], respectively. Each of the three methods gave one non-faulted section the same possibility value as the actual faulted section. If we consider the three fault location methods together, the three sections obtained group possibility values (1 0.95 0.92), (1 0.4 0.92), and (0 0.95 0.6), respectively. Therefore, no non-faulted section had the same group possibility values as the actual faulted section. However, even when three fault location methods were considered together, some non-faulted sections might still have the same group possibility values as the actual faulted section, which are called non-distinguishable sections hereafter. Since all three fault location methods cannot distinguish these non-distinguishable sections from the actual faulted section, there is no way that a fuzzy resolver can distinguish them. The number of total non-faulted sections and non-distinguishable sections in the training cases and test cases is listed in Table 4.8.

TABLE 4.7 PERCENTAGE OF FAULT CASES WHERE AT LEAST ONE NON-FAULTED SECTION HAS DIFFERENT POSSIBILITY VALUE FROM THE ACTUAL FAULTED SECTION

	Bolted Fault	Middle Impedance	High Impedance
Phase Selector	100%	100%	100%
Fault Distance	100%	0%	0%
ODIM	100%	100%	32.94%

TABLE 4.8 NUMBER OF NON-DISTINGUISHABLE SECTIONS

	# of total non-faulted sections	# of non-distinguishable sections
Training case	5504	1983
Test cases	10752	4196

#### **4.6 CHAPTER SUMMARY**

In this chapter, the model of components in the IEEE 34 node test feeder and the system model were introduced. The general protective device model was presented, and the appropriate protective devices used in this feeder were presented. These devices were selected based on load flow and short circuit analysis studies. The steady state results of the modeled system were compared with the IEEE published results. The error of node voltages was less than 1.5%, with most less than 1.0%, and the error of most line currents was less than 2.5%. Ten types of faults were simulated at each three-phase line segment, while a phase to ground fault was simulated at each single-phase line segment. For each type of fault at each line segment, three fault resistance levels were used: high resistance, middle resistance, and low resistance. The values of these resistances vary with each line segment. The method used to determine these resistance values was also discussed. The chosen resistance values were listed.

## CHAPTER V

### METHODOLOGY FOR DESIGNING A FUZZY RESOLVER

#### 5.1 INTRODUCTION

In the new fault location scheme discussed in section 3.2.1, there is a fuzzy resolver that is used to combine the three fault location methods' outputs to produce the final possibility value for each line section of a distribution feeder. The methodology for designing a fuzzy resolver is to solve a fuzzy aggregation problem, and fuzzy aggregation operators are used to design fuzzy resolvers. After investigating fuzzy aggregation operators in Chapter III, three fuzzy aggregation operators, the min, OWA, and uninorm operators, were chosen as candidates to design fuzzy resolvers. In order to consider the different accuracy of the three fault location methods, weights need to be assigned to these fault location methods. In addition, the OWA operator has parameters that affect its behavior, and these parameters need to be determined. However, these weights and parameters cannot be determined arbitrarily and they need to be optimized.

In order to obtain optimal weights and parameters, genetic algorithms were chosen as the optimization method, and two objective functions were proposed. The first objective function was to maximize the number of fault cases whose actual faulted sections have possibility values equal to or larger than a preset possibility value  $p_1$ , which was shown in (3.32); the other was to maximize the number of non-faulted line sections whose possibility values are less than a preset possibility value  $p_2$ , which was shown in (3.34).

In this chapter, the author first introduces genetic algorithms. After that, the methodology for designing fuzzy resolvers with respect to a single objective function is discussed. GA-based multi-objective optimization methods are reviewed and evaluated. The methodology for designing fuzzy resolvers with respect to two objective functions together is also presented.

## 5.2 GENETIC ALGORITHMS (GA)

### 5.2.1 Overview

As random search based optimization methods, genetic algorithms mimic biological evolution in nature [74]-[76],[85]. In the very beginning, many potential individuals are generated randomly to form the first generation, and these individuals are called chromosomes. Crossover and mutation operators are used on these selected individuals to create the intermediate generation. Objective functions are evaluated at the individuals of the intermediate generation, and objective values are obtained. Based on these objective values, fitness values are assigned to each individual. The selection probabilities of these individuals are calculated based on their fitness values. Then, individuals are selected based on their selection probabilities to form the next generation. This process continues until some criteria are met, or the number of generations is reached to a preset value.

In the following sections, the commonly used operations for genetic algorithms such as the fitness assignment, selection, crossover, and mutation, are introduced.

### 5.2.2 Fitness Assignment

There are two ways to assign fitness values, the value-based method and rank-based method [85]. The value-based method obtains fitness values by using the average of all individuals' objective values to normalize each individual's objective value. For example, there are  $n$  individuals, and their objective values are  $a_1, \dots, a_n$ . The average of these objective values is  $\bar{a} = (a_1 + \dots + a_n)/n$ . The fitness value of the  $i^{\text{th}}$  individual is  $f_i = \frac{a_i}{\bar{a}}$ . Based on these fitness values, selection probabilities are calculated.

This value-based method is straightforward. However, the individuals having a large objective value have too many duplicates in the next generation, which causes the search to narrow down too quickly so that it is possible not to find the actual optimal points [74],[85]. The rank-based method overcomes this shortcoming. In this method, fitness values are not calculated based on objective values directly. Objective values are ranked

first. Then, fitness values are calculated based on these ranks. The linear ranking fitness assignment is commonly used. It is shown in (5.1), where  $SP$  is the selective pressure, which represents the probability of the best individuals being selected compared to the average probability of selection of all individuals,  $N_{ind}$  is the number of individuals in the population,  $pos$  is the rank of an individuals in this population, the least fit individual has  $pos=1$ , and the fittest individual has  $pos=N_{ind}$ .

$$Fitness(pos) = 2 - SP + 2 \times (SP - 1) \times \frac{pos - 1}{N_{ind} - 1} \quad (5.1)$$

### 5.2.3 Selection

After fitness values are obtained, selection probabilities are calculated based on (5.2), where  $p_i$  is the selection possibility of the  $i^{\text{th}}$  individual,  $f_i$  is the fitness value of the  $i^{\text{th}}$  individual. Based on these selection probabilities, individuals are selected. There are three commonly used selection methods, the Roulette wheel selection, the stochastic universal sampling, and the tournament selection [74],[75],[85].

$$p_i = \frac{f_i}{(f_1 + \dots + f_n)} \quad (5.2)$$

In the Roulette wheel selection [74],[85], individuals are mapped to contiguous segments of a wheel based on their selection probabilities. A pointer points to the wheel. Then the wheel is spun repeatedly. Each time the individual pointed by the pointer is chosen. From the description, it is known that the Roulette wheel selection is a stochastic selection with replacement.

Another selection method is the stochastic universal sampling [74]. In this method, the mapping method is exactly the same as the Roulette wheel selection. The difference is that equally spaced pointers are placed over the wheel. The number of pointers is equal to the number of individuals to be selected. For example, there are  $n$  individuals to be selected. Then  $n$  equally spaced pointers are placed over the wheel. The wheel is spun



once to pick up  $n$  individuals. The stochastic universal sampling method selects offspring that is closer to what is deserved than the Roulette wheel selection method [85].

The last commonly used selection method is tournament selection [74],[75],[85], which chooses individuals based on their objective values directly. In this method, the individuals are randomly selected to form a tour and the best individual of the tour is selected. The number of tours is determined by the number of individuals to be chosen. The size of a tour ranges from 2 to the number of individuals in the population.

#### 5.2.4 Crossover

As for crossover methods, there are the single-point crossover, the multi-point crossover, and the uniform crossover [74],[75],[85]. In all crossover methods, a pair of individuals is chosen randomly, and all individuals are coded as binary numbers. There is a crossover probability,  $p_c$ . For each crossover operation, a random number within  $[0,1]$  is generated. If the number is less than  $p_c$ , the crossover operation is executed. Otherwise, it is not implemented. In the single-point crossover, a position is selected uniformly at random. The two individuals exchange part of their bits at this point. This process is shown in Figure 5.1. In this figure, there are two individuals  $x=110101001$  and  $y=101100011$  and position 3 is chosen to implement the crossover operation. These two individuals exchange their bits between positions 4 to 9. Therefore, two offspring  $x'=110100011$  and  $y'=101101001$  emerge. In this method, the probability of two bits being separated is different based on their relative positions. For example, for an  $L$  length binary number, the first two bits only have  $1/(L-1)$  probability of being separated during the single-point crossover. However, the first bit and the last bit have  $(L-1)/(L-1)$  probability of being disrupted. This makes the positions of bits important in the single-point crossover.

The multiple-point crossover is similar to the single-point crossover. However, in this operation, several positions, let us say  $m$ , are randomly selected without duplicates. The multiple-point crossover overcomes the problem of the single-point, that is, the positions

of bits influence the probability of two bits of being separated, to some extent. A three-point crossover is shown in Figure 5.2. In this figure, positions 1, 3, and 7, are chosen to implement the crossover operation. The single-point crossover operation implements three times at these positions. First the crossover is implemented at position 1. After that, two new individuals  $x_1=101100011$  and  $y_1=110101001$  emerge. Then the crossover is implemented on  $x_1$  and  $y_1$  at position 3. After that, two new individuals  $x_2=101101001$  and  $y_2=110100011$  emerge. Last the crossover is implemented on  $x_2$  and  $y_2$  at position 7. Two offspring  $x'=101101001$  and  $y'=110100011$  emerge.

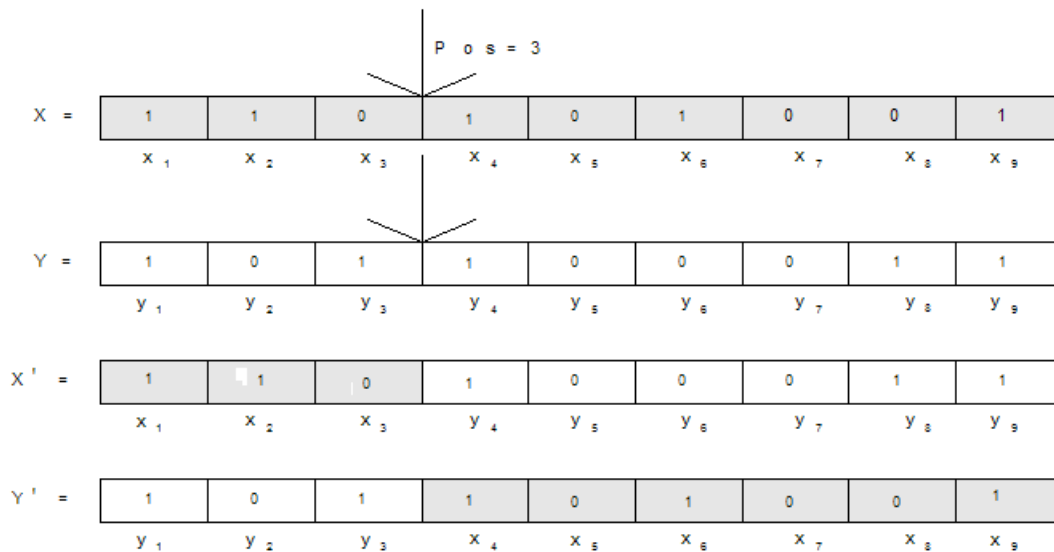


Figure 5.1 Single-point crossover

However, probabilities of separating two bits still depend on their positions and are not constant. To overcome this problem completely, the uniform crossover was developed. Uniform crossover generalizes the multi-point crossover idea and makes each point to be a potential crossover point. In this method, a mask is used. The mask has the

same length as the individuals and is created randomly. The parity of the mask's bits indicates which parent will supply the offspring. If one of the mask's bits is 1, it means this bit of the offspring is from parent 1. If it is 0, the bit of the offspring is from parent 2. The other offspring is created using the inverse of the mask. An example is shown in Figure 5.3. There are two 9-bit individuals  $x=011100110$  (parent 1) and  $y=101011001$  (parent 2). The mask that is randomly created is  $m1=011000110$ . Based on this mask, the first bit of the first offspring comes from parent 2, and it is 1. The second bit of the first offspring comes from parent 1, and it is 1. Repeating this process, the first offspring is  $x'=111011111$ . The inverse of the mask,  $m2$ , is  $001110001$ . The other offspring  $y'$  corresponding to  $m2$  is  $001100000$ . Hence, the two offspring are  $111011111$  and  $001100000$ .

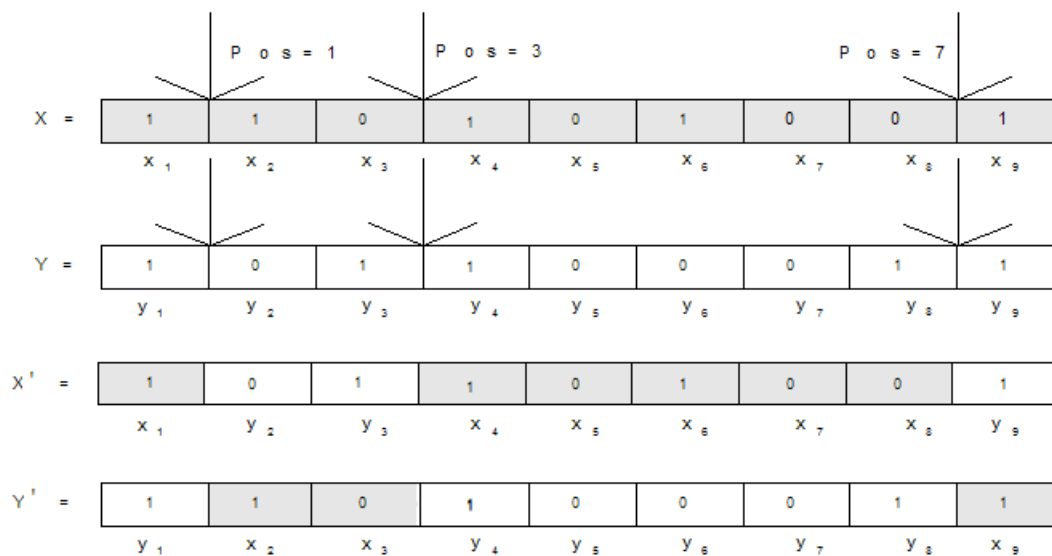


Figure 5.2 Three-point crossover

X =	0	1	1	1	0	0	1	1	0
	$x_1$	$x_2$	$x_3$	$x_4$	$x_5$	$x_6$	$x_7$	$x_8$	$x_9$

Y =	1	0	1	0	1	1	0	0	1
	$y_1$	$y_2$	$y_3$	$y_4$	$y_5$	$y_6$	$y_7$	$y_8$	$y_9$

m 1 =	0	1	1	0	0	0	1	1	0
-------	---	---	---	---	---	---	---	---	---

m 2 =	1	0	0	1	1	1	0	0	1
-------	---	---	---	---	---	---	---	---	---

X' =	1	1	1	0	1	1	1	1	1
	$y_1$	$x_2$	$x_3$	$y_4$	$y_5$	$y_6$	$x_7$	$x_8$	$y_9$

Y' =	0	0	1	1	0	0	0	0	0
	$x_1$	$y_2$	$y_3$	$x_4$	$x_5$	$x_6$	$y_7$	$y_8$	$x_9$

Figure 5.3 Uniform crossover

### 5.2.5 Mutation

Compared with the crossover operation, the mutation operation is very simple. There is a mutation probability,  $p_m$ . For each bit of an individual, a random number within  $[0,1]$  is generated. If the random number is less than  $p_m$ , the bit should be mutated. If any of the bits of an individual needs to be mutated, the bit is inverted [74],[75],[85]. For example, if the first bit of an individual needs to be mutated, and the value of the bit is 1, after the mutation the first bit of the individual becomes 0.

## 5.3 METHODOLOGY FOR DESIGNING A FUZZY RESOLVER WITH RESPECT TO A SINGLE OBJECTIVE FUNCTION

The author proposed two objective functions for designing a fuzzy resolver. The min, OWA, and uninorm operators were used to design fuzzy resolvers. For the min and OWA operators, two transformation methods mentioned in (3.27)-(3.31) were used to design

fuzzy resolvers. In this section, a methodology for designing a fuzzy resolver with respect to a single objective function is discussed.

### 5.3.1 Methodology for Obtaining Optimal Weights and Parameters

In the design process, 172 simulated fault cases were randomly chosen as the training set. For each fault case, the three fault location methods were executed individually. Each method assigned possibility values for all line sections. These possibility values were used as the input data for a fuzzy resolver, and a genetic algorithm was used to obtain optimal weights for the three fault location methods and optimal parameters for the OWA operator. The process for obtaining these optimal weights and parameters was the same for all three fuzzy aggregation operators and all transformation methods. The only difference was that the representation of a chromosome for the OWA operator was different from the representation of a chromosome for the min and uninorm operators. The process for obtaining these optimal values is shown in Figure 5.4 and introduced below.

First, 200 chromosomes were generated randomly to represent the weights of the three fault location methods and the parameters of the OWA operator, and they composed the population of the first generation. Each chromosome in the first generation was used in a transformation method mentioned in (3.27)-(3.31) to transform three fault location methods' outputs (possibility values of all line sections for all fault cases) into effective values. For the min operator, (3.27) and (3.28) were used. For the OWA operator, (3.29) and (3.30) were used. For the uninorm operator, (3.31) was used. After that, a fuzzy aggregation operator introduced in 2.2.7: the min operator, OWA operator, or uninorm operator, was used to aggregate these effective values to produce aggregation possibility values of all line sections for all fault cases. After aggregation possibility values were obtained, an objective value, either (3.32) or (3.34), was evaluated. After the objective values of all chromosomes were obtained, these objective values were ranked. The fitness value of each chromosome was assigned using (5.1), and its selection probability was

calculated as (5.2). Based on their selection probabilities, some chromosomes were chosen using the stochastic universal sampling approach introduced in 5.2.3.

In this paragraph, an example is used to illustrate the method to choose two chromosomes from five chromosomes. These five chromosomes have selection probabilities 0.2, 0.12, 0.24, 0.36, 0.8. Using the stochastic universal sampling approach, the chromosomes would be mapped to contiguous segments of a wheel as shown in Figure 5.5. Two equally spaced pointers point to the wheel. The wheel is spun once. The two pointed chromosomes, which have selection probabilities 0.12 and 0.36, are chosen.

The uniform crossover and the mutation operations introduced in section 5.2 were implemented over the chosen chromosomes to generate the second generation. In the crossover operation, the chosen chromosomes randomly formed pairs. For each pair, a random number was generated. If the random number was less than  $p_c$ , the crossover between this pair needed to be implemented. For each bit of the first mask  $m_1$ , a random number was generated. If the number was less than 0.5, the bit was equal to 1. Otherwise it was equal to 0. The second mask  $m_2$  was the inverse of  $m_1$ . In the mutation operation, for each bit of a chromosome, a random number was generated. If the number was less than  $p_m$ , the bit was mutated. Otherwise it was not mutated. The same process was used to produce the third generation from the second generation. This process continued for 100 generations, and the optimal chromosomes were obtained. In the following sections, the representation of a chromosome for different fuzzy aggregation operators is introduced.

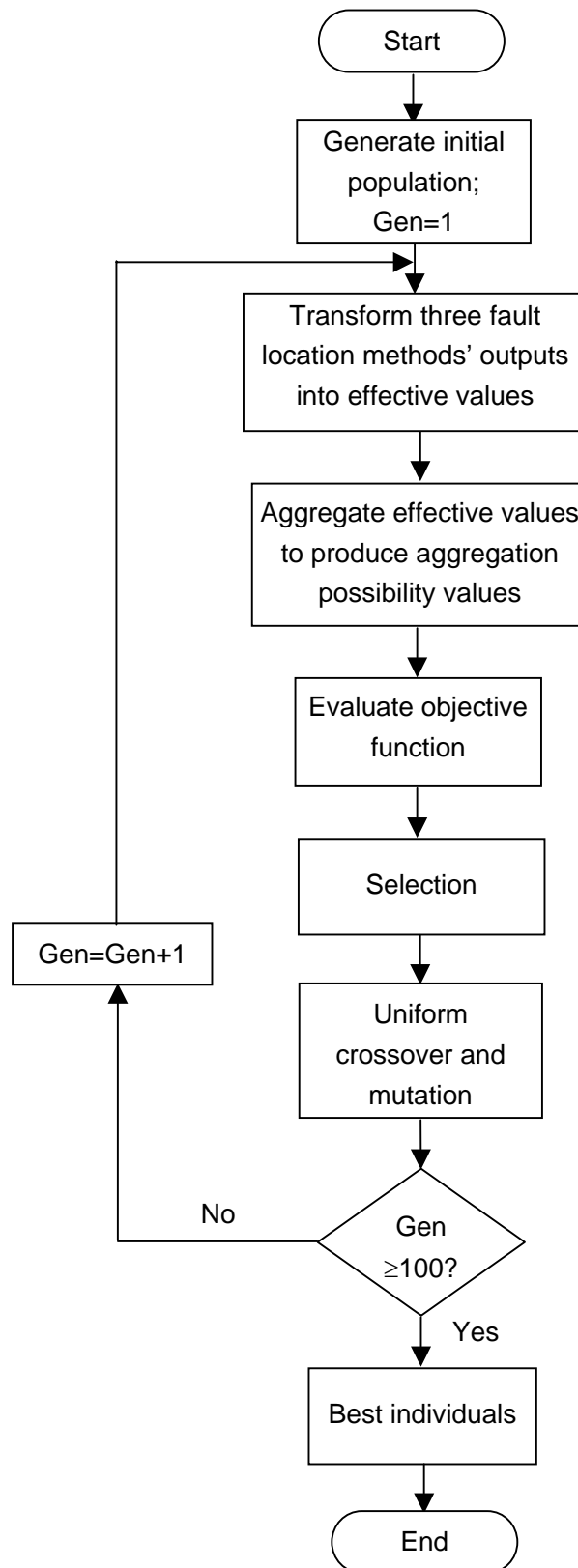


Figure 5.4 Process for obtaining optimal weights and parameters

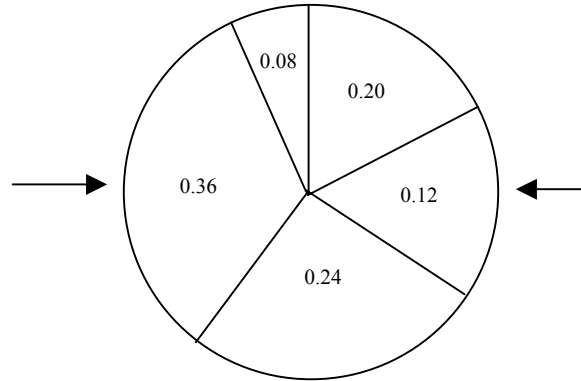


Figure 5.5 Stochastic universal sampling approach

### 5.3.1.1 Representation of a Chromosome

The min operator and uninorm operator do not have parameters. For these operators, only weights of the three fault location methods need to be optimized. These weights are real numbers within  $[0,1]$ . In this methodology, each weight was represented as an 8-bit integer in a chromosome. Each chromosome had 24 bits. In order to represent these weights as 8-bit integers, the formula in (5.3) was used, where  $w$  was a weight of a fault location method, and  $Int$  was the integer that was used in a chromosome to represent the weight of the fault location method. With using the 8-bit integer, the accuracy of the quantization was  $\frac{1}{2} \times \frac{1}{(2^8 - 1)} = 0.00196$ . To produce a chromosome, three random

numbers were generated to represent the weights of the three fault location methods  $w_1$ ,  $w_2$ , and  $w_3$ . Then these random numbers were converted to integers using (5.3). These integers were used in a chromosome. For example, if three random numbers, 0.252, 0.768, and 0.589 were generated to represent  $w_1$ ,  $w_2$ , and  $w_3$ . Based on (5.3), they were converted to three integers, 64, 196, and 150. These three integers were represented as binary numbers that constitute a chromosome. The chromosome for this example is shown as Figure 5.6.



$$Int = round((2^8 - 1) \times w) \quad (5.3)$$

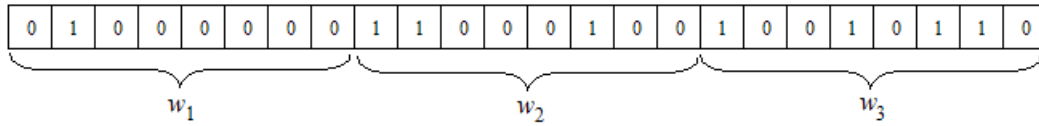


Figure 5.6 Representation of a chromosome for the min and uninorm operator

For the OWA operator, there are three parameters in addition to the weights of the three fault location methods. Therefore, a chromosome represents the three weights and three parameters. The three parameters are  $W_1$ ,  $W_2$ , and  $W_3$  as was discussed in (2.11). These weights and parameters are real numbers within  $[0,1]$ , and the sum of the three parameters should be equal to 1. These weights and parameters were converted to integers using (5.3), and each of them has 8 bits. Therefore, a chromosome has 64 bits. To produce a chromosome, three random numbers were generated to represent the weights of the three fault location methods  $w_1$ ,  $w_2$ , and  $w_3$  and two random numbers were generated to represent the first two parameters of the OWA operator  $W_1$  and  $W_2$ . If  $W_1 + W_2 \leq 1$ ,  $W_3$  was computed as  $1 - W_1 - W_2$ ; if  $W_1 + W_2 > 1$ , another two random numbers were generated for  $W_1$  and  $W_2$  until  $W_1 + W_2 \leq 1$ . For example, if three random numbers, 0.252, 0.768, and 0.589 were generated to represent  $w_1$ ,  $w_2$ , and  $w_3$ , and two random numbers 0.025 and 0.268 were generated to represent  $W_1$  and  $W_2$ .  $W_3 = 1 - W_1 - W_2 = 0.707$ . Based on (5.3), they were converted to three integers, 64, 196, 150, 6, 68, and 180. These six integers were represented as binary numbers that constitute a chromosome. The chromosome for this example is shown as Figure 5.7.

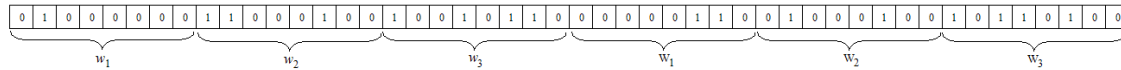


Figure 5.7 Representation of a chromosome for the OWA operator

### 5.3.2 Optimal Weights with Respect to the First Objective Function

In this section, the methodology for obtaining optimal weights for the min operator, OWA operator, and uninorm operator with respect to the first objective function was introduced. The first objective function was to maximize the number of fault cases whose actual faulted section has a possibility value no less than a preset value  $p_1$  and was represented as (3.32). After obtaining the optimal weights, the objective function and the number of non-faulted sections whose possibility values  $< p_2$  were evaluated at these optimal weights, where  $p_2$  was a small possibility value. The performance of these optimal weights was discussed. Various studies were performed to obtain optimal weights and parameters using different values of  $p_1$ . In these studies, three values were used for  $p_1$ , 0.95, 0.9, and 0.8, respectively, and three values were used for  $p_2$ , 0.2, 0.3, and 0.4, respectively.

#### 5.3.2.1 Optimal Weights for the Min Operator

For the min operator, only the optimal weights of the three fault location methods need to be found. The process for obtaining these optimal weights is the same as the process introduced in 5.3.1. Transformation methods (3.27) and (3.28) were used to transform three fault location methods' outputs into effective values. The min operator was used to aggregate effective values into aggregation possibility values. For the fitness assignment, the selective pressure  $SP=1.5$ . For the crossover operation,  $p_c=0.65$ . For the mutation operation,  $p_m=0.05$ .

Fuzzy resolver 1 used the transformation method in (3.28). There were several weights that maximized the objective function but gave a different number of non-faulted sections whose possibility value  $< p_2$ . 9 optimal weights are arbitrarily selected and listed in Table 5.1, where  $w_1$  is the weight for the operated device identification method,  $w_2$  is the weight for the phase selector method,  $w_3$  is the weight for the fault distance method. After obtaining these optimal weights, the objective function and the number of non-faulted sections whose possibility values  $< p_2$  were evaluated at these weights, where  $p_2$  is equal to 0.2, 0.3, and 0.4.

TABLE 5.1 OPTIMAL WEIGHTS OF THE MIN OPERATOR WITH RESPECT TO THE FIRST OBJECTIVE FUNCTION AND USING THE FIRST TRANSFORMATION METHOD

Optimal weights			Objective value 1	Number of non-faulted sections whose possibility value $< p_2$		
$w_1$	$w_2$	$w_3$		$p_2=0.2$	$p_2=0.3$	$p_2=0.4$
Optimal weights when $p_1=0.95$						
0.1059	0.0078	0.0039	172	2819	2825	2834
0.0431	0.0549	0.0000	172	2059	2059	2059
0.0000	0.0235	0.0000	172	0	0	0
Optimal weights when $p_1=0.9$						
0.2392	0.0863	0.0588	172	2860	2881	2943
0.1059	0.0745	0.0471	172	2819	2825	2834
0.0000	0.1137	0.0000	172	0	0	0
Optimal weights when $p_1=0.8$						
0.5255	0.1569	0.0745	172	2997	3133	3217
0.1451	0.2980	0.0941	172	2825	2910	2941
0.0000	0.1020	0.0000	172	0	0	0

Fuzzy resolver 2 used the transformation method in (3.27) to transform three fault location methods' outputs to effective values and the min operator to aggregate these effective values. There were several weights that maximized the objective function but

gave the different number of non-faulted sections whose possibility value  $< p_2$ . Optimal weights that gave an extreme number of non-faulted sections whose possibility value  $< p_2$  are selected and listed in Table 5.2. After obtaining these optimal weights, the objective function and the number of non-faulted sections whose possibility values  $< p_2$  were evaluated at these weights, where  $p_2$  is equal to 0.2, 0.3, and 0.4.

TABLE 5.2 OPTIMAL WEIGHTS OF THE MIN OPERATOR WITH RESPECT TO THE FIRST OBJECTIVE FUNCTION AND USING THE SECOND TRANSFORMATION METHOD

Optimal weights			Objective value 1	Number of non-faulted sections whose possibility value $< p_2$		
$w_1$	$w_2$	$w_3$		$p_2=0.2$	$p_2=0.3$	$p_2=0.4$
Optimal weights when $p_1=0.95$						
0.0980	0.0980	0.8000	172	1682	1682	1682
0.0275	0.0431	0.0039	172	0	0	0
Optimal weights when $p_1=0.9$						
0.1961	0.2000	0.8000	172	1682	1682	1682
0.2431	0.1333	0.0824	172	0	0	0
Optimal weights when $p_1=0.8$						
0.0000	0.1176	0.0000	172	0	0	0
0.4980	0.4000	0.9804	172	1682	1682	1682

Comparing the results in Table 5.1 and Table 5.2, the optimal weights using the first transformation method (3.28) had better performance than the optimal weights using the second transformation method (3.27) because the fuzzy resolver designed using the first transformation method made more non-faulted sections have a possibility value  $< p_2$ . For example, when  $p_1=0.95$ , fuzzy resolver 1 made 2819 non-faulted sections have a possibility value  $< 0.2$ , while fuzzy resolver 2 at most made 1682 non-faulted sections have a possibility value  $< 0.2$ .

### 5.3.2.2 *Optimal Weights for the OWA Operator*

For the OWA operator, in addition to the optimal weights of three fault location methods, the optimal parameters of the OWA operator need to be found. The process for obtaining these optimal weights is the same as the process introduced in 5.3.1. Transformation methods (3.29) and (3.30) were used to transform the outputs of the three fault location methods into effective values. The OWA operator was used to aggregate effective values into aggregation possibility values. For the fitness assignment, the selective pressure  $SP=1.5$ . For the crossover operation,  $p_c=0.65$ . For the mutation operation,  $p_m=0.05$ .

Fuzzy resolver 3 used the OWA operator and the transformation method in (3.30). There were several weights that maximized the objective function but gave a different number of non-faulted sections whose possibility value  $< p_2$ . 9 optimal weights are arbitrarily selected and listed in Table 5.3, where  $w_1$  is the weight for the operated device identification method,  $w_2$  is the weight for the phase selector method,  $w_3$  is the weight for the fault distance method,  $W_1$ ,  $W_2$ , and  $W_3$  are the parameters of the OWA operator. After obtaining these optimal weights, the objective function and the number of non-faulted sections whose possibility values  $< p_2$  were evaluated at these weights, where  $p_2$  is equal to 0.2, 0.3, and 0.4.

Fuzzy resolver 4 used the transformation method in (3.29) to transform three fault location methods' outputs to effective values and the OWA operator to aggregate these effective values. There were several weights that maximized the objective function but gave a different number of non-faulted sections whose possibility value  $< p_2$ . Optimal weights that gave an extreme number of non-faulted sections whose possibility value  $< p_2$  and another optimal weight are selected and listed in Table 5.4. After obtaining these optimal weights, the objective function and the number of non-faulted sections whose possibility values  $< p_2$  were evaluated at these weights, where  $p_2$  is equal to 0.2, 0.3, and 0.4.

TABLE 5.3 OPTIMAL WEIGHTS OF THE OWA OPERATOR WITH RESPECT TO THE FIRST OBJECTIVE FUNCTION AND USING THE FIRST TRANSFORMATION METHOD

Optimal weights						Objective value 1	Number of non-faulted sections whose possibility value < $p_2$		
$w_1$	$w_2$	$w_3$	$W_1$	$W_2$	$W_3$		$p_2=0.2$	$p_2=0.3$	$p_2=0.4$
Optimal weights when $p_1=0.95$									
0.0000	0.0078	0.0000	0.0000	0.0000	1.0000	172	0	0	0
1.0000	1.0000	0.9020	0.8824	0.1137	0.0039	172	550	552	559
0.1020	0.0118	0.8000	0.0000	0.0039	0.9961	172	2819	2822	2834
Optimal weights when $p_1=0.9$									
0.0000	0.1137	0.0000	0.0000	0.0000	1.0000	172	0	0	0
0.9961	0.9882	0.9098	0.7216	0.1294	0.1490	172	550	557	560
0.2490	0.1098	0.9804	0.0000	0.0000	1.0000	172	2860	2888	2943
Optimal weights when $p_1=0.8$									
0.0000	0.0039	0.0000	0.0000	0.0000	1.0000	172	0	0	0
0.9686	0.9451	0.8745	0.9098	0.0078	0.0824	172	550	552	557
0.5294	0.2510	0.9020	0.0000	0.0039	0.9961	172	2997	3139	3235

TABLE 5.4 OPTIMAL WEIGHTS OF THE OWA OPERATOR WITH RESPECT TO THE FIRST OBJECTIVE FUNCTION AND USING THE SECOND TRANSFORMATION METHOD

Optimal weights						Objective value 1	Number of non-faulted sections whose possibility value < $p_2$		
$w_1$	$w_2$	$w_3$	$W_1$	$W_2$	$W_3$		$p_2=0.2$	$p_2=0.3$	$p_2=0.4$
Optimal weights when $p_1=0.95$									
0.1098	0.0118	0.3922	0.0000	0.0039	0.9961	172	0	0	0
0.9882	0.9961	0.9333	0.9137	0.0196	0.0667	172	550	552	557
0.1137	0.0157	0.8902	0.0000	0.0078	0.9922	172	1682	1682	1682
Optimal weights when $p_1=0.9$									
0.1137	0.0196	0.1569	0.0039	0.0000	0.9961	172	0	0	0
0.9647	0.9804	0.9137	0.9451	0.0039	0.0510	172	550	551	557
0.2118	0.1255	0.8627	0.0039	0.0000	0.9961	172	1682	1682	1682
Optimal weights when $p_1=0.8$									
0.0980	0.0275	0.1961	0.0000	0.0078	0.9922	172	0	0	0
0.9529	0.9765	0.8588	0.7765	0.0275	0.1961	172	550	553	560
0.1098	0.0392	0.9804	0.0000	0.0078	0.9922	172	1682	1682	1682

Comparing the results in Table 5.3 and Table 5.4, the optimal weights using transformation method (3.30) had better performance than the optimal weights using transformation method (3.29) because it achieved the larger number of non-faulted sections whose possibility values  $< p_2$ . For example, when  $p_1=0.95$ , fuzzy resolver 3 made 2819 non-faulted sections have a possibility value  $< 0.2$ , while fuzzy resolver 4 at most made 1682 non-faulted sections have a possibility value  $< 0.2$ .

### 5.3.2.3 *Optimal Weights for the Uninorm Operator*

For the uninorm operator, only the optimal weights of the three fault location methods need to be found. The process for obtaining these optimal weights is the same as the process introduced in 5.3.1. Transformation method (3.31) was used to transform three fault location methods' outputs into effective values. The uninorm operator was used to aggregate effective values into aggregation possibility values. For the fitness assignment, the selective pressure  $SP=1.5$ . For the crossover operation,  $p_c=0.65$ . For the mutation operation,  $p_m=0.05$ .

Fuzzy resolver 5 used the transformation method in (3.31) to transform three fault location methods' outputs to effective values and the uninorm operator to aggregate these effective values. There were several weights that maximized the objective function but gave a different number of non-faulted sections whose possibility value  $< p_2$ . 6 optimal weights are arbitrarily selected and listed in Table 5.5. After obtaining these optimal weights, the objective function and the number of non-faulted sections whose possibility values  $< p_2$  were evaluated at these weights, where  $p_2$  is equal to 0.2, 0.3, and 0.4.

In summary, when the optimal weights were obtained with respect to the first objective function, it was not guaranteed that these optimal weights gave the best performance on the number of non-faulted sections whose possibility value  $< p_2$ . For example, when  $p_1=0.95$ , fuzzy resolver 5 obtained some weights that made 2664 non-faulted sections have a possibility value  $< 0.2$ , while there were some other weights that made 3255 non-faulted sections have a possibility value  $< 0.2$ . Based on results from

Table 5.1-Table 5.5, for the min operator and OWA operator, some weights were obtained that made the number of non-faulted sections whose possibility value  $< p_2$  equal to 0 because without the constraint of non-faulted section's possibility values, the optimization program may find optimal weights that made all line sections have large possibility values.

TABLE 5.5 OPTIMAL WEIGHTS OF THE UNIFORM OPERATOR WITH RESPECT TO THE FIRST OBJECTIVE FUNCTION

Optimal weights			Objective value 1	Number of non-faulted sections whose possibility value $< p_2$		
$w_1$	$w_2$	$w_3$		$p_2=0.2$	$p_2=0.3$	$p_2=0.4$
Optimal weights when $p_1=0.95$						
0.9961	0.9608	0.7843	172	3255	3369	3469
0.7608	0.7804	0.5961	172	2664	3294	3445
Optimal weights when $p_1=0.9$						
0.9137	0.6627	0.3216	172	2714	2822	3413
0.7843	0.7451	0.7333	172	3214	3294	3441
Optimal weights when $p_1=0.8$						
0.9176	0.9451	0.5176	172	2714	3367	3469
0.4980	0.4000	0.5020	172	1629	3138	3369

### 5.3.3 Optimal Weights with Respect to the Second Objective Function

In this section, the methodology for obtaining optimal weights for the min, OWA, and uniform operators with respect to the second objective function was introduced. After obtaining these optimal weights, the objective function and the number of faulted sections whose possibility values  $\geq p_1$  were evaluated at these optimal weights. The performance of these optimal weights was discussed. The second objective function was to maximize the number of non-faulted line sections whose possibility value is less than a



preset value  $p_2$  and was represented as (3.34). Various studies were performed to obtain optimal weights and parameters using different  $p_1$ . In these studies, three values were used for  $p_2$ , 0.2, 0.3, and 0.4, respectively.

### ***5.3.3.1 Optimal Weights for the Min Operator***

For the min operator, only the optimal weights of the three fault location methods need to be found. The process for obtaining these optimal weights is the same as the process introduced in 5.3.1. Transformation methods (3.27) and (3.28) were used to transform three fault location methods' outputs into effective values. The min operator was used to aggregate effective values into aggregation possibility values. For the fitness assignment, the selective pressure  $SP=1.5$ . For the crossover operation,  $p_c=0.65$ . For the mutation operation,  $p_m=0.05$ .

Fuzzy resolver 6 used the transformation method in (3.28). All optimal weights that maximized the objective function and gave the different number of faulted sections whose possibility value  $\geq p_1$  are listed in Table 5.6. After obtaining these optimal weights, the objective function and the number of faulted sections whose possibility value  $\geq p_1$  were evaluated at these weights, where  $p_1$  is equal to 0.95, 0.9, and 0.8.

Fuzzy resolver 7 used the transformation method in (3.27). All optimal weights that maximized the objective function and gave the different number of faulted sections whose possibility value  $\geq p_1$  are listed in Table 5.7. After obtaining these optimal weights, the objective function and the number of faulted sections whose possibility value  $\geq p_1$  were evaluated at these weights, where  $p_1$  is equal to 0.95, 0.9, and 0.8.

Comparing the results in Table 5.6 and Table 5.7, the optimal weights using transformation methods (3.28) and (3.27) had the same performance in terms of the number of faulted sections whose possibility value  $\geq p_1$  when  $p_2=0.4$  and 0.3. When  $p_2=0.2$ , transformation method (3.28) found three optimal weights while the transformation method (3.27) only found one optimal weights. In addition, two of the three optimal weights found using transformation method (3.28) made more faulted

sections whose possibility value  $\geq p_I$  than the optimal weight found using transformation method (3.27).

TABLE 5.6 OPTIMAL WEIGHTS OF THE MIN OPERATOR WITH RESPECT TO THE SECOND OBJECTIVE FUNCTION AND USING THE FIRST TRANSFORMATION METHOD

Optimal weights			Objective value 2	Number of faulted sections whose possibility value $\geq p_I$		
$w_1$	$w_2$	$w_3$		$p_I=0.8$	$p_I=0.9$	$p_I=0.95$
Optimal weights when $p_2=0.4$						
0.9176	1.0000	0.0824	3485	147	144	134
0.9843	1.0000	0.6980	3485	147	144	133
Optimal weights when $p_2=0.3$						
0.9843	0.9725	0.1922	3369	147	144	133
Optimal weights when $p_2=0.2$						
0.9569	0.4824	0.5100	3255	154	145	135
0.9608	0.8118	0.2400	3255	147	144	133
0.9961	0.6667	0.5200	3255	149	144	134

TABLE 5.7 OPTIMAL WEIGHTS OF THE MIN OPERATOR WITH RESPECT TO THE SECOND OBJECTIVE FUNCTION AND USING THE SECOND TRANSFORMATION METHOD

Optimal weights			Objective value 2	Number of faulted sections whose possibility value $\geq p_I$		
$w_1$	$w_2$	$w_3$		$p_I=0.8$	$p_I=0.9$	$p_I=0.95$
Optimal weights when $p_2=0.4$						
1.0000	1.0000	0.9725	3485	147	144	133
0.9490	1.0000	0.8000	3485	147	144	134
Optimal weights when $p_2=0.3$						
0.9961	0.9882	0.9020	3369	147	144	133
Optimal weights when $p_2=0.2$						
0.9922	0.9294	0.8300	3255	147	144	133

### 5.3.3.2 Optimal Weights for the OWA Operator

For the OWA operator, in addition to the optimal weights of the three fault location methods, the optimal parameters of the OWA operator need to be found. The process for obtaining these optimal weights is the same as the process introduced in 5.3.1. Transformation methods (3.29) and (3.30) were used to transform three fault location methods' outputs into effective values. The OWA operator was used to aggregate effective values into aggregation possibility values. For the fitness assignment, the selective pressure  $SP=1.5$ . For the crossover operation,  $p_c=0.65$ . For the mutation operation,  $p_m=0.05$ .

Fuzzy resolver 8 used the transformation method in (3.30). All optimal weights that maximized the objective function are listed in Table 5.8. After obtaining these optimal weights, the objective function and the number of faulted sections whose possibility value  $\geq p_1$  were evaluate at these weights, where  $p_1$  is equal to 0.95, 0.9 and 0.8. It is seen that these optimal weights made the number of faulted sections have possibility values  $\geq p_1$  equal to 0.

TABLE 5.8 OPTIMAL WEIGHTS OF THE OWA OPERATOR WITH RESPECT TO THE SECOND OBJECTIVE FUNCTION AND USING THE FIRST TRANSFORMATION METHOD

Optimal weights						Objective value 2	Number of faulted sections whose possibility value $\geq p_1$		
$w_1$	$w_2$	$w_3$	$W_1$	$W_2$	$W_3$		$p_2=0.8$	$p_2=0.9$	$p_2=0.95$
Optimal weights when $p_2=0.4$									
0.4235	0.3020	0.1373	0.7216	0.1647	0.1137	5504	0	0	0
Optimal weights when $p_2=0.3$									
0.2235	0.0784	0.0431	0.7529	0.2196	0.0275	5504	0	0	0
Optimal weights when $p_2=0.2$									
0.1961	0.1490	0.1400	0.9400	0.0000	0.0600	5504	0	0	0

Fuzzy resolver 9 used the transformation method in (3.29). All optimal weights that maximized the objective function are listed in Table 5.9. After obtaining these optimal weights, the objective function and the number of faulted sections whose possibility value  $\geq p_1$  were evaluated at these weights, where  $p_1$  is equal to 0.95, 0.9, and 0.8. It is seen that these optimal weights made the number of faulted sections have possibility values  $\geq p_1$  equal to 0.

TABLE 5.9 OPTIMAL WEIGHTS OF THE OWA OPERATOR WITH RESPECT TO THE SECOND OBJECTIVE FUNCTION AND USING THE SECOND TRANSFORMATION METHOD

Optimal weights						Objective value 2	Number of faulted sections whose possibility value $\geq p_1$		
$w_1$	$w_2$	$w_3$	$W_1$	$W_2$	$W_3$		$p_2=0.8$	$p_2=0.9$	$p_2=0.95$
Optimal weights when $p_2=0.4$									
0.2353	0.2196	0.1765	0.7843	0.0392	0.1765	5504	0	0	0
Optimal weights when $p_2=0.3$									
0.2431	0.2353	0.1529	0.9451	0.0549	0.0000	5504	0	0	0
Optimal weights when $p_2=0.2$									
0.0118	0.0510	0.0000	0.8900	0.1100	0.0100	5504	0	0	0

Comparing the results in Table 5.8 and Table 5.9, the optimal weights using transformation methods (3.30) and (3.29) had the same performance in terms of the number of faulted sections whose possibility values  $\geq p_1$ .

### 5.3.3.3 Optimal Weights for the Uninorm Operator

For the uninorm operator, only the optimal weights of three fault location methods need to be found. The process for obtaining these optimal weights is the same as the process introduced in 5.3.1. Transformation method (3.31) was used to transform three fault location methods' outputs into effective values. The uninorm operator was used to

aggregate effective values into aggregation possibility values. For the fitness assignment, the selective pressure  $SP=1.5$ . For the crossover operation,  $p_c=0.65$ . For the mutation operation,  $p_m=0.05$ .

Fuzzy resolver 10 used transformation method (3.31) to transform three fault location methods' outputs to effective values and the uninorm operator to aggregate these effective values. There were several weights that maximized the objective function but gave the different number of faulted sections whose possibility values  $\geq 0.95$ . 5 optimal weights are arbitrarily selected and listed in Table 5.5. After obtaining these optimal weights, the objective function and the number of faulted sections whose possibility values  $\geq 0.95$  were evaluated at these weights, where  $p_2$  is equal to 0.95, 0.9, and 0.8.

TABLE 5.10 OPTIMAL WEIGHTS OF THE UNINORM OPERATOR WITH RESPECT TO THE SECOND OBJECTIVE FUNCTION

Optimal weights			Objective value 2	Number of faulted sections whose possibility value $\geq p_1$		
$w_1$	$w_2$	$w_3$		$p_1=0.8$	$p_1=0.9$	$p_1=0.95$
Optimal weights when $p_2=0.4$						
0.7294	1.0000	0.5059	3485	172	172	156
0.9490	1.0000	0.5412	3485	172	172	172
0.6902	1.0000	0.3490	3485	172	171	148
Optimal weights when $p_2=0.3$						
1.0000	0.8588	0.7608	3369	172	172	172
Optimal weights when $p_2=0.2$						
0.9804	0.9569	0.7500	3255	172	172	172

### 5.3.4 Summary

The optimal weights that were obtained with respect to the first objective function using three fuzzy aggregation operators and their corresponding objective functions were listed in Table 5.1-Table 5.5. It was seen that several weights maximized the number of

faulted sections that had possibility values  $\geq p_1$  but they gave the different number of non-faulted sections that had possibility values  $< p_2$ . For the min and OWA operators, when they maximized the number of faulted sections whose possibility values are  $\geq p_1$ , some optimal weights made the number of non-faulted sections whose possibility value  $< p_2$  equal to 0 because without the constraint of non-faulted section's possibility values the optimization program may find optimal weights that made all line sections have large possibility values. Therefore, without the second objective function, it was not guaranteed to find optimal weights that maximized the first objective function and gave the best performance on the number of non-fault sections that had possibility values  $< p_2$ . These fuzzy resolvers identified some distinguishable non-faulted sections as potential faulted sections. Therefore, system operators needed to spend more time to locate a fault.

The optimal weights that were obtained with respect to the second objective function using three fuzzy aggregation operators and their corresponding objective functions were listed in Table 5.6-Table 5.10. It was seen that there might be several weights that maximized the number of non-faulted sections whose possibility values are less than  $p_2$ , but these weights gave the different number of faulted sections whose possibility values  $\geq p_1$ . For the min and OWA operators, these weights could not make all actual fault sections have possibility values  $\geq p_1$ . For the OWA operator, when they maximized the number of non-faulted sections whose possibility values are less than  $p_2$ , the optimal weights and parameters caused all sections to have a low possibility value. Hence, no actual faulted sections had possibility values  $\geq p_1$ . These fuzzy resolvers may not identify the actual faulted section as potential faulted sections for some fault cases. Therefore, it was difficult for system operators to find the actual faulted section for these fault cases. In summary, the optimal weights should be obtained with respect to two objective functions instead of one of them to achieve better performance.

## **5.4 METHODOLOGY FOR DESIGNING A FUZZY RESOLVER WITH RESPECT TO TWO OBJECTIVE FUNCTIONS**

When weights and parameters are optimized using two objective functions, the problem becomes a multi-objective optimization problem. There were several GA-based multi-objective optimization methods. In the following sections, the author reviews these GA-based multi-objective optimization methods. Then, the method that was used for this dissertation work is presented.

### **5.4.1 Review of GA-based Multi-objective Optimization Methods**

There are three ways to solve a multi-objective problem using GA. The simplest way is to scale these multiple objectives and combine them into a single objective based on the knowledge of the problem, and then GA is applied to find solutions that optimize the single objective. However, by using this method the obtained solutions are sensitive to the weights, and the user must have thorough knowledge of the problem. The second way is non-Pareto methods that treat objective functions separately. A fraction of optimal solutions is obtained based on only one of these objective functions. The last way is Pareto-based approaches, in which optimal weights are obtained based on some Pareto-based ranking methods.

In single-objective optimization problems, it is theoretically possible to find a global optimum. However, in multi-objective problems, there may not exist a global optimum with respect to all objectives. Usually there is a set of solutions that are superior to the rest of the solutions with respect to all objectives. The solutions in this set are called Pareto-optimal solutions (or non-dominated solutions) [74],[86],[88]. No Pareto-optimal solution is superior to other Pareto-optimal solutions in terms of all objectives. The user may be interested in all Pareto-optimal solutions, not just one Pareto-optimal solution. As a population-based algorithm, genetic algorithms are well suited to find Pareto-optimal solutions. In the following paragraphs, the non-Pareto methods and Pareto-based methods are discussed.

#### **5.4.1.1 Non-Pareto Methods**

Non-Pareto methods treat the objective functions separately in the reproduction process. There are two non-Pareto methods introduced in the literature to solve a multi-objective problem. The first one is the vector evaluated genetic algorithm (VEGA) [86]. In this method, the parallel selection that reproduced a fraction of the next generation (subpopulation) from the current generation according to each of the objectives separately was used. After all subpopulations were generated, they were shuffled and merged together to perform the crossover and mutation operations. Fourman [87] proposed a method that produced the next generation based on one of the objective functions. The tournament selection method introduced in 5.2.3 was used, and two individuals formed a tour. The objective function used in each tournament was selected either randomly or according to the pre-assigned priorities of the objective functions.

These kinds of methods can be easily implemented. However, they have a drawback. They tend to generate solutions that make one of the objectives extremely good but other objectives are not so good [88]. They do not produce all Pareto-optimal solutions.

#### **5.4.1.2 Pareto-based Methods**

Pareto-based methods treat the objective functions together in the reproduction process. They reproduce individuals based on the Pareto-optimality concept. Some Pareto-based methods [74],[88],[89] reproduce the next generation based on the Pareto-based rank, and some ranking methods have been developed to rank each individual [74],[89]. Other methods [90] reproduce individuals based on individuals' values directly without ranking them.

In [74],[89], two Pareto-based ranking methods were proposed. After ranking individuals, the rank-based fitness assignment introduced in 5.2.2 was used to produce the fitness value and the selection probability. Then, individuals were chosen to survive based on their selection probability using the Roulette wheel selection method or stochastic universal sampling selection method introduced in 5.2.3. In Goldberg's



ranking method [74], the non-dominated individuals were assigned the rank of 1. Then, the non-dominated individuals were removed, and the non-dominated individuals in the remaining population were assigned the rank of 2. This process continued until all individuals in the current generation were assigned a rank. The process is shown as Figure 5.8. In the figure, two objective functions,  $f_1$  and  $f_2$ , are minimized. It is seen that individuals A, C, E, and F are non-dominated because no individual has smaller objective functions than they do in both  $f_1$  and  $f_2$  domain. Hence, they are assigned the rank of 1. After removing these four individuals, B and G become non-dominated individuals. Therefore, they are assigned the rank of 2. After removing these two individuals, D is non-dominated and assigned the rank of 3. Fonseca and Fleming [89] proposed a slightly different ranking method. In their method, the rank of each individual was defined as one plus the number of individuals in the current population that dominate this individual. In Figure 5.9, there are no individuals that dominate A, C, E, and F. They are assigned the rank of 1. For individual G, there are two individuals E and F that dominate it. Hence, the rank of G is  $1+2=3$ . For individual B, there is one individual C that dominates it. Hence, the rank of B is  $1+1=2$ . For individual D, there are three individuals A, B and C that dominate it. Hence, the rank of D is  $1+3=4$ .

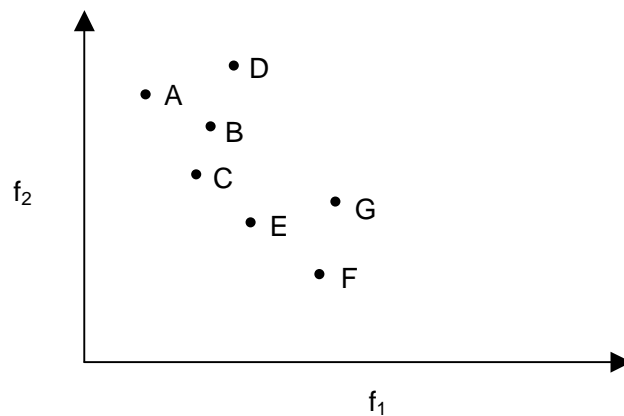


Figure 5.8 Pareto-based ranking (Goldberg's ranking)

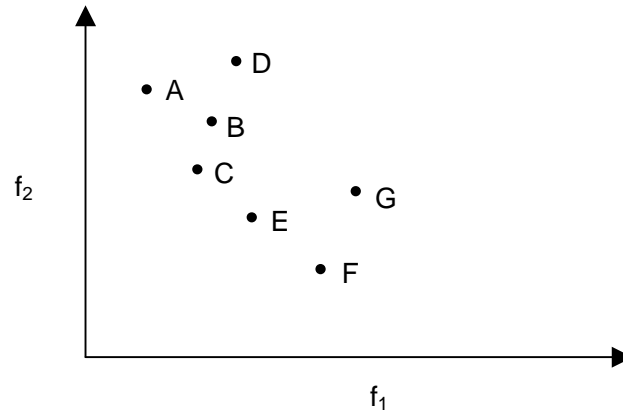


Figure 5.9 Pareto-based ranking (Fonseca and Fleming's ranking)

Tanaka, Yamamura, and Kobayashi [88] proposed a different selection method. Before the selection operation, crossover and mutation operations were applied to produce many individuals as the intermediate population. Then, all the non-dominated individuals (rank 1) in the intermediate population were selected, and the dominated individuals were discarded. Thus, the population size varied over generations. In some cases, another slightly modified version of the selection method was utilized [88], where not only the non-dominated individuals but also individuals with a favorable rank (say, less than or equal to three) were selected for survival.

In addition to the above three methods, some other Pareto-based methods reproduce the next generation without depending on individuals' values. Horn et al. [90] proposed a tournament selection for multi-objective optimization. In his method, the selection did not depend on individuals' rank but on their objective values directly. It was similar to the tournament selection method introduced in 5.2.3. Two individuals were randomly selected to form a tour. However, in each tournament, two individuals did not compete with each other. They competed using a set of other individuals in the population that was called a comparison set (the individuals surrounded by the dash line in Figure 5.10). If one individual was not dominated by anyone in the comparison set and the other was dominated by at least one individual in the comparison set, then the first individual was

selected for survival. If both competitors are either dominated or non-dominated, the fitness sharing [89] technique was used. In the fitness sharing methods, the fitness value of each individual was reduced if there existed other individuals in its neighborhood, and therefore an individual located in a more crowded area left less offspring. Thus, the population was distributed more uniformly over the Pareto-optimal set. While the Pareto-based methods mentioned above can find a variety of the Pareto-optimal solutions, they use much computational time [91].

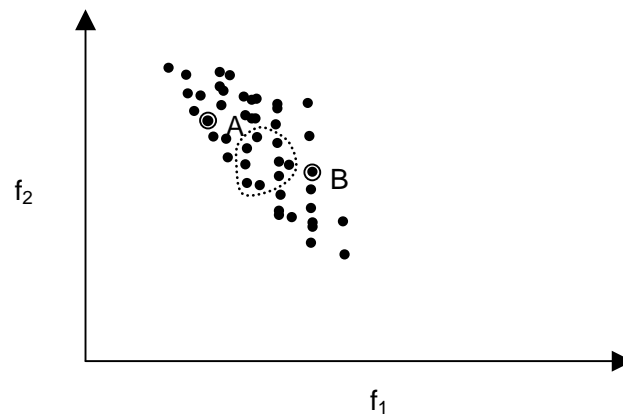


Figure 5.10 Pareto-based tournament selection

Non-Pareto and Pareto-based methods were introduced to solve a multi-objective problem. While the first one does not produce all Pareto-optimal solutions, the second one uses much computational time. In order to overcome the computational time problem, Tamaki [91] proposed a method that utilized the parallel selection method of the VEGA without considering the Pareto-based ranking. In order to overcome the VEGA's problem, that is, generating solutions that make one of the objectives extremely good but the other objectives not so good, the Pareto reservation strategy was developed [91]; that is, non-dominated individuals in a population at each generation were all reserved in the next generation. The procedure of this method is shown as Figure 5.11. First, the

crossover and mutation operations were implemented on the  $i^{\text{th}}$  generation to produce the intermediate population. Then, the non-dominated individuals in the intermediate population were found. If the number of non-dominated individuals was less than the population size of the next generation, the rest of the population in the next generation was produced using the parallel selection method introduced in 5.4.1.1. On the other hand, if the number of non-dominated individuals was larger than the population size, individuals in the next generation were selected from the non-dominated individuals by using the fitness sharing technique [89],[90]. By combining the parallel selection method with the Pareto reservation strategy, Tamaki's method can find a variety of Pareto-optimal results with less computational time than the Pareto-based methods.

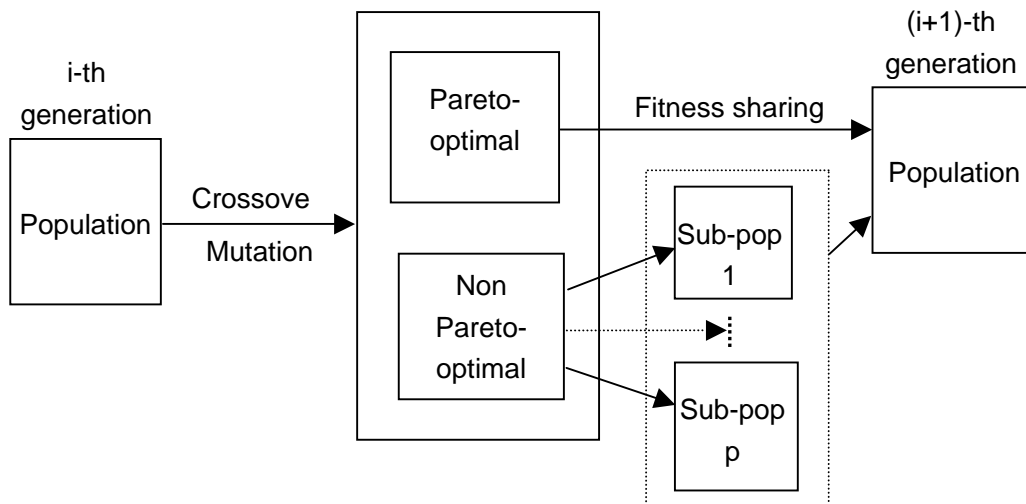


Figure 5.11 Pareto-based method proposed by Tamaki

#### 5.4.2 Methodology for Obtaining Optimal Weights and Parameters

Tamaki's method [91] was used to determine the optimal weights of the three aggregation operators and the optimal parameters of the OWA operator. Of 508 fault

cases simulated on the IEEE 34 node test feeder, 172 fault cases were randomly chosen as the training set. For each fault case in the training set, the three fault location methods were executed to calculate possibility values for all line sections. These possibility values were used as the input data for a fuzzy resolver, and a genetic algorithm was used to obtain optimal weights for the three fault location methods and optimal parameters for the OWA operator. The process for obtaining these optimal weights and parameters is the same for all three fuzzy aggregation operators and all transformation methods. The only difference is that the representation of a chromosome for the OWA operator is different from the representation of a chromosome for the min and uninorm operators. The process for obtaining these optimal values is shown in Figure 5.11 and introduced below.

First, 200 chromosomes were generated randomly to represent the weights of three fault location methods and the parameters of the OWA operator, and they composed the population of the first generation. Then, the uniform crossover and the mutation operations introduced in 5.2 were implemented over the first generation to generate the intermediate population. The size of the intermediate population was 400.

Each chromosome in the intermediate population was used in a transformation process mentioned in (3.27)-(3.31) to transform the three fault location methods' outputs (possibility values of all line sections for all fault cases) into effective values. Then a fuzzy aggregation operator introduced in 2.2.7 was used to aggregate these effective values to produce aggregation possibility values of all line sections for all fault cases. After the aggregation possibility values were obtained, the two objective values, both the number of faulted sections that had a possibility value no less than a preset value  $p_1$  and the number of non-faulted sections that had a possibility value less than a preset value  $p_2$ , were evaluated.

After the objective values of all chromosomes were obtained, the non-dominated chromosomes were found. The non-dominated chromosomes were chromosomes to which other chromosomes were not superior in terms of two objective values. For

example, if the evaluation of two objective functions (3.32) and (3.34) at three chromosomes produced objective values (123, 2313) (127, 1982) (98, 983). The chromosomes corresponding to (123, 2313) and (127, 1982) were non-dominated chromosomes because no chromosome could produce larger objective values in terms of two objective functions. These non-dominated chromosomes were kept in the second generation.

If the number of the non-dominated chromosomes was less than the population size, the parallel selection technique was used on the dominated chromosomes to fill the rest of the second generation. For example, if the size of the second generation was 200 and there were 60 non-dominated chromosomes and 340 dominated chromosomes. These 60 non-dominated chromosomes were kept in the second generation. Then the 340 dominated chromosomes were ranked based on their first objective values. The fitness value of each chromosome was assigned using (5.1), and its selection probability was calculated as (5.2). Based on their selection probabilities, 70 chromosomes were chosen to form half of the rest 140 population of the second generation using the stochastic universal sampling introduced in 5.2.3. The other half of the rest 140 population of the second generation was filled based on the second objective values of the 340 dominated chromosomes.

If the number of the non-dominated chromosomes was larger than the population size of the second generation, the fitness sharing technique [89],[90] was used to choose chromosomes to survive in the second generation. In the fitness sharing technique, all non-dominated chromosomes had a fitness value 1 and the fitness value of a non-dominated chromosome was degraded using its niche count  $m_i$ . This degradation was obtained by dividing the fitness value 1 by the niche count to find the shared fitness value:  $1/m_i$ . Then the selection probabilities of all chromosomes were obtained based on these shared fitness values using the method introduced in section 5.2.3. The stochastic universal sampling was used to choose chromosomes that survive in the next generation.

An example is used to explain how to calculate the niche count of a chromosome. For example, for the  $i^{\text{th}}$  chromosome, there are two objective values  $g_i$  and  $h_i$ . These objective values are normalized using (5.4) and (5.5), where  $\max(g_i)$  is the maximum value of  $g_i$  for all chromosomes,  $\max(h_i)$  is the maximum value of  $h_i$  for all chromosomes. The niche count of this chromosome is calculated using (5.6), where  $d[i,j]$  is the distance between chromosome  $i$  and  $j$ . The sharing function  $Sh(d)$  is defined as  $Sh(d)=1-d/\sigma_{\text{share}}$  for  $d \leq \sigma_{\text{share}}$  and  $Sh(d)=0$  for  $d > \sigma_{\text{share}}$ . Here  $\sigma_{\text{share}}$  is the niche radius that is fixed at some estimate of the minimal separation expected between the chromosome's objective values. The distance between chromosome  $i$  and  $j$  is calculated using (5.7).

$$\text{norm}_{-}g_i = \frac{g_i}{\max(g_i)} \quad (5.4)$$

$$\text{norm}_{-}h_i = \frac{h_i}{\max(h_i)} \quad (5.5)$$

$$m_i = \sum_{j \in \text{Pop}} Sh(d[i, j]) \quad (5.6)$$

$$d[i, j] = \sqrt{(\text{norm}_{-}h_i - \text{norm}_{-}h_j)^2 + (\text{norm}_{-}g_i - \text{norm}_{-}g_j)^2} \quad (5.7)$$

Then the third generation was produced from the second generation using the same procedure. This procedure continued for 100 generations, and the optimal chromosomes were obtained. The representation of a chromosome used in this procedure was introduced in 5.3.1.1.

In the following sections, the above methodology was used on the min, OWA, and uninorm operators to obtain the optimal weights of the three fault location methods and the optimal parameters of the OWA operator. After obtaining these optimal weights, the two objective functions (3.32) and (3.34) were evaluated at these optimal weights. The performance of these optimal weights was discussed. The first objective function was to maximize the number of fault cases whose actual faulted section has a possibility value no less than a preset value  $p_l$  as shown in (3.32). The second objective function was to maximize the number of non-faulted line sections whose possibility value is less than a

preset value  $p_2$  as shown in (3.34). Various studies were performed to obtain optimal weights and parameters with different  $p_1$  and  $p_2$ . In these studies, three values were used for  $p_1$ , 0.95, 0.9, and 0.8, respectively. Three values were used for  $p_2$ , 0.2, 0.3, and 0.4, respectively.

### 5.4.3 Optimal Weights for the Min Operator

For the min operator, only the optimal weights of the three fault location methods need to be determined. The process to obtain these optimal weights is the same as the process introduced in section 0. Transformation methods (3.27) and (3.28) were used to transform the outputs of the three fault location methods into effective values. The min operator was used to aggregate effective values into aggregation possibility values. For the fitness assignment, the selective pressure  $SP=1.5$ . For the crossover operation,  $p_c=0.65$ . For the mutation operation,  $p_m=0.05$ .

Before obtaining optimal weights, the author investigated the performance of the min operator without weights in terms of the two objective functions. The objective values obtained using the min operators without weights are listed in Table 5.11.

TABLE 5.11 OBJECTIVE VALUES OBTAINED USING THE MIN OPERATOR WITHOUT WEIGHTS

	Objective value 1	Objective value 2
$p_1=0.95, p_2=0.2$	133	3255
$p_1=0.95, p_2=0.3$	133	3369
$p_1=0.95, p_2=0.4$	133	3485
$p_1=0.9, p_2=0.2$	144	3255
$p_1=0.9, p_2=0.3$	144	3369
$p_1=0.9, p_2=0.4$	144	3485
$p_1=0.8, p_2=0.2$	147	3255
$p_1=0.8, p_2=0.3$	147	3369
$p_1=0.8, p_2=0.4$	147	3485



Fuzzy resolver 11 used the transformation method in (3.28). 12 optimal weights that gave different objective values were obtained for  $p_1=0.95$  and  $p_2=0.2$ . 14 optimal weights that gave different objective values were obtained for  $p_1=0.95$  and  $p_2=0.3$ . 13 optimal weights that gave different objective values were obtained for  $p_1=0.95$  and  $p_2=0.4$ . 7 optimal weights that gave different objective values were obtained for  $p_1=0.9$  and  $p_2=0.2$ . 9 optimal weights that gave different objective values were obtained for  $p_1=0.9$  and  $p_2=0.3$ . 11 optimal weights that gave different objective values were obtained for  $p_1=0.9$  and  $p_2=0.4$ . 6 optimal weights that gave different objective values were obtained for  $p_1=0.8$  and  $p_2=0.2$ . 6 optimal weights that gave different objective values were obtained for  $p_1=0.8$  and  $p_2=0.3$ . 4 optimal weights that gave different objective values were obtained for  $p_1=0.8$  and  $p_2=0.4$ . Optimal weights that gave the extreme objective values and some other optimal weights are listed in Table 5.12. Comparing Table 5.12 with Table 5.11, when no weights were used, the second objective function obtained its maximum values. With using weights, it may be possible to increase the first objective value while keeping the second objective value equal to its maximum value. For example, when  $p_1=0.95$ ,  $p_2=0.2$ , the objective value 1 was equal to 133 without weights; it was increased to 135 with using weights. In addition, there were some optimal weights that increased the first objective value but simultaneously decreased the second objective value.

TABLE 5.12 OPTIMAL WEIGHTS OF THE MIN OPERATOR WITH RESPECT TO TWO OBJECTIVE FUNCTIONS AND USING THE FIRST TRANSFORMATION METHOD

Optimal weights			Objective value 1	Objective value 2
$w_1$	$w_2$	$w_3$		
Optimal weights when $p_1=0.95$ , $p_2=0.2$				
0.9843	0.5843	0.2275	135	3255
0.9490	0.0706	0.0118	161	3221
0.1216	0.0706	0.0275	172	2819

TABLE 5.12 CONTINUED

Optimal weights			Objective value 1	Objective value 2
$w_1$	$w_2$	$w_3$		
Optimal weights when $p_1=0.95, p_2=0.3$				
1.0000	1.0000	1.0000	133	3369
0.9490	0.9059	0.4824	134	3367
0.7176	0.0706	0.0392	165	3239
0.1216	0.0706	0.0039	172	2831
Optimal weights when $p_1=0.95, p_2=0.4$				
0.9059	1.0000	0.3725	134	3485
0.7255	1.0000	0.6000	138	3463
0.6039	0.0706	0.0471	168	3254
0.1216	0.0706	0.0196	172	2845
Optimal weights when $p_1=0.9, p_2=0.2$				
1.0000	0.4902	0.3020	145	3255
0.7961	0.1490	0.0157	170	3216
0.2510	0.1490	0.0980	172	2860
Optimal weights when $p_1=0.9, p_2=0.3$				
1.0000	1.0000	1.0000	144	3369
0.7765	0.1490	0.0667	170	3254
0.2510	0.1490	0.0667	172	2888
Optimal weights when $p_1=0.9, p_2=0.4$				
1.0000	1.0000	1.0000	144	3485
0.8078	0.1490	0.0314	170	3325
0.2510	0.1490	0.0471	172	2956
Optimal weights when $p_1=0.8, p_2=0.2$				
0.9725	0.4941	0.0078	154	3255
0.9961	0.3216	0.0157	171	3243
0.5216	0.3216	0.0784	172	3003
Optimal weights when $p_1=0.8, p_2=0.3$				
1.0000	1.0000	1.0000	147	3369
0.9765	0.3216	0.1255	171	3338
0.5294	0.3216	0.1922	172	3163
Optimal weights when $p_1=0.8, p_2=0.4$				
1.0000	1.0000	1.0000	147	3485
0.9137	0.3216	0.1255	171	3361
0.4392	0.3216	0.3098	172	3233

Fuzzy resolver 12 used the transformation method in (3.27). 4 optimal weights that gave different objective values were obtained for  $p_1=0.95$  and  $p_2=0.2$ . 8 optimal weights that gave different objective values were obtained for  $p_1=0.95$  and  $p_2=0.3$ . 10 optimal weights that gave different objective values were obtained for  $p_1=0.95$  and  $p_2=0.4$ . 4 optimal weights that gave different objective values were obtained for  $p_1=0.9$  and  $p_2=0.2$ . 4 optimal weights that gave different objective values were obtained for  $p_1=0.9$  and  $p_2=0.3$ . 5 optimal weights that gave different objective values were obtained for  $p_1=0.9$  and  $p_2=0.4$ . 3 optimal weights that gave different objective values were obtained for  $p_1=0.8$  and  $p_2=0.2$ . 4 optimal weights that gave different objective values were obtained for  $p_1=0.8$  and  $p_2=0.3$ . 5 optimal weights that gave different objective values were obtained for  $p_1=0.8$  and  $p_2=0.4$ . Optimal weights that gave the extreme objective values and some other optimal weights are listed in Table 5.13. Comparing Table 5.13 with Table 5.11, when no weights were used, the second objective function obtained its maximum values. With using weights, it may be possible to increase the first objective value while keeping the second objective value equal to its maximum value. For example, when  $p_1=0.95$ ,  $p_2=0.4$ , the objective value 1 was equal to 133 without weights; it was increased to 134 with using weights. In addition, there were some optimal weights that increased the first objective value but simultaneously decreased the second objective value.

TABLE 5.13 OPTIMAL WEIGHTS OF THE MIN OPERATOR WITH RESPECT TO TWO OBJECTIVE FUNCTIONS AND USING THE SECOND TRANSFORMATION METHOD

Optimal weights			Objective value 1	Objective value 2
$w_1$	$w_2$	$w_3$		
Optimal weights when $p_1=0.95, p_2=0.2$				
1.0000	1.0000	1.0000	133	3255
0.9451	0.0196	0.8039	161	3217
0.0353	0.0824	0.9608	172	1682

TABLE 5.13 CONTINUED

Optimal weights			Objective value 1	Objective value 2
$w_1$	$w_2$	$w_3$		
Optimal weights when $p_1=0.95, p_2=0.3$				
1.0000	1.0000	1.0000	133	3369
0.9961	0.7412	0.7961	134	3341
0.7333	0.0353	0.8118	165	2997
0.0706	0.0627	0.7020	172	1682
Optimal weights when $p_1=0.95, p_2=0.4$				
0.9333	1.0000	0.9686	134	3485
0.7373	1.0000	0.8275	138	3379
0.6118	0.0196	0.7765	168	2940
0.0314	0.0157	0.9686	172	1682
Optimal weights when $p_1=0.9, p_2=0.2$				
1.0000	1.0000	1.0000	144	3255
0.8196	0.0471	0.8902	170	2943
0.1294	0.1686	0.9451	172	1682
Optimal weights when $p_1=0.9, p_2=0.3$				
1.0000	1.0000	1.0000	144	3369
0.8078	0.1373	0.7882	170	3216
0.2863	0.0196	0.7843	172	1682
Optimal weights when $p_1=0.9, p_2=0.4$				
1.0000	1.0000	1.0000	144	3485
0.8157	0.1294	0.6588	170	3269
0.0667	0.1490	0.6118	172	1682
Optimal weights when $p_1=0.8, p_2=0.2$				
1.0000	1.0000	1.0000	147	3255
0.9843	0.0196	0.9490	171	3239
0.1647	0.0157	0.9294	172	1682
Optimal weights when $p_1=0.8, p_2=0.3$				
1.0000	1.0000	1.0000	147	3369
0.9922	0.2471	0.9020	171	3325
0.3882	0.0706	0.8275	172	1682
Optimal weights when $p_1=0.8, p_2=0.4$				
1.0000	1.0000	1.0000	147	3485
0.9843	0.0078	0.8314	171	3345
0.2706	0.1176	0.7490	172	1682

Comparing Table 5.12 with Table 5.13, fuzzy resolver 11 had better performance than fuzzy resolver 12 in terms of two objective values. That is, fuzzy resolver 11 made either more actual faulted sections have possibility values  $\geq p_1$  or more non-faulted sections have possibility values  $\leq p_2$  than fuzzy resolver 12. For example, when  $p_1=0.95$ ,  $p_2=0.2$ , fuzzy resolver 11 found optimal weights that gave objective values (135, 3255), (161, 3221), and (172, 2819); fuzzy resolver 12 found optimal weights that gave objective values (133, 3255), (161, 3217), and (172, 1682). When both fuzzy resolvers made the first objective value equal to 172, fuzzy resolver 11 made the second objective value equal to 2819 while fuzzy resolver 12 made the first objective value equal to 1682. Therefore, transformation method (3.28) was used to design the fuzzy resolver for the min operator.

Comparing Table 5.12 with Table 5.1, fuzzy resolver 1 may not be able to find a Pareto-optimal solution. For example, when  $p_1=0.95$  and  $p_2=0.3$ , fuzzy resolver 1 found optimal weights that made the two objective values equal to (172, 2059) while the Pareto-optimal solution in fuzzy resolver 11 was (172, 2831). The Pareto-optimal solution had better performance than the non Pareto-optimal solution because the Pareto-optimal solution achieved the same objective value in the first objective function but made more non-faulted sections have possibility values  $< p_2$ . Comparing Table 5.12 with Table 5.6, the similar observation could be found. Fuzzy resolver 6 may not be able to find a Pareto-optimal solution. Further, even when fuzzy resolver 1 or fuzzy resolver 6 was able to find a Pareto-optimal solution, fuzzy resolver 11 found the same Pareto-optimal solution. In addition, fuzzy resolver 11 found more Pareto-optimal solutions than fuzzy resolver 1 and fuzzy resolver 6.

#### 5.4.4 Optimal Weights for the OWA Operator

For the OWA operator, in addition to the optimal weights of three fault location methods, the optimal parameters of the OWA operator need to be found. The process for obtaining these optimal weights and optimal parameters is the same as the process

introduced in section 0. Transformation methods (3.29) and (3.30) were used to transform three fault location methods' outputs into effective values. The OWA operator was used to aggregate effective values into aggregation possibility values. For the fitness assignment, the selective pressure  $SP=1.5$ . For the crossover operation,  $p_c=0.65$ . For the mutation operation,  $p_m=0.05$ .

Before obtaining optimal weights, the author investigated the performance of the OWA operator in terms of the two objective functions without weights. 12 optimal parameters that gave different objective values were obtained for  $p_1=0.95$  and  $p_2=0.2$ . 11 optimal parameters that gave different objective values were obtained for  $p_1=0.95$  and  $p_2=0.3$ . 16 optimal parameters that gave different objective values were obtained for  $p_1=0.95$  and  $p_2=0.4$ . 5 optimal parameters that gave different objective values were obtained for  $p_1=0.9$  and  $p_2=0.2$ . 7 optimal parameters that gave different objective values were obtained for  $p_1=0.9$  and  $p_2=0.3$ . 9 optimal parameters that gave different objective values were obtained for  $p_1=0.9$  and  $p_2=0.4$ . 7 optimal parameters that gave different objective values were obtained for  $p_1=0.8$  and  $p_2=0.2$ . 11 optimal parameters that gave different objective values were obtained for  $p_1=0.8$  and  $p_2=0.3$ . 13 optimal parameters that gave different objective values were obtained for  $p_1=0.8$  and  $p_2=0.4$ . Optimal parameters that gave extreme objective values are listed in Table 5.14, where  $W_1$ ,  $W_2$ , and  $W_3$  are the parameters of the OWA operator.

TABLE 5.14 OBJECTIVE VALUES OBTAINED USING THE OWA OPERATOR WITHOUT WEIGHTS

Parameters			Objective value 1	Objective value 2
$W_1$	$W_2$	$W_3$		
Optimal weights when $p_1=0.95, p_2=0.2$				
0.0000	0.0000	1.0000	133	3255
0.0000	0.9020	0.0980	172	1626
Optimal weights when $p_1=0.95, p_2=0.3$				
0.0000	0.0000	1.0000	133	3369
0.0000	0.9059	0.0941	172	1633

TABLE 5.14 CONTINUED

Parameters			Objective value 1	Objective value 2
$W_1$	$W_2$	$W_3$		
Optimal weights when $p_1=0.95, p_2=0.4$				
0.0000	0.0000	1.0000	133	3485
0.0039	0.9020	0.0941	172	1635
Optimal weights when $p_1=0.9, p_2=0.2$				
0.0000	0.0000	1.0000	144	3255
0.0000	0.8000	0.2000	172	1626
Optimal weights when $p_1=0.9, p_2=0.3$				
0.0000	0.0000	1.0000	144	3369
0.0000	0.8078	0.1922	172	1633
Optimal weights when $p_1=0.9, p_2=0.4$				
0.0000	0.0000	1.0000	144	3485
0.0039	0.8000	0.1961	172	1647
Optimal weights when $p_1=0.8, p_2=0.2$				
0.0000	0.0000	1.0000	147	3255
0.0000	0.6196	0.3804	172	1633
Optimal weights when $p_1=0.8, p_2=0.3$				
0.0000	0.0000	1.0000	147	3369
0.0039	0.5961	0.4000	172	1647
Optimal weights when $p_1=0.8, p_2=0.4$				
0.0000	0.0000	1.0000	147	3485
0.0078	0.6039	0.3883	172	1688

Fuzzy resolver 13 used the transformation method in (3.30). 13 optimal weights and parameters that gave different objective values were obtained for  $p_1=0.95$  and  $p_2=0.2$ . 15 optimal weights and parameters that gave different objective values were obtained for  $p_1=0.95$  and  $p_2=0.3$ . 14 optimal weights and parameters that gave different objective values were obtained for  $p_1=0.95$  and  $p_2=0.4$ . 8 optimal weights and parameters that gave different objective values were obtained for  $p_1=0.9$  and  $p_2=0.2$ . 10 optimal weights and parameters that gave different objective values were obtained for  $p_1=0.9$  and  $p_2=0.3$ . 12 optimal weights and parameters that gave different objective values were obtained for  $p_1=0.9$  and  $p_2=0.4$ . 7 optimal weights and parameters that gave different objective values

were obtained for  $p_1=0.8$  and  $p_2=0.2$ . 7 optimal weights and parameters that gave different objective values were obtained for  $p_1=0.8$  and  $p_2=0.3$ . 5 optimal weights and parameters that gave different objective values were obtained for  $p_1=0.8$  and  $p_2=0.4$ . Optimal weights that gave the extreme objective values and some other optimal weights are listed in Table 5.15, where  $w_1$  is the weight for the operated device identification method,  $w_2$  is the weight for the phase selector method,  $w_3$  is the weight for the fault distance method,  $W_1$ ,  $W_2$ , and  $W_3$  are the parameters of the OWA operator. Comparing Table 5.15 with Table 5.14, fuzzy resolver 13 had better performance than the fuzzy resolver without weights in terms of two objective values. That is, fuzzy resolver 13 made either more actual faulted sections have possibility values  $\geq p_1$  or more non-faulted sections have possibility values  $\leq p_2$  than the fuzzy resolver without weights. For example, when  $p_1=0.95$ ,  $p_2=0.2$ , the fuzzy resolver without weights found optimal weights that gave objective values (133, 3255) and (172, 1626); fuzzy resolver 13 found optimal weights that gave objective values (135, 3255) and (172, 2819). When both fuzzy resolvers made the first objective value equal to 172, fuzzy resolver 13 made the second objective value equal to 2819 while the fuzzy resolver without weights made the first objective value equal to 1626.

TABLE 5.15 OPTIMAL WEIGHTS OF THE OWA OPERATOR WITH RESPECT TO TWO OBJECTIVE FUNCTIONS AND USING THE FIRST TRANSFORMATION METHOD

Optimal weights						Objective value 1	Objective value 2
$w_1$	$w_2$	$w_3$	$W_1$	$W_2$	$W_3$		
Optimal weights when $p_1=0.95, p_2=0.2$							
1.0000	0.5405	0.1529	0.0000	0.0039	0.9961	135	3255
0.9294	0.0706	0.0039	0.0000	0.0000	1.0000	161	3221
0.1216	0.0706	0.1216	0.0000	0.0000	1.0000	172	2819
0.1412	0.0824	0.0353	0.7137	0.2706	0.0157	0	5504



TABLE 5.15 CONTINUED

Optimal weights						Objective value 1	Objective value 2
$w_1$	$w_2$	$w_3$	$W_1$	$W_2$	$W_3$		
Optimal weights when $p_1=0.95, p_2=0.3$							
1.0000	0.9961	0.7216	0.0000	0.0118	0.9882	133	3369
0.9490	0.9333	0.5529	0.0000	0.0000	1.0000	134	3367
0.7176	0.0706	0.0235	0.0000	0.0000	1.0000	165	3239
0.1216	0.0706	0.2941	0.0000	0.0000	1.0000	172	2831
0.1451	0.2235	0.0196	0.9373	0.0627	0.0000	0	5504
Optimal weights when $p_1=0.95, p_2=0.4$							
0.9098	1.0000	0.1137	0.0000	0.0000	1.0000	134	3485
0.7294	1.0000	0.1059	0.0000	0.0000	1.0000	138	3463
0.6039	0.0706	0.0353	0.0000	0.0000	1.0000	168	3254
0.1216	0.0706	0.0353	0.0000	0.0000	1.0000	172	2845
0.2353	0.2353	0.1529	0.9451	0.0431	0.0117	0	5504
Optimal weights when $p_1=0.9, p_2=0.2$							
0.9843	0.4902	0.3098	0.0000	0.0039	0.9961	145	3255
0.7922	0.1490	0.0549	0.0000	0.0039	0.9961	170	3216
0.2510	0.1490	0.0549	0.0000	0.0000	1.0000	172	2860
0.0588	0.2000	0.0275	0.7686	0.1490	0.0824	0	5504
Optimal weights when $p_1=0.9, p_2=0.3$							
0.9882	0.8824	0.6863	0.0039	0.0039	0.9922	144	3369
0.7686	0.1490	0.0314	0.0000	0.0000	1.0000	170	3254
0.2510	0.1490	0.1059	0.0000	0.0000	1.0000	172	2888
0.0706	0.0588	0.0235	0.5843	0.3333	0.0824	0	5504
Optimal weights when $p_1=0.9, p_2=0.4$							
0.9804	1.0000	0.7569	0.0000	0.0000	1.0000	144	3485
0.7490	0.1490	0.2275	0.0000	0.0039	0.9961	170	3325
0.2510	0.1490	0.0588	0.0000	0.0000	1.0000	172	2956
0.2353	0.2353	0.1529	0.9451	0.0431	0.0117	0	5504
Optimal weights when $p_1=0.8, p_2=0.2$							
0.9765	0.4980	0.1765	0.0000	0.0039	0.9961	154	3255
0.9569	0.3216	0.1255	0.0000	0.0000	1.0000	171	3243
0.5216	0.3216	0.0784	0.0000	0.0000	1.0000	172	3003
0.0745	0.0549	0.0078	0.7176	0.2157	0.0667	0	5504

TABLE 5.15 CONTINUED

Optimal weights						Objective value 1	Objective value 2
$w_1$	$w_2$	$w_3$	$W_1$	$W_2$	$W_3$		
Optimal weights when $p_1=0.8, p_2=0.3$							
0.9882	0.9294	0.3647	0.0039	0.0039	0.9922	147	3369
0.9961	0.3216	0.0980	0.0000	0.0039	0.9961	171	3338
0.5294	0.3216	0.0588	0.0000	0.0000	1.0000	172	3163
0.0941	0.2784	0.0353	0.4549	0.5333	0.0118	0	5504
Optimal weights when $p_1=0.8, p_2=0.4$							
1.0000	1.0000	0.6549	0.0000	0.0000	1.0000	147	3485
0.9765	0.3216	0.2275	0.0000	0.0000	1.0000	171	3361
0.4902	0.3216	0.0392	0.0000	0.0000	1.0000	172	3233
0.2353	0.2353	0.1529	0.9451	0.0431	0.0118	0	5504

Fuzzy resolver 14 used the transformation method in (3.29). 5 optimal weights and parameters that gave different objective values were obtained for  $p_1=0.95$  and  $p_2=0.2$ . 9 optimal weights and parameters that gave different objective values were obtained for  $p_1=0.95$  and  $p_2=0.3$ . 11 optimal weights and parameters that gave different objective values were obtained for  $p_1=0.95$  and  $p_2=0.4$ . 5 optimal weights and parameters that gave different objective values were obtained for  $p_1=0.9$  and  $p_2=0.2$ . 5 optimal weights and parameters that gave different objective values were obtained for  $p_1=0.9$  and  $p_2=0.3$ . 6 optimal weights and parameters that gave different objective values were obtained for  $p_1=0.9$  and  $p_2=0.4$ . 4 optimal weights and parameters that gave different objective values were obtained for  $p_1=0.8$  and  $p_2=0.2$ . 5 optimal weights and parameters that gave different objective values were obtained for  $p_1=0.8$  and  $p_2=0.3$ . 6 optimal weights and parameters that gave different objective values were obtained for  $p_1=0.8$  and  $p_2=0.4$ . Optimal weights that gave the extreme objective values and some other optimal weights are listed in Table 5.16. Comparing Table 5.16 with Table 5.14, fuzzy resolver 14 had better performance than the fuzzy resolver without weights in terms of two objective values. That is, fuzzy resolver 14 made more actual faulted sections have possibility

values  $\geq p_1$ , or made more non-faulted sections have possibility values  $\leq p_2$  than the fuzzy resolver without weights. For example, when  $p_1=0.95$ ,  $p_2=0.2$ , the fuzzy resolver without weights found optimal weights that gave objective values (133, 3255) and (172, 1626); fuzzy resolver 14 found optimal weights that gave objective values (133, 3255) and (172, 1682). When both fuzzy resolvers made the first objective value equal to 172, fuzzy resolver 13 made the second objective value equal to 1682 while the fuzzy resolver without weights made the first objective value equal to 1626.

TABLE 5.16 OPTIMAL WEIGHTS OF THE OWA OPERATOR WITH RESPECT TO TWO OBJECTIVE FUNCTIONS AND USING THE SECOND TRANSFORMATION METHOD

Optimal weights						Objective value 1	Objective value 2
$w_1$	$w_2$	$w_3$	$W_1$	$W_2$	$W_3$		
Optimal weights when $p_1=0.95, p_2=0.2$							
1.0000	0.9333	0.9608	0.0000	0.0078	0.9922	133	3255
0.9529	0.0392	0.9922	0.0000	0.0039	0.9961	161	3217
0.0784	0.0078	0.9529	0.0000	0.0000	1.0000	172	1682
0.0902	0.1451	0.0353	0.9098	0.0471	0.0431	0	5504
Optimal weights when $p_1=0.95, p_2=0.3$							
0.9882	0.9843	0.9098	0.0000	0.0000	1.0000	133	3369
0.9961	0.7333	0.9725	0.0000	0.0039	0.9961	134	3341
0.7373	0.0235	0.9137	0.0000	0.0000	1.0000	165	2997
0.1020	0.0235	0.9725	0.0000	0.0078	0.9922	172	1682
0.1608	0.0157	0.1686	0.9137	0.0039	0.0824	0	5504
Optimal weights when $p_1=0.95, p_2=0.4$							
0.9255	1.0000	0.9333	0.0000	0.0000	1.0000	134	3485
0.7373	1.0000	0.9961	0.0000	0.0000	1.0000	138	3379
0.6118	0.0941	0.7843	0.0000	0.0000	1.0000	168	2940
0.0235	0.0392	0.9176	0.0000	0.0000	1.0000	172	1682
0.1333	0.1333	0.1529	0.8157	0.0235	0.1608	0	5504
Optimal weights when $p_1=0.9, p_2=0.2$							
0.9961	0.8667	0.9176	0.0000	0.0078	0.9922	144	3255
0.8196	0.1804	0.8392	0.0000	0.0039	0.9961	170	2943
0.0039	0.1294	0.9804	0.0000	0.0000	1.0000	172	1682
0.0000	0.1020	0.0392	0.8353	0.1490	0.0157	0	5504

TABLE 5.16 CONTINUED

Optimal weights						Objective value 1	Objective value 2
w <sub>1</sub>	w <sub>2</sub>	w <sub>3</sub>	W <sub>1</sub>	W <sub>2</sub>	W <sub>3</sub>		
Optimal weights when $p_1=0.9, p_2=0.3$							
1.0000	0.9412	0.9216	0.0000	0.0118	0.9882	144	3369
0.8118	0.0706	0.7098	0.0000	0.0000	1.0000	170	3216
0.0353	0.0784	0.8392	0.0000	0.0000	1.0000	172	1682
0.0314	0.0000	0.2627	0.8196	0.1725	0.0078	0	5504
Optimal weights when $p_1=0.9, p_2=0.4$							
0.9804	1.0000	0.8824	0.0000	0.0000	1.0000	144	3485
0.8196	0.1098	0.9725	0.0000	0.0039	0.9961	170	3269
0.0784	0.1059	0.9961	0.0000	0.0078	0.9922	172	1682
0.0941	0.0157	0.2863	0.8157	0.1647	0.0157	0	5504
Optimal weights when $p_1=0.8, p_2=0.2$							
1.0000	0.8549	0.8784	0.0000	0.0157	0.9843	147	3255
0.9922	0.0980	0.8863	0.0000	0.0039	0.9961	171	3239
0.1647	0.1373	0.8980	0.0000	0.0000	1.0000	172	1682
0.1725	0.0706	0.1725	0.9569	0.0392	0.0039	0	5504
Optimal weights when $p_1=0.8, p_2=0.3$							
1.0000	0.9412	0.8784	0.0000	0.0078	0.9922	147	3369
1.0000	0.3176	0.7843	0.0000	0.0000	1.0000	171	3325
0.2078	0.0196	0.8980	0.0000	0.0000	1.0000	172	1682
0.1333	0.2118	0.1569	0.8431	0.1490	0.0078	0	5504
Optimal weights when $p_1=0.8, p_2=0.4$							
0.9882	1.0000	0.9686	0.0000	0.0000	1.0000	147	3485
0.9922	0.1961	0.9059	0.0000	0.0039	0.9961	171	3345
0.2706	0.1137	0.9529	0.0000	0.0000	1.0000	172	1682
0.0510	0.0353	0.1765	0.4824	0.4667	0.0510	0	5504

Comparing Table 5.15 with Table 5.16, fuzzy resolver 13 had better performance than fuzzy resolver 14 in terms of two objective values. That is, fuzzy resolver 13 made either more actual faulted sections have possibility values  $\geq p_1$  or more non-faulted sections have possibility values  $\leq p_2$  than fuzzy resolver 14 does. For example, when  $p_1=0.95, p_2=0.2$ , fuzzy resolver 13 found optimal weights that gave objective values (0, 5504), (135, 3255), (161, 3221), and (172, 2819); fuzzy fuzzy resolver 14 found optimal weights

that gave objective values (0, 5504), (133, 3255), (161, 3217), and (172, 1682). When both fuzzy resolvers made the first objective value equal to 172, fuzzy resolver 13 made the second objective value equal to 2819 while fuzzy resolver 12 made the first objective value equal to 1682. Therefore, transformation method (3.30) was used to design the fuzzy resolver for the OWA operator.

Comparing Table 5.15 with Table 5.3, fuzzy resolver 3 may not be able to find a Pareto-optimal solution. For example, when  $p_1=0.95$  and  $p_2=0.3$ , fuzzy resolver 3 might find optimal weights that made two objective values equal to (172, 2822) while the Pareto-optimal solution in fuzzy resolver 13 was (172, 2831). The Pareto-optimal solution had better performance than the non Pareto-optimal solution because the Pareto-optimal solution achieved the same objective value in the first objective function but made more non-faulted sections have possibility values  $< p_2$ . Comparing Table 5.15 with Table 5.8, the solution of fuzzy resolver 8 was one of the Pareto-optimal solutions of fuzzy resolver 13. Further, even when fuzzy resolver 3 was able to find a Pareto-optimal solution, fuzzy resolver 13 found the same Pareto-optimal solution. In addition, fuzzy resolver 13 found more Pareto-optimal solutions than fuzzy resolver 3.

#### **5.4.5 Optimal Weights for the Uninorm Operator**

For the uninorm operator, only the optimal weights of three fault location methods need to be found. The process for obtaining these optimal weights is the same as the process introduced in 0. Transformation method (3.31) was used to transform three fault location methods' outputs into effective values. The uninorm operator was used to aggregate effective values into aggregation possibility values. For the fitness assignment, the selective pressure  $SP=1.5$ . For the crossover operation,  $p_c=0.65$ . For the mutation operation,  $p_m=0.05$ .

Before obtaining optimal weights, the author investigated the performance of the uninorm operator without weights in terms of the two objective functions. The objective values obtained using the uninorm operators without weights are listed in Table 5.17.

TABLE 5.17 OBJECTIVE VALUES OBTAINED USING THE UNINORM OPERATOR WITHOUT WEIGHTS

	Objective value 1	Objective value 2
$p_1=0.95, p_2=0.2$	172	3255
$p_1=0.95, p_2=0.3$	172	3369
$p_1=0.95, p_2=0.4$	172	3485
$p_1=0.9, p_2=0.2$	172	3255
$p_1=0.9, p_2=0.3$	172	3369
$p_1=0.9, p_2=0.4$	172	3485
$p_1=0.8, p_2=0.2$	172	3255
$p_1=0.8, p_2=0.3$	172	3369
$p_1=0.8, p_2=0.4$	172	3485

Fuzzy resolver 15 used the transformation method in (3.31). 1 optimal weight was obtained for  $p_1=0.95$  and  $p_2=0.2$ . 1 optimal weight was obtained for  $p_1=0.95$  and  $p_2=0.3$ . 1 optimal weight was obtained for  $p_1=0.95$  and  $p_2=0.4$ . 1 optimal weight was obtained for  $p_1=0.9$  and  $p_2=0.2$ . 1 optimal weight was obtained for  $p_1=0.9$  and  $p_2=0.3$ . 1 optimal weight was obtained for  $p_1=0.9$  and  $p_2=0.4$ . 1 optimal weight was obtained for  $p_1=0.8$  and  $p_2=0.2$ . 1 optimal weight was obtained for  $p_1=0.8$  and  $p_2=0.3$ . 1 optimal weight was obtained for  $p_1=0.8$  and  $p_2=0.4$ . All of these obtained optimal weights and their corresponding objective values are listed in Table 5.18, where  $w_1$  is the weight for the operated device identification method,  $w_2$  is the weight for the phase selector method,  $w_3$  is the weight for the fault distance method. Comparing Table 5.18 with Table 5.17, fuzzy resolver 15 obtained the same objective values as the fuzzy resolver without weights. From (3.31), it is seen that the effective value  $a'$  is equal to  $a$  when the weight  $w$  is 1. That is, no weight is equivalent to  $w=1$ . It is also observed that when  $w$  decreases, the transformation method tries to make the effective value closer to  $g$ . That is, when  $a > g$ ,  $a' < a$ ; when  $a < g$ ,  $a' > a$ . Therefore, this transformation tends to reduce the difference between high possibility values and low possibility values when  $w$  decreases. Hence, the

fuzzy resolver without weights has better performance than fuzzy resolver 15 in terms of the difference between high possibility values and low possibility values.

TABLE 5.18 OPTIMAL WEIGHTS OF THE UNINORM OPERATOR WITH RESPECT TO TWO OBJECTIVE FUNCTIONS

Optimal weights			Objective value 1	Objective value 2
$w_1$	$w_2$	$w_3$		
Optimal weights when $p_1=0.95, p_2=0.2$				
1.0000	1.0000	1.0000	172	3255
Optimal weights when $p_1=0.95, p_2=0.3$				
1.0000	1.0000	0.9569	172	3369
Optimal weights when $p_1=0.95, p_2=0.4$				
1.0000	1.0000	0.8510	172	3485
Optimal weights when $p_1=0.9, p_2=0.2$				
0.9961	1.0000	0.8000	172	3255
Optimal weights when $p_1=0.9, p_2=0.3$				
1.0000	1.0000	0.8941	172	3369
Optimal weights when $p_1=0.9, p_2=0.4$				
0.9961	1.0000	0.8980	172	3485
Optimal weights when $p_1=0.8, p_2=0.2$				
1.0000	1.0000	0.8078	172	3255
Optimal weights when $p_1=0.8, p_2=0.3$				
1.0000	1.0000	0.9843	172	3369
Optimal weights when $p_1=0.8, p_2=0.4$				
1.0000	1.0000	0.9294	172	3485

Comparing Table 5.15 with Table 5.3, fuzzy resolver 3 may not be able to find a Pareto-optimal solution. For example, when  $p_1=0.95$  and  $p_2=0.3$ , fuzzy resolver 3 might found optimal weights that made two objective values equal to (172, 2822) while the Pareto-optimal solution in fuzzy resolver 13 was (172, 2831). The Pareto-optimal solution had better performance than the non Pareto-optimal solution because the Pareto-optimal solution achieved the same objective value in the first objective function

but made more non-faulted sections have possibility values  $< p_2$ . Comparing Table 5.15 with Table 5.8, the solution of fuzzy resolver 8 was one of the Pareto-optimal solutions of fuzzy resolver 13. Further, even when fuzzy resolver 3 was able to find a Pareto-optimal solution, fuzzy resolver 13 found the same Pareto-optimal solution. In addition, fuzzy resolver 13 found more Pareto-optimal solutions than fuzzy resolver 3.

Comparing Table 5.18 with Table 5.5, fuzzy resolver 5 may not be able to find a Pareto-optimal solution. For example, when  $p_1=0.9$  and  $p_2=0.3$ , fuzzy resolver 5 might find optimal weights that made two objective values equal to (172, 3294), while the Pareto-optimal solution in fuzzy resolver 13 was (172, 3369). Comparing Table 5.18 with Table 5.10, a similar observation was made. Fuzzy resolver 10 may not be able to find a Pareto-optimal solution. Further, even when fuzzy resolver 5 or fuzzy resolver 10 was able to find a Pareto-optimal solution, fuzzy resolver 15 found the same Pareto-optimal solution.

Comparing the objective values of three aggregation operators, the OWA operator achieved the same objective values as the min operator. In addition, it had one set of weights that made all non-faulted sections (5504) have possibility values  $< p_2$  and 0 actual faulted sections have possibility values  $\geq p_1$ . For both of these two operators, there were several Pareto-optimal solutions. One Pareto-optimal solution maximized the first objective function. Another Pareto-optimal solution maximized the second objective function. Other Pareto-optimal made a compromise between these two objective functions and had moderate performance on two objective functions. The uninorm operator had better performance than the min operator in terms of two objective values. That is, fuzzy resolver 15 made more actual faulted sections have possibility values  $\geq p_1$ , or more non-faulted sections have possibility values  $\leq p_2$  than fuzzy resolver 11. For example, when  $p_1=0.95$ ,  $p_2=0.2$ , fuzzy resolver 11 found optimal weights that gave objective values (135, 3255), (161, 3221), and (172, 2819); fuzzy fuzzy resolver 15 found optimal weights that gave objective values (172, 3255). Obviously, (172, 3255)



dominated (135, 3255), (161, 3221), and (172, 2819). Similarly, the solution of the uninorm operator dominated most solutions of the OWA operator except solution (0, 5504).

#### 5.4.6 Summary

In the above sections, the author studied fuzzy resolvers with respect to two objective functions. Three fuzzy aggregation operators were used. For the min operator and OWA operator, fuzzy resolvers were designed using two transformation methods. From the results, the better transformation method for the min operator is (3.28), and the better transformation method for the OWA operator is (3.30). Comparing fuzzy resolvers designed using two objective functions with fuzzy resolvers designed using only one objective function, fuzzy resolvers designed using only one objective function may not be able to find Pareto-optimal solutions. Even when resolvers designed using only one objective function can find Pareto-optimal solutions, fuzzy resolvers using two objective functions can find not only the same solutions but also other Pareto-optimal solutions. For the min operator and OWA operator, the fuzzy resolver with weights has better performance than the fuzzy resolver without weights in terms of two objective functions. For the uninorm operators, the fuzzy resolver with using weights has the same performance as the fuzzy resolver without weights in terms of two objective functions. In terms of the difference between high possibility values and low possibility values, the fuzzy resolver without weights gives better performance than the fuzzy resolver using weights. Comparing three fuzzy aggregation operators, the uninorm operator has better performance than the min operator and OWA operator.

In summary, the fuzzy resolver designed using the uninorm operator without weights yields the best performance. The fuzzy resolver designed using the min operator and OWA operator with weights make all actual faulted sections have possibility values  $\geq p_1$  but they make less non-faulted sections have possibility values  $< p_2$  than the fuzzy resolver designed using the uninorm operator. For the fuzzy resolvers designed using the

min operator, fuzzy resolver 11 (which uses weights) is better than fuzzy resolver 12 (which uses weights). For the fuzzy resolvers designed using the OWA operator, fuzzy resolver 13 (which uses weights) is better than fuzzy resolver 14 (which uses weights). The author compared the performance of various fuzzy resolvers in term of two objective functions. The different fuzzy resolvers and their performance are listed in Table 5.19.

The methodology for designing a fuzzy resolver would entail selecting the most effective operator and optimal weights. Based on the training analysis, using simulated data, performed on the fifteen fuzzy resolvers studied in this chapter, fuzzy resolver 11, 13, 15, and the fuzzy resolver using the uninorm operator without weights showed the best potential. These fuzzy resolvers identified all faulted line sections as potential faulted sections and identified as many as possible non-faulted sections as non-faulted sections. Therefore, system operators just need to locate a fault from a small number of line sections. These fuzzy resolvers were studied further using the test set of the simulated data. Results of the studies are presented in chapter 6.

## **5.5 CHAPTER SUMMARY**

In this chapter, three fuzzy aggregation operators were used to design various fuzzy resolvers using the training set of the simulated data. For the min operator and OWA operator, two transformation methods were used to design two different fuzzy resolvers. The optimal weights and parameters of fuzzy resolvers were obtained with respect to each objective function separately, and with respect to two objective functions together.

In the next chapter, 336 test cases are used in some performance studies. The performance of these fuzzy resolvers designed using three operators with respect to two objective functions (fuzzy resolver 11, 13, and 15) are compared with each other. The performance of fuzzy resolvers designed with respect to two objective functions (fuzzy resolver 11, 13, and 15) are compared with fuzzy resolvers designed with respect to the first objective function (fuzzy resolver 1, 3, and 5). The performance of fuzzy resolvers designed with respect to two objective functions (fuzzy resolver 11, 13, and 15) are

compared with fuzzy resolvers without weights. For these studies, transformation method (3.28) is used for the min operator, and transformation method (3.30) is used for the OWA operator.

TABLE 5.19 SUMMARIES OF FUZZY RESOLVERS

Fuzzy resolver	Operator	Transformation	Objective function	Performance
1	Min	(3.28)	(3.32)	May not achieve the Pareto-optimal solution. Even when achieving the Pareto-optimal solution, it is one of the Pareto-optimal solutions obtained using fuzzy resolvers 11, 12, 13, 14, and 15
2	Min	(3.27)	(3.32)	
3	OWA	(3.30)	(3.32)	
4	OWA	(3.29)	(3.32)	
5	Uninorm	(3.31)	(3.32)	
6	Min	(3.28)	(3.34)	May not achieve the Pareto-optimal solution. Even when achieving the Pareto-optimal solution, it is one of the Pareto-optimal solutions obtained using fuzzy resolvers 11, 12, 13, 14, and 15
7	Min	(3.27)	(3.34)	
8	OWA	(3.30)	(3.34)	
9	OWA	(3.29)	(3.34)	
10	Uninorm	(3.31)	(3.34)	
11	Min	(3.28)	Both	Achieves Pareto-optimal solutions that dominate Pareto-optimal solutions obtained using fuzzy resolver 12
12	Min	(3.27)	Both	
13	OWA	(3.30)	Both	Achieves Pareto-optimal solutions that dominate Pareto-optimal solutions obtained using fuzzy resolver 14
14	OWA	(3.29)	Both	
15	Uninorm	(3.31)	Both	Achieves a Pareto-optimal solution that dominates the solutions of fuzzy resolvers 11, 12, 13, and 14
	Min		Without weights	May not achieve the Pareto-optimal solution. Even when achieving the Pareto-optimal solution, it is one of the Pareto-optimal solutions obtained using fuzzy resolvers 11 and 12.
	OWA		Without weights	May not achieve the Pareto-optimal solution. Even when achieving the Pareto-optimal solution, it is one of the Pareto-optimal solutions obtained using fuzzy resolvers 13 and 14.
	Uninorm		Without weights	Achieves the same Pareto-optimal solution as fuzzy resolver 15. It has better performance than fuzzy resolver 15 because it keeps the difference between low possibility values and high possibility values as large as possible.

## **CHAPTER VI**

### **STUDIES AND RESULTS**

#### **6.1 INTRODUCTION**

In the previous chapter, three fuzzy aggregation operators and several transformation methods were used to design various fuzzy resolvers. The optimal weights of these fuzzy resolvers were obtained using the training data set. The two objective values obtained from the fuzzy resolvers designed with respect to two objective functions were compared with those obtained from the fuzzy resolvers designed with respect to a single objective function. The two objective values obtained from the fuzzy resolvers designed using weights were compared with those obtained from the fuzzy resolvers designed without weights. The two objective values obtained from the fuzzy resolvers designed using different fuzzy aggregation operators were compared with each other. The purpose of these studies was to find the most effective operators and optimal weights. Based on the training analysis performed on the fifteen studied fuzzy resolvers, fuzzy resolvers designed with respect to two objective functions (fuzzy resolver 11, 13, 15) and the fuzzy resolver using the uninorm operator without weights showed the best potential. These fuzzy resolvers were studied further using a test set of simulated data.

The remaining 336 simulated fault cases were used to test the performance of the four promising fuzzy resolvers. Some selected results of those studies are presented in the following sections. For these studies, transformation method (3.28) was used for the min operator, and transformation method (3.30) was used for the OWA operator. Through these studies, the optimal weights that obtained the best performance were chosen for each aggregation operator. A case study was implemented using these optimal weights.

In order to study the performance of fuzzy resolvers, the maximum achievable number of actual faulted sections that could be designated as potential faulted sections and the maximum achievable number of non-faulted sections whose possibility values were distinguishable from faulted sections in the test set was used as a benchmark. There were

336 cases in the test set. Therefore, the maximum achievable number of actual faulted sections that could be designated as potential faulted sections was 336. In Table 4.8, it was stated that there were 4196 non-distinguishable non-faulted line sections in the test set, and there were 10,752 total non-faulted sections. Hence, the maximum achievable number of non-faulted sections whose possibility values were distinguishable from faulted sections was 6556 ( $=10752-4196$ ). Therefore, the maximum achievable percentage of actual faulted sections that were designated as potential faulted sections was 100%. The maximum achievable percentage of non-faulted sections whose possibility values were distinguishable from faulted sections was 60.97% ( $=6556/10752$ ).

## 6.2 CASE STUDY

Through the design process, for the min and OWA operator, one of the Pareto-optimal weights that made all the actual faulted sections have a possibility value  $\geq p_1$  ( $=0.8$ ) was  $[0.5216 \ 0.3216 \ 0.0784]$  and  $[0.5294 \ 0.3216 \ 0.0588 \ 0.0000 \ 0.0000 \ 1.0000]$ , respectively. For the uninorm operator, the fuzzy resolver without weights obtained the best performance. In this section, a case study was performed to show the results of the fuzzy resolvers designed using the min and OWA operators with the optimal weights  $[0.5216 \ 0.3216 \ 0.0784]$  and  $[0.5294 \ 0.3216 \ 0.0588 \ 0.0000 \ 0.0000 \ 1.0000]$ , respectively, and the fuzzy resolver designed using the uninorm operator without weights. In this case study and the following performance studies, the  $\alpha$ -level as shown in Figure 6.1 was used to classify faulted sections and non-faulted sections. The line sections with a possibility value greater than or equal to the  $\alpha$ -level were identified as potential faulted sections, while the line sections with a possibility value less than the  $\alpha$ -level were identified as non-faulted sections. In Figure 6.1, line sections within  $[a, b]$  and  $[c, d]$  are identified as potential faulted sections. In this case study and the following performance studies, 0.8 was used as the  $\alpha$ -level.

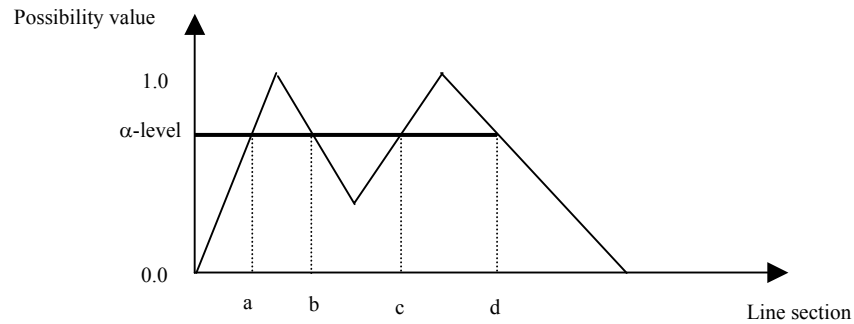


Figure 6.1 Illustration of the  $\alpha$ -level

A phase A to G fault staged on line section 8 (between node 816 and 818) with an  $80\Omega$  fault resistance was used for this study. For this case, the three fault location methods assigned possibility values for each line section as shown in Table 6.1 and Figure 6.2. In the table, PS stands for the phase selector method; FD stands for the fault distance method; ODIM stands for the operated device identification method. From this table, it is seen that the phase selector method identified 28 sections (1, 2, 3, 5, 6, 7, 8, 9, 10, 11, 13, 14, 15, 16, 17, 18, 19, 20, 21, 22, 23, 24, 25, 26, 28, 29, 30, 31, and 33) as potential faulted sections with a possibility value 0.9933. The fault distance method identified all 33 line sections as potential faulted sections with a possibility value 1.0000. The operated device identification method assigned the largest possibility value 0.6581 to sections 8, 10, and 11. Since no line sections were assigned a possibility value greater than or equal to 0.8, this method did not identify any sections as potential faulted sections.

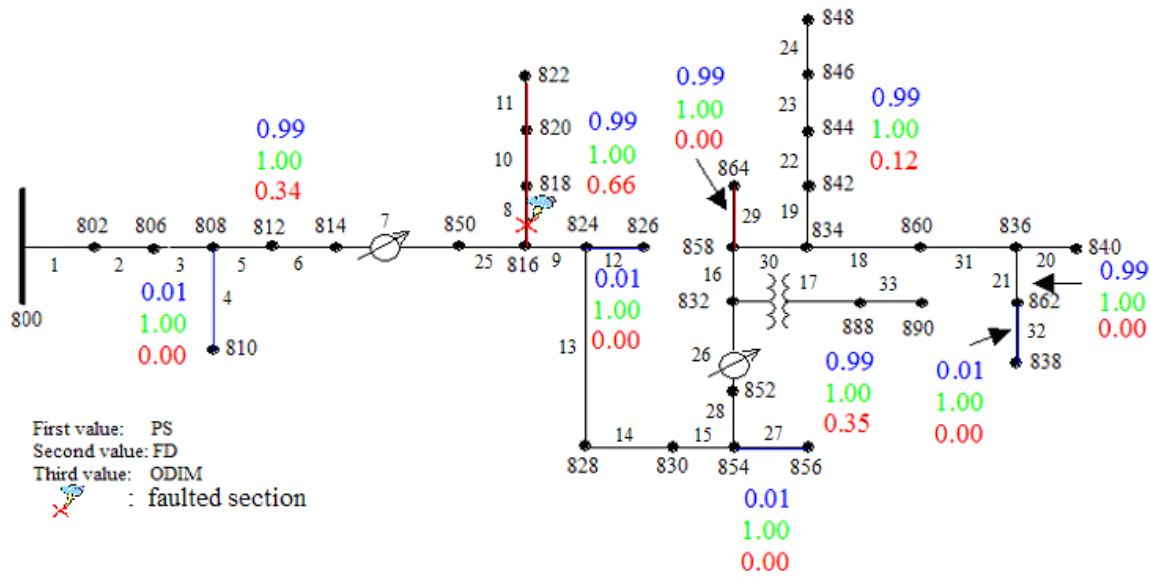


Figure 6.2 Outputs of the three fault location methods

TABLE 6.1 OUTPUTS OF THE THREE FAULT LOCATION METHODS

	Section								
	1	2	3	4	5	6	7	8	9
PS	0.9933	0.9933	0.9933	0.0067	0.9933	0.9933	0.9933	0.9933	0.9933
FD	1.0000	1.0000	1.0000	1.0000	1.0000	1.0000	1.0000	1.0000	1.0000
ODIM	0.3419	0.3419	0.3419	0.0000	0.3419	0.3419	0.3419	0.6581	0.3419
	10	11	12	13	14	15	16	17	18
PS	0.9933	0.9933	0.0067	0.9933	0.9933	0.9933	0.9933	0.9933	0.9933
FD	1.0000	1.0000	1.0000	1.0000	1.0000	1.0000	1.0000	1.0000	1.0000
ODIM	0.6581	0.6581	0.0000	0.3419	0.3419	0.3419	0.3419	0.3468	0.3419
	19	20	21	22	23	24	25	26	27
PS	0.9933	0.9933	0.9933	0.9933	0.9933	0.9933	0.9933	0.9933	0.0067
FD	1.0000	1.0000	1.0000	1.0000	1.0000	1.0000	1.0000	1.0000	1.0000
ODIM	0.1231	0.3419	0.0000	0.1231	0.1231	0.1231	0.3419	0.3419	0.0000
	28	29	30	31	32	33			
PS	0.9933	0.9933	0.9933	0.9933	0.0067	0.9933			
FD	1.0000	1.0000	1.0000	1.0000	1.0000	1.0000			
ODIM	0.3419	0.0000	0.3419	0.3419	0.0000	0.3468			



The outputs of three fuzzy resolvers are shown in Table 6.2 and Figure 6.3. From this table, it can be observed that all three fuzzy resolvers identified sections 8, 10, and 11 as potential faulted sections because they had possibility values larger than 0.8 (the  $\alpha$ -level), and identified all other sections as non-faulted sections. For these output results, the operator would have only three of 33 sections identified as potential faulted sections. The min operator based method gave potential faulted sections a possibility value 0.8039; the OWA operator based method gave potential faulted sections a possibility value 0.8013; and the uninorm operator based method gave potential faulted sections a possibility value 1.0000. The maximum possibility values of non-faulted sections were 0.5714, 0.5666, and 0.3419 for the min, OWA, and uninorm operator based methods, respectively. From this study, the uninorm operator based method has better performance than the other two operators because it gives the faulted section a larger possibility value and gives distinguishable non-faulted sections lower possibility values.

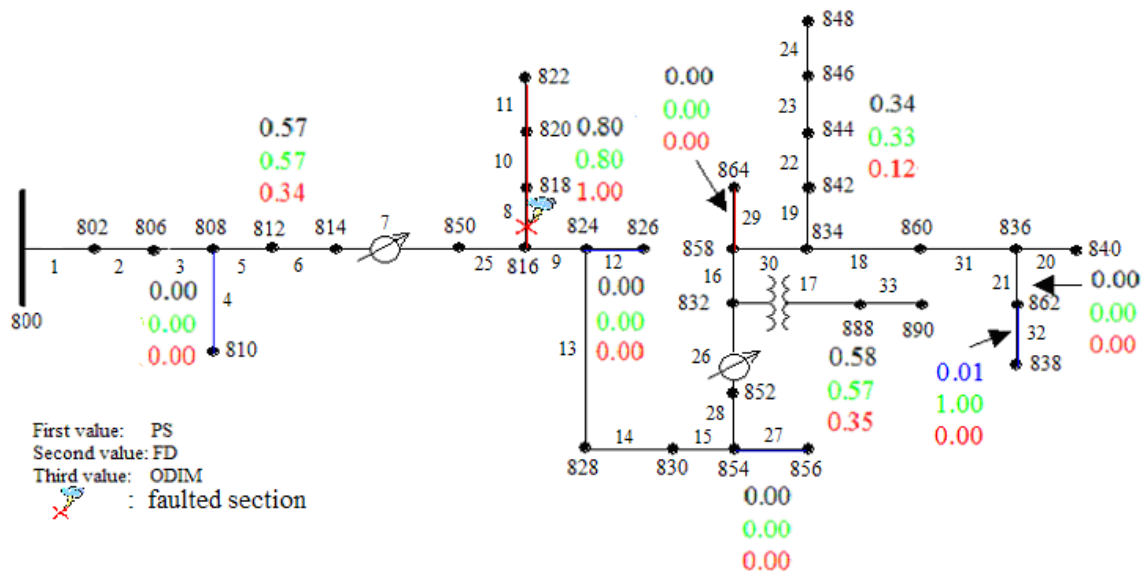


Figure 6.3 Outputs of fuzzy resolvers

TABLE 6.2 OUTPUTS OF FUZZY RESOLVERS

	Section								
	1	2	3	4	5	6	7	8	9
Min	0.5714	0.5714	0.5714	0.0000	0.5714	0.5714	0.5714	0.8039	0.5714
OWA	0.5666	0.5666	0.5666	0.0000	0.5666	0.5666	0.5666	0.8013	0.5666
Uninorm	0.3419	0.3419	0.3419	0.0000	0.3419	0.3419	0.3419	1.0000	0.3419
	10	11	12	13	14	15	16	17	18
Min	0.8039	0.8039	0.0000	0.5714	0.5714	0.5714	0.5714	0.5756	0.5714
OWA	0.8013	0.8013	0.0000	0.5666	0.5666	0.5666	0.5666	0.5709	0.5666
Uninorm	1.0000	1.0000	0.0000	0.3419	0.3419	0.3419	0.3419	0.3468	0.3419
	19	20	21	22	23	24	25	26	27
Min	0.3353	0.5714	0.0000	0.3353	0.3353	0.3353	0.5714	0.5714	0.0000
OWA	0.3299	0.5666	0.0000	0.3299	0.3299	0.3299	0.5666	0.5666	0.0000
Uninorm	0.1231	0.3419	0.0000	0.1231	0.1231	0.1231	0.3419	0.3419	0.0000
	28	29	30	31	32	33			
Min	0.5714	0.0000	0.5714	0.5714	0.0000	0.5756			
OWA	0.5666	0.0000	0.5666	0.5666	0.0000	0.5709			
Uninorm	0.3419	0.0000	0.3419	0.3419	0.0000	0.3468			

### 6.3 FUZZY FAULT LOCATION SCHEME

There were three fault location methods in the new fault location scheme. The fault resistance affected the accuracy of the fault distance method significantly. When a fault was a middle resistance fault or high resistance fault, the method identified all line sections as potential faulted sections and assigned the possibility value 1 to all line sections. The phase selector method assigned each phase a possibility value to represent the possibility that the phase was involved in the fault. A line section was assigned a possibility value based on the presence of phases on the line section. The fault resistance affected the magnitude of the fault current increment and therefore affected the possibility values assigned to all line sections. For some high resistance faults where the fault current increments were too small, the phase selector method might assign a small possibility value to the faulted phases and did not identify any line section as potential faulted sections. For a fault, the operated device identification method assigned

possibility values to each protective device indicating the possibility that the protective device was involved in the fault (operated when the fault occurred). For some high impedance faults where the fault currents were less than protective device's pickup values, no protective devices operated and no protective devices were identified as being involved in the fault. Therefore, the ODIM method identified all line sections as potential faulted sections. For some single phase to ground faults staged on laterals, the ODIM method assigned a small possibility value ( $<0.8$ ) to the operated protective device and therefore did not identify any line section as potential faulted sections. Hence, each method had its own individual shortcomings and did not give satisfactory results for some situations.

The fuzzy resolvers were designed to reduce these problems and identify a smaller subset of line sections as potential faulted sections than individual fault location methods. By aggregating the three fault location methods' outputs, the fuzzy resolvers achieved this objective. However, for a line section for which all three fault location methods assigned the same possibility values as the actual faulted section, fuzzy resolvers were not able to distinguish this non-faulted section from the actual faulted section.

#### **6.4 PERFORMANCE STUDIES**

The performance of a fuzzy resolver fault location method was measured based on its ability for a fault occurrence to assign a high possibility value to the actual faulted section and low possibility values to the non-faulted sections. Since, practically speaking, the methods usually identify some of the non-faulted sections as faulted sections, the quality of the performance of the fuzzy resolver fault location ultimately is measured by the number of potential faulted sections the method identifies. The smaller value of this number, the better a fuzzy resolver performs.

A good fuzzy resolver should be able to correctly identify the actual faulted line section as one of the potential faulted sections and should not identify distinguishable non-faulted sections as potential faulted sections. The best fuzzy resolver should achieve

the result that both the percentage of correctly identified actual faulted sections and the percentage of correctly identified distinguishable non-faulted sections are equal to 100%. The three fault location methods were executed for the 336 fault cases in the test set. The output results were possibility values for all line sections. Nine fuzzy resolvers were executed which aggregated the outputs of the three fault location methods and assigned an aggregation possibility value to each line section for each test case. After these aggregation possibility values were obtained, the percentage of faulted sections that were identified as potential faulted sections (correctly identified actual faulted sections), the percentage of distinguishable non-faulted sections that were identified as non-faulted sections (correctly identified distinguishable non-faulted sections), and the percentage of non-faulted sections that were identified as non-faulted sections (identified non-faulted sections) were obtained. These percentages were used to evaluate the performance of the nine fuzzy resolvers. In the following sections, the results of three studies are discussed. The three studies and the fuzzy resolvers used in each study are listed in Table 6.3.

#### **6.4.1 Comparison of the Performance of the Fuzzy Resolvers Designed Using Different Operators with Respect to Two Objective Functions**

This study is to evaluate the performance of the fuzzy resolvers designed using three aggregation operators with respect to two objective functions. The three fuzzy resolvers were used to aggregate three fault location methods' outputs. The percentage of correctly identified actual faulted sections ( $=\frac{\text{the number of correctly identified actual faulted sections}}{336}$ ), the percentage of correctly identified distinguishable non-faulted sections ( $=\frac{\text{the number of correctly identified distinguishable non-faulted sections}}{6556}$ ), and the percentage of identified non-faulted sections ( $=\frac{\text{the number of identified non-faulted sections}}{10752}$ ) are summarized in Table 6.4-Table 6.6, respectively.

TABLE 6.3 FUZZY RESOLVERS USED IN STUDIES

	Study	Fuzzy resolver
1	Comparison of the performance of the fuzzy resolvers designed using different operators with respect to two objective functions	(a) Min operator with respect to two objective functions and with transformation method (3.28); (b) OWA operator with respect to two objective functions and with transformation method (3.30); (c) Uninorm operator with respect to two objective functions and with transformation method (3.31)
2	Comparison of the performance of the fuzzy resolvers designed with respect to the first objective function and the fuzzy resolvers designed with respect to two objective functions	(a) Fuzzy resolvers in study 1; (b) Min operator with respect to the first objective function and with transformation method (3.28); (c) OWA operator with respect to the first objective function and with transformation method (3.30); (d) Uninorm operator with respect to the first objective function and with transformation method (3.31)
3	Comparison of the performance of the fuzzy resolvers designed with respect to two objective functions and the fuzzy resolvers without weights	(a) Fuzzy resolvers in study 1; (b) Min operator without weights; (c) OWA operator without weights; (d) Uninorm operator without weights

From Table 6.4 and Table 6.5, for the fuzzy resolvers designed using the min and OWA operators, a set of weights achieved a larger percentage of correctly identified actual faulted sections than another set of weights while it achieved a smaller percentage of correctly identified distinguishable non-faulted sections and a smaller percentage of identified non-faulted sections than that set of weights. Only several optimal weights of the fuzzy resolvers designed using the min operator and OWA operator identified all actual faulted sections as potential faulted sections. However, most of these weights identified some distinguishable non-faulted sections as potential faulted sections. For example, with using the optimal weight [0.2510 0.1490 0.0667] in Table 6.4 that was obtained when  $p_1=0.9$  and  $p_2=0.3$ , the fuzzy resolver designed using the min operator

identified 92.68% of distinguishable non-faulted sections as non-faulted sections. 7.32% of distinguishable non-faulted sections were identified as potential faulted sections. For the optimal weights that identified 100% of actual faulted sections as potential faulted sections, when  $p_1$  was closer to the  $\alpha$ -level, the percentage of correctly identified distinguishable non-faulted became closer to 100%; when  $p_1$  was equal to the  $\alpha$ -level, which was 0.8, the percentage of correctly identified distinguishable non-faulted sections was equal to 100%. For example, for the optimal weights that identified 100% of actual faulted sections as potential faulted sections, when the  $\alpha$ -level was equal to 0.95, 0.9, and 0.8, the percentage of correctly identified distinguishable sections was equal to 92.68%, 96.89%, and 100%, respectively. In addition, for the fuzzy resolver designed using the OWA operator, there was a set of weights that identified all non-faulted sections as non-faulted sections, i.e., the percentage of identified non-faulted sections was equal to 100%. However, for this set of weights, the percentage of correctly identified non-distinguishable sections was equal to 0%. Therefore, it was not a desirable set of weights.

TABLE 6.4 RESULTS OF THE FUZZY RESOLVER DESIGNED USING THE MIN OPERATOR WITH RESPECT TO TWO OBJECTIVE FUNCTIONS

Optimal weights			% of faulted sect $\geq$ 0.8	% of distinguishable non-faulted sect $<$ 0.8	% of non-Faulted Sect $<$ 0.8
$w_1$	$w_2$	$w_3$			
Pareto-optimal weights when $p_1=0.95, p_2=0.2$					
0.9843	0.5843	0.2275	89.29	100.00	68.15
0.9490	0.0706	0.0118	98.81	96.75	59.09
0.1216	0.0706	0.0275	100.00	92.68	56.48
Pareto-optimal weights when $p_1=0.95, p_2=0.3$					
1.0000	1.0000	1.0000	87.80	100.00	68.66
0.9490	0.9059	0.4824	88.39	100.00	68.42
0.7176	0.0706	0.0392	99.40	96.77	59.03
0.1216	0.0706	0.0039	100.00	92.68	56.48

TABLE 6.4 CONTINUED

Optimal weights			% of faulted sect $\geq$ 0.8	% of distinguishable non-faulted sect $<$ 0.8	% of non-Faulted Sect $<$ 0.8
w <sub>1</sub>	w <sub>2</sub>	w <sub>3</sub>			
Pareto-optimal weights when $p_1=0.95, p_2=0.4$					
0.9059	1.0000	0.3725	87.80	100.00	68.66
0.7255	1.0000	0.6000	88.39	100.00	68.60
0.6039	0.0706	0.0471	99.70	96.77	59.02
0.1216	0.0706	0.0196	100.00	92.68	56.48
Pareto-optimal weights when $p_1=0.9, p_2=0.2$					
1.0000	0.4902	0.3020	89.88	100.00	67.66
0.7961	0.1490	0.0157	98.81	96.89	59.16
0.2510	0.1490	0.0980	100.00	96.89	59.08
Pareto-optimal weights when $p_1=0.9, p_2=0.3$					
1.0000	1.0000	1.0000	87.80	100.00	68.66
0.7765	0.1490	0.0667	98.81	96.89	59.16
0.2510	0.1490	0.0667	100.00	96.89	59.08
Pareto-optimal weights when $p_1=0.9, p_2=0.4$					
1.0000	1.0000	1.0000	87.80	100.00	68.66
0.8078	0.1490	0.0314	98.81	96.89	59.16
0.2510	0.1490	0.0471	100.00	96.89	59.08
Pareto-optimal weights when $p_1=0.8, p_2=0.2$					
0.9725	0.4941	0.0078	89.58	100.00	67.92
0.9961	0.3216	0.0157	98.81	100.00	61.06
0.5216	0.3216	0.0784	100.00	100.00	60.97
Pareto-optimal weights when $p_1=0.8, p_2=0.3$					
1.0000	1.0000	1.0000	87.80	100.00	68.66
0.9765	0.3216	0.1255	98.81	100.00	61.06
0.5294	0.3216	0.1922	100.00	100.00	60.97
Pareto-optimal weights when $p_1=0.8, p_2=0.4$					
1.0000	1.0000	1.0000	87.80	100.00	68.66
0.9137	0.3216	0.1255	98.81	100.00	61.06
0.4392	0.3216	0.3098	100.00	100.00	60.97

TABLE 6.5 RESULTS OF THE FUZZY RESOLVER DESIGNED USING THE OWA OPERATOR WITH RESPECT TO TWO OBJECTIVE FUNCTIONS

Optimal weights						% of faulted sect $\geq$ 0.8	% of non-faulted distinguishable sect $<$ 0.8	% of non-faulted sect $<$ 0.8
$w_1$	$w_2$	$w_3$	$W_1$	$W_2$	$W_3$			
Pareto-optimal weights when $p_1=0.95, p_2=0.2$								
1.0000	0.5405	0.1529	0.0000	0.0039	0.9961	89.29	100.00	68.15
0.9294	0.0706	0.0039	0.0000	0.0000	1.0000	98.81	96.77	59.09
0.1216	0.0706	0.1216	0.0000	0.0000	1.0000	100.00	92.68	56.51
0.1412	0.0824	0.0353	0.7137	0.2706	0.0157	0.00	100.00	100.00
Pareto-optimal weights when $p_1=0.95, p_2=0.3$								
1.0000	0.9961	0.7216	0.0000	0.0118	0.9882	87.80	100.00	68.66
0.9490	0.9333	0.5529	0.0000	0.0000	1.0000	87.80	100.00	68.66
0.7176	0.0706	0.0235	0.0000	0.0000	1.0000	99.40	96.77	59.03
0.1216	0.0706	0.2941	0.0000	0.0000	1.0000	100.00	92.68	56.51
0.1451	0.2235	0.0196	0.9373	0.0627	0.0000	0.00	100.00	100.00
Pareto-optimal weights when $p_1=0.95, p_2=0.4$								
0.9098	1.0000	0.1137	0.0000	0.0000	1.0000	87.80	100.00	68.66
0.7294	1.0000	0.1059	0.0000	0.0000	1.0000	88.39	99.91	68.60
0.6039	0.0706	0.0353	0.0000	0.0000	1.0000	99.70	96.77	59.02
0.1216	0.0706	0.0353	0.0000	0.0000	1.0000	100.00	92.68	56.51
0.2353	0.2353	0.1529	0.9451	0.0431	0.0117	0.00	100.00	100.00
Pareto-optimal weights when $p_1=0.9, p_2=0.2$								
0.9843	0.4902	0.3098	0.0000	0.0039	0.9961	89.88	100.00	67.66
0.7922	0.1490	0.0549	0.0000	0.0039	0.9961	98.81	96.89	59.16
0.2510	0.1490	0.0549	0.0000	0.0000	1.0000	100.00	96.89	59.08
0.0588	0.2000	0.0275	0.7686	0.1490	0.0824	0.00	100.00	100.00
Pareto-optimal weights when $p_1=0.9, p_2=0.3$								
0.9882	0.8824	0.6863	0.0039	0.0039	0.9922	88.39	100.00	68.42
0.7686	0.1490	0.0314	0.0000	0.0000	1.0000	98.81	96.89	59.16
0.2510	0.1490	0.1059	0.0000	0.0000	1.0000	100.00	96.89	59.08
0.0706	0.0588	0.0235	0.5843	0.3333	0.0824	0.00	100.00	100.00
Pareto-optimal weights when $p_1=0.9, p_2=0.4$								
0.9804	1.0000	0.7569	0.0000	0.0000	1.0000	87.80	100.00	68.66
0.7490	0.1490	0.2275	0.0000	0.0039	0.9961	98.81	96.89	59.16
0.2510	0.1490	0.0588	0.0000	0.0000	1.0000	100.00	96.89	59.08
0.2353	0.2353	0.1529	0.9451	0.0431	0.0117	0.00	100.00	100.00



TABLE 6.5 CONTINUED

Optimal weights						% of faulted sect $\geq$ 0.8	% of non-faulted distinguishable sect $<$ 0.8	% of non-faulted sect $<$ 0.8
$w_1$	$w_2$	$w_3$	$W_1$	$W_2$	$W_3$			
Pareto-optimal weights when $p_1=0.8, p_2=0.2$								
0.9765	0.4980	0.1765	0.0000	0.0039	0.9961	89.58	100.00	67.92
0.9569	0.3216	0.1255	0.0000	0.0000	1.0000	98.81	100.00	61.06
0.5216	0.3216	0.0784	0.0000	0.0000	1.0000	100.00	100.00	60.97
0.0745	0.0549	0.0078	0.7176	0.2157	0.0667	0.00	100.00	100.00
Pareto-optimal weights when $p_1=0.8, p_2=0.3$								
0.9882	0.9294	0.3647	0.0039	0.0039	0.9922	89.58	100.00	67.92
0.9961	0.3216	0.0980	0.0000	0.0039	0.9961	98.81	100.00	61.06
0.5294	0.3216	0.0588	0.0000	0.0000	1.0000	100.00	100.00	60.97
0.0941	0.2784	0.0353	0.4549	0.5333	0.0118	0.00	100.00	100.00
Pareto-optimal weights when $p_1=0.8, p_2=0.4$								
1.0000	1.0000	0.6549	0.0000	0.0000	1.0000	89.58	100.00	67.92
0.9765	0.3216	0.2275	0.0000	0.0000	1.0000	98.81	100.00	61.06
0.4902	0.3216	0.0392	0.0000	0.0000	1.0000	100.00	100.00	60.97
0.2353	0.2353	0.1529	0.9451	0.0431	0.0118	0.00	100.00	100.00

From Table 6.6, for the fuzzy resolver designed using the uninorm, all Pareto-optimal weights achieved the best achievable results, that is, both the percentage of correctly identified actual faulted sections and the percentage of correctly identified distinguishable non-faulted sections were equal 100%.

#### 6.4.1.1 Summary

In the above performance study, it was found that for all three fuzzy resolvers, there were some sets of weights that achieved the result that both the percentage of correctly identified actual faulted sections and the percentage of correctly identified distinguishable non-faulted sections were equal to 100%. However, for the min operator and OWA operator, only when  $p_1$  was equal to the  $\alpha$ -level did the fuzzy resolvers achieve this result. For the uninorm operator, the fuzzy resolver always achieved this result for the three

values of  $p_1$ . Therefore, when the fuzzy resolver was designed using the uninorm operator, it achieved high performance even when  $p_1$  was not equal to the  $\alpha$ -level.

TABLE 6.6 RESULTS OF THE FUZZY RESOLVER DESIGNED USING THE UNINORM OPERATOR WITH RESPECT TO TWO OBJECTIVE FUNCTIONS

Optimal weights			% of faulted sect $\geq$ 0.8	% of distinguishable non-faulted sect $<$ 0.8	% of non-faulted sect $<$ 0.8
$w_1$	$w_2$	$w_3$			
Pareto-optimal weights when $p_1=0.95, p_2=0.2$					
1.0000	1.0000	1.0000	100.00	100.00	60.97
Pareto-optimal weights when $p_1=0.95, p_2=0.3$					
1.0000	1.0000	0.9569	100.00	100.00	60.97
Pareto-optimal weights when $p_1=0.95, p_2=0.4$					
1.0000	1.0000	0.8510	100.00	100.00	60.97
Pareto-optimal weights when $p_1=0.9, p_2=0.2$					
0.9961	1.0000	0.8000	100.00	100.00	60.97
Pareto-optimal weights when $p_1=0.9, p_2=0.3$					
1.0000	1.0000	0.8941	100.00	100.00	60.97
Pareto-optimal weights when $p_1=0.9, p_2=0.4$					
0.9961	1.0000	0.8980	100.00	100.00	60.97
Pareto-optimal weights when $p_1=0.8, p_2=0.2$					
1.0000	1.0000	0.8078	100.00	100.00	60.97
Pareto-optimal weights when $p_1=0.8, p_2=0.3$					
1.0000	1.0000	0.9843	100.00	100.00	60.97
Pareto-optimal weights when $p_1=0.8, p_2=0.4$					
1.0000	1.0000	0.9294	100.00	100.00	60.97

#### **6.4.2 Comparison of the Performance of the Fuzzy Resolvers Designed with Respect to the First Objective Function and the Fuzzy Resolvers Designed with Respect to Two Objective Functions**

This study investigates the comparison of the fuzzy resolvers designed with respect to two objective functions and the fuzzy resolvers designed with respect to the first objective function. In this study, the fuzzy resolvers designed with respect to the first objective function were used to calculate the aggregation possibility values for the test cases. Based on these possibility values, the percentage of correctly identified actual faulted sections, the percentage of correctly identified distinguishable non-faulted sections, and the percentage of identified non-faulted sections were evaluated. The fuzzy resolvers designed with respect to two objective functions were compared with fuzzy resolvers designed with respect to the first objective function in terms of these percentages.

The fuzzy resolvers designed with respect to the first objective function are listed in section 5.3.2. The performance of the fuzzy resolvers designed using different operators with respect to the first objective function is summarized in Table 6.7-Table 6.9. From Table 6.7 and Table 6.8, for the fuzzy resolvers designed using the min operator and OWA operator, even when  $p_1$  was equal to the  $\alpha$ -level, these fuzzy resolvers did not achieve the result that the percentage of correctly identified distinguishable non-faulted sections was equal to 100%. Without the constraint of the second objective function, some optimal weights might be found that increased all line sections' possibility values too much so that too many sections had possibility values larger than or equal to the  $\alpha$ -level. For example, for  $p_1=0.95$ , fuzzy resolver 1 generated one set of the optimal weights [0.0000 0.0235 0.0000]. These weights achieved the result that the percentage of correctly identified distinguishable non-faulted sections was equal to 0%. Therefore, all line sections were identified as potential faulted sections. Comparing Table 6.7 and Table 6.8 with Table 6.4 and Table 6.5, for the min operator and OWA operator, when

achieving the percentage of correctly identified actual faulted sections equal to 100%, the fuzzy resolvers designed with respect to two objective functions achieved the percentage of correctly identified distinguishable non-faulted sections equal to 92.68%, 96.89%, and 100% for  $p_1=0.95$ , 0.9, and 0.8, respectively. The fuzzy resolvers with respect to the first objective function achieved the maximum percentage of correctly identified distinguishable non-faulted sections equal to 91.82%, 96.77%, and 96.89% for  $p_1=0.95$ , 0.9, and 0.8, respectively. Therefore, for the min and OWA operators, the fuzzy resolvers designed with respect to two objective functions had better performance than the fuzzy resolvers designed with respect to the first objective function for these test cases.

TABLE 6.7 RESULTS OF THE FUZZY RESOLVER DESIGNED USING THE MIN OPERATOR WITH RESPECT TO THE FIRST OBJECTIVE FUNCTION

Optimal weights			% of faulted sect $\geq$ 0.8	% of distinguishable non-faulted sect $<$ 0.8	% of non-faulted sect $<$ 0.8
$w_1$	$w_2$	$w_3$			
Optimal weights when $p_1=0.95$					
0.1059	0.0078	0.0039	100.00	91.82	55.99
0.0431	0.0549	0.0000	100.00	70.76	43.15
0.0000	0.0235	0.0000	100.00	0.00	0.00
Optimal weights when $p_1=0.9$					
0.2392	0.0863	0.0588	100.00	96.77	59.00
0.1059	0.0745	0.0471	100.00	92.07	56.39
0.0000	0.1137	0.0000	100.00	32.21	19.64
Optimal weights when $p_1=0.8$					
0.5255	0.1569	0.0745	100.00	96.89	59.08
0.1451	0.2980	0.0941	100.00	95.79	58.41
0.0000	0.1020	0.0000	100.00	32.09	19.57

From Table 6.9, the fuzzy resolver designed using the uninorm operator with respect to the first objective function correctly identified all actual faulted sections and achieved the result that both the percentage of correctly identified actual faulted sections and the

percentage of correctly identified distinguishable non-faulted sections were equal to 100%. Comparing Table 6.9 with Table 6.6, the fuzzy resolver designed with respect to the first objective function had the same performance as the fuzzy resolver designed with respect to two objective functions.

TABLE 6.8 RESULTS OF THE FUZZY RESOLVER DESIGNED USING THE OWA OPERATOR WITH RESPECT TO THE FIRST OBJECTIVE FUNCTION

Optimal weights						% of faulted sect $\geq$ 0.8	% of distinguishable non-Faulted sect $\geq$ 0.8	% of non-faulted sect $<$ 0.8
w <sub>1</sub>	w <sub>2</sub>	w <sub>3</sub>	W <sub>1</sub>	W <sub>2</sub>	W <sub>3</sub>			
Optimal weights when $p_I=0.95$								
0.0000	0.0078	0.0000	0.0000	0.0000	1.0000	100.00	0.00	0.00
1.0000	1.0000	0.9020	0.8824	0.1137	0.0039	100.00	29.94	18.26
0.1020	0.0118	0.8000	0.0000	0.0039	0.9961	100.00	91.55	55.82
Optimal weights when $p_I=0.9$								
0.0000	0.1137	0.0000	0.0000	0.0000	1.0000	100.00	32.21	19.64
0.9961	0.9882	0.9098	0.7216	0.1294	0.1490	100.00	53.00	32.32
0.1176	0.1098	0.9804	0.0000	0.0078	0.9922	100.00	92.68	56.51
Optimal weights when $p_I=0.8$								
0.0000	0.0039	0.0000	0.0000	0.0000	1.0000	100.00	0.00	0.00
0.9686	0.9451	0.8745	0.9098	0.0078	0.0824	100.00	32.20	19.63
0.3059	0.2510	0.9020	0.0039	0.0000	0.9961	100.00	99.21	60.49

#### 6.4.2.1 Summary

The above study found that for the min operator and OWA operator, fuzzy resolvers designed with respect to two objective functions had better performance than fuzzy resolvers designed with respect to the first objective function because the fuzzy resolvers designed with respect to the first objective function did not achieve the result that both the percentage of correctly identified actual faulted sections and the percentage of

correctly identified distinguishable non-faulted sections were equal to 100%. For the uninorm operator, the fuzzy resolver designed with respect to two objective functions had the same performance as the fuzzy resolver designed with respect to the first objective function because they all achieved the result that both the percentage of correctly identified actual faulted sections and the percentage of correctly identified distinguishable non-faulted sections were equal to 100%.

TABLE 6.9 RESULTS OF THE FUZZY RESOLVER DESIGNED USING THE UNINORM OPERATOR WITH RESPECT TO THE FIRST OBJECTIVE FUNCTION

Optimal weights			% of faulted sect $\geq$ 0.8	% of distinguishable non-faulted Sect $<$ 0.8	% of non-faulted Sect $<$ 0.8
w <sub>1</sub>	w <sub>2</sub>	w <sub>3</sub>			
Optimal weights when $p_I=0.95$					
0.9961	0.9608	0.7843	100.00	100.00	60.97
0.7608	0.7804	0.5961	100.00	100.00	60.97
Optimal weights when $p_I=0.9$					
0.9137	0.6627	0.3216	100.00	100.00	60.97
0.7843	0.7451	0.7333	100.00	100.00	60.97
Optimal weights when $p_I=0.8$					
0.9176	0.9451	0.5176	100.00	100.00	60.97
0.4980	0.4000	0.5020	100.00	100.00	60.97

#### 6.4.3 Comparison of the Performance of the Fuzzy Resolvers Designed with Respect to Two Objective Functions and the Fuzzy Resolvers without Weights

This study investigates the comparison of the fuzzy resolvers designed with respect to two objective functions and the fuzzy resolvers without weights. In this study, the fuzzy resolvers without weights were used to calculate the aggregation possibility values for the

test cases. Based on these possibility values, the percentage of correctly identified actual faulted sections, the percentage of correctly identified distinguishable non-faulted sections, and the percentage of identified non-faulted sections were evaluated. The fuzzy resolvers designed with respect to two objective functions were compared with fuzzy resolvers without weights in terms of these percentages.

The results of the min operator without weights are shown in Table 6.10. The results of the OWA operator without weights on the fault location method outputs are shown in Table 6.11, where  $W_1$ ,  $W_2$ , and  $W_3$  are the optimal parameters of the OWA operator. From Table 6.10, it is observed that for the min operator, when no weights were used, only 87.80% of actual faulted sections were correctly identified as potential faulted sections but all distinguishable non-faulted sections were correctly identified. From Table 6.11, it is seen that the OWA operator was able to achieve the result that the percentage of correctly identified actual faulted sections equal to 100% by choosing appropriate parameters when no weights were used. However, most of the parameters that achieved 100% of correctly identified actual faulted sections achieved the percentage of correctly identified distinguishable non-faulted sections less than 100%.

TABLE 6.10 RESULTS OF THE FUZZY RESOLVER DESIGNED USING THE MIN OPERATOR WITHOUT WEIGHTS

Optimal weights	% of faulted sect $\geq$ 0.8	% of distinguishable non-faulted sect $<$ 0.8	% of non-faulted sect $<$ 0.8
No weight	87.80	100.00	68.66

Comparing Table 6.11 with Table 6.5, without weights, the OWA operator usually achieved more distinguishable non-faulted sections to be identified as potential faulted

sections than the fuzzy resolver designed with respect to two objective functions. For example, the OWA operator using optimal parameters obtained when  $p_1=0.95$  and  $p_2=0.2$  but without weights achieved 52.56% of distinguishable non-faulted sections as non-faulted sections while the fuzzy resolver designed with respect to two objective functions achieved 92.68% of distinguishable non-faulted sections as non-faulted sections when  $p_1=0.95$  and  $p_2=0.2$ .

TABLE 6.11 RESULTS OF THE FUZZY RESOLVER DESIGNED USING THE OWA OPERATOR WITHOUT WEIGHTS

Optimal parameters			% of faulted sect $\geq$ 0.8	% of distinguishable non-faulted sect $<$ 0.8	% of non-faulted sect $<$ 0.8
$W_1$	$W_2$	$W_3$			
Optimal weights when $p_1=0.95, p_2=0.2$					
0.0000	0.0000	1.0000	87.80	100.00	68.66
0.0000	0.9020	0.0980	100.00	52.56	32.05
Optimal weights when $p_1=0.95, p_2=0.3$					
0.0000	0.0000	1.0000	87.80	100.00	68.66
0.0000	0.9059	0.0941	100.00	52.33	31.91
Optimal weights when $p_1=0.95, p_2=0.4$					
0.0000	0.0000	1.0000	87.80	100.00	68.66
0.0039	0.9020	0.0941	100.00	52.33	31.91
Optimal weights when $p_1=0.9, p_2=0.2$					
0.0000	0.0000	1.0000	87.80	100.00	68.66
0.0000	0.8000	0.2000	100.00	91.29	55.66
Optimal weights when $p_1=0.9, p_2=0.3$					
0.0000	0.0000	1.0000	87.80	100.00	68.66
0.0000	0.8078	0.1922	100.00	72.61	44.27
Optimal weights when $p_1=0.9, p_2=0.4$					
0.0000	0.0000	1.0000	87.80	100.00	68.66
0.0039	0.8000	0.1961	100.00	90.60	55.25
Optimal weights when $p_1=0.8, p_2=0.2$					
0.0000	0.0000	1.0000	87.80	100.00	68.66
0.0000	0.6196	0.3804	100.00	99.88	60.90



TABLE 6.11 CONTINUED

Optimal parameters			% of faulted sect $\geq$ 0.8	% of distinguishable non-faulted sect $<$ 0.8	% of non-faulted sect $<$ 0.8
Optimal weights when $p_1=0.8, p_2=0.3$					
0.0000	0.0000	1.0000	87.80	100.00	68.66
0.0039	0.5961	0.4000	100.00	100.00	60.97
Optimal weights when $p_1=0.8, p_2=0.4$					
0.0000	0.0000	1.0000	87.80	100.00	68.66
0.0078	0.6039	0.3883	100.00	99.94	60.94

TABLE 6.12 RESULTS OF THE FUZZY RESOLVER DESIGNED USING THE UNINORM OPERATOR WITHOUT WEIGHTS

Optimal weights	% of faulted sect $\geq$ 0.8	% of distinguishable non-faulted sect $<$ 0.8	% of non-faulted sect $<$ 0.8
No weight	100.00	100.00	60.97

From Table 6.12, it is observed that the fuzzy resolver designed using the uninorm operator without weights achieved the result that both the percentage of correctly identified actual faulted sections and the percentage of correctly identified distinguishable non-faulted sections were equal to 100%. Comparing Table 6.6 with Table 6.12, the performance of the fuzzy resolver without weights was the same as the fuzzy resolver designed with respect to two objective functions. There was no need for weights for this operator. As discussed in section 5.4.5, transformation method (3.31) tends to reduce the difference between high possibility values and low possibility values when  $w$  decreases, and no weight is equivalent to  $w=1$ . When using weights, the difference between high possibility values and low possibility values is reduced. Therefore, for the uninorm

operator, the fuzzy resolver designed without weights performed better than the fuzzy resolver with weights.

#### **6.4.3.1 Summary**

From the above study, for the min operator, the fuzzy resolver without weights did not identify all actual faulted sections as potential faulted sections; however, the fuzzy resolver with respect to two objective functions achieved this result. For the OWA operator, the fuzzy resolver without weights usually did not achieve the same performance as the fuzzy resolver designed with respect two objective functions because the fuzzy resolver without weights did not achieve the result that both the percentage of correctly identified actual faulted sections and the percentage of correctly identified distinguishable non-faulted sections were equal to 100%. For the uninorm operator, the fuzzy resolver without weights had the same performance as the fuzzy resolver with weights. When the difference between high possibility values and low possibility values was considered, the fuzzy resolver without weights was better than the fuzzy resolver with weights.

### **6.5 SUMMARY OF THE STUDIES AND RECOMMENDATIONS**

All Pareto-optimal weights in Table 6.4-Table 6.12 that achieved the best achievable results were shaded. From the first study, it was found that for the min operator and OWA operator, the fuzzy resolver designed with respect to two objective functions achieved the best results when  $p_1$  was equal to the  $\alpha$ -level as shown in Table 6.4 and Table 6.5; that is, they identified all actual faulted sections as potential faulted sections and all distinguishable non-faulted sections as non-faulted sections. As shown in Table 6.6, for the uninorm operator, the fuzzy resolver designed with respect to two objective functions always achieved the best results for the three values of  $p_1$ .

From the second study, as shown in Table 6.4, Table 6.5, Table 6.7 and Table 6.8, for the min operator and OWA operator, the fuzzy resolvers designed with respect to the first objective function did not achieve the best results because these fuzzy resolvers only

maximized the percentage of faulted sections whose possibility values  $\geq 0.8$  but did not achieve the optimal percentage of distinguishable non-faulted sections whose possibility values  $< 0.8$ . For example, the fuzzy resolver designed using the min operator with respect to the first objective function achieved a set of weights as [0.0431 0.0549 0.0000]. This set of weights caused some distinguishable non-faulted sections to have a possibility value larger than 0.8. Therefore, the weights achieved the result that only 70.76% distinguishable non-faulted sections were identified as non-faulted sections. For the uninorm operator, both the fuzzy resolver designed with respect to two objective functions and the fuzzy resolver designed with respect to the first objective function achieved the best results as shown in Table 6.6 and Table 6.9.

From the third study, as shown in Table 6.4, Table 6.5, Table 6.10, and Table 6.11, for the min and OWA operator, the fuzzy resolvers designed with respect to two objective functions had better performance than the fuzzy resolvers without weights because the fuzzy resolvers without weights did not achieve the result that both the percentage of correctly identified actual faulted sections and the percentage of correctly identified distinguishable non-faulted sections were equal to 100%. As shown in Table 6.6 and Table 6.12, for the uninorm operator, the fuzzy resolver without weights had better performance than the fuzzy resolver designed with weights because it generated the largest difference between high possibility values for actual faulted sections and low possibility values for distinguishable non-faulted sections.

In order to compare the performance of individual fault location methods and the fuzzy resolver designed using the uninorm operator without weights in terms of fault location, the number of potential faulted sections identified by the individual fault location methods and the fuzzy resolver designed using the uninorm operator without weights for the test cases are listed in Table 6.13. The number of cases represents how many fault cases have the same combination of the number of potential faulted sections. From this table, it can be seen that the fuzzy resolver identified a smaller number of line

sections as potential faulted sections than the individual fault location methods for 43 fault cases. For 37 fault cases with high or middle fault resistance levels, the phase selector method identified all line sections as non-faulted sections while the fuzzy resolver identified some line sections as potential faulted sections. For 4 fault cases staged on laterals, the ODIM method identified all line sections as non-faulted sections while the fuzzy resolver identified some line sections as potential faulted sections. For 119 fault cases with a middle or high fault resistance level, the fault distance method identified all line sections as potential faulted sections while the fuzzy resolver identified a smaller subset of line sections as potential fault sections. For 34 fault cases with a high fault resistance level, the ODIM method identified all line sections as potential faulted sections while the fuzzy resolver identified a smaller subset of line sections as potential fault sections. For the fault cases where all individual methods identified a non-zero number of line sections as potential faulted sections, the fuzzy resolver always identified a smaller or same number of line sections as potential faulted sections.

Based on these performance studies, some recommendations about designing desirable fuzzy resolvers are obtained. The author recommends designing a fuzzy resolver using the min operator without weights. If fuzzy resolvers are designed using the min operator and OWA operator, the author suggests the methodology for designing fuzzy resolvers with respect to two objective functions, and  $p_1$  of the first objective function should be equal to the  $\alpha$ -level.

TABLE 6.13 PERFORMANCE OF INDIVIDUAL FAULT LOCATION METHODS AND THE FUZZY RESOLVER DESIGNED USING THE UNINORM OPERATOR WITHOUT WEIGHTS

# of cases	Fault resistance	ODIM	PS	FD	Fuzzy Resolver	# of cases	Fault resistance	ODIM	PS	FD	Fuzzy Resolver
106	Middle/high	18	25	33	18	2	Low	18	29	6	6
27	Middle/high	18	29	33	18	2	Low	18	29	10	10
21	High	33	0	33	25	2	Low	18	29	13	13

TABLE 6.13 CONTINUED

# of cases	Fault resistance	ODIM	PS	FD	Fuzzy Resolver	# of cases	Fault resistance	ODIM	PS	FD	Fuzzy Resolver
12	Low	18	25	10	10	2	Low	18	29	15	14
11	High	33	0	33	29	2	Low	18	29	17	15
8	Low	18	25	13	13	2	Low	18	29	17	17
8	Low	18	25	17	17	2	Low	18	29	18	18
7	Low	18	25	4	4	2	High	33	25	33	25
6	Low	18	25	2	2	1	Middle	3	25	33	1
6	Low	18	25	6	6	1	Middle	2	25	33	1
6	Low	18	25	18	18	1	Low	18	25	1	1
5	Middle	2	0	33	2	1	Low	5	25	19	1
5	Low	4	25	17	2	1	Low	3	25	22	1
5	Low	18	25	3	3	1	Low	18	29	1	1
5	Low	18	25	7	7	1	Low	5	29	12	1
5	Low	18	25	8	8	1	Low	5	29	15	1
5	Low	18	25	14	14	1	Middle	6	25	33	1
5	Low	18	25	15	15	1	Low	0	29	11	1
4	Low	4	25	18	3	1	Low	3	25	19	1
4	Middle	5	29	33	5	1	Low	3	29	18	1
4	Middle	6	25	33	6	1	Low	6	25	18	1
3	Low	6	25	17	2	1	Low	5	29	19	1
3	Low	2	25	15	2	1	Low	0	29	9	2
3	Low	18	25	11	11	1	Low	6	29	17	2
2	Low	4	25	16	1	1	Middle	3	29	33	2
2	Middle	5	25	33	1	1	Low	6	29	19	3
2	Low	6	25	15	2	1	Low	4	29	18	3
2	Middle	2	25	33	2	1	Low	0	29	10	3
2	Low	18	29	2	2	1	Low	6	29	18	3
2	Low	18	29	3	3	1	Low	6	25	19	4
1	Low	6	25	20	4	1	Low	18	25	9	8
1	Low	4	29	19	4	1	Low	18	25	10	9
1	Low	18	29	4	4	1	Low	18	29	9	9
1	Low	6	25	21	6	1	Low	18	29	11	11
1	Low	18	29	7	7	1	Low	18	25	17	15
1	High	0	29	33	7	1	Low	18	25	16	16

## 6.6 CHAPTER SUMMARY

In this chapter, the performance of the fuzzy resolver designed using the min, OWA, and uninorm operators with respect to two objective functions, and the fuzzy resolver designed using the uninorm operator without weights was studied using fault cases in the test set. The performance of fuzzy resolvers designed with respect to two objective functions was compared with the performance of fuzzy resolvers designed with respect to the first objective function. The performance of fuzzy resolvers without weights was compared with the performance of fuzzy resolvers using weights. The performance of fuzzy resolvers designed using three fuzzy aggregation operators with weights was compared with each other. The results showed that the fuzzy resolver designed using the uninorm operator without weights achieved the best fuzzy performance.

In the next chapter, conclusions and future work are discussed.

## CHAPTER VII

### CONCLUSIONS AND FUTURE WORK

#### 7.1 SUMMARIES

A new fault location scheme that uses measurements at the substation and distribution system's topological data was developed in the Power System Automation Lab at Texas A&M University. This new scheme has three stages: the input stage, the fault location methods stage, and the output stage. In order to be used for most utilities, the input data for this scheme should be available from most utilities. In this new fault location scheme, only the current and voltage measurements at the substation, feeder topological data, and protective device settings and locations are required. The input stage is used to process and format the data to a form useable by the fault location methods stage. The fault location methods stage consists of three independent fault location methods. The fault distance method locates faults by calculating the fault distance. The phase selector method locates faults by identifying faulted phases and based on the presence of phases on each line section. The operated device identification method locates faults by identifying the operated protective device for a fault. Since there are uncertainties in the load component of the fault current, the fault resistance, the raw data, etc., fuzzy logic was utilized in the development of these methods. Each fault location method determines possibility values to each line section of a distribution feeder. These possibility values represent how possible a line section is involved in a fault. In the last stage, a fuzzy resolver is used to aggregate the outputs of the three fault location methods and produce one final aggregation possibility value for each line section. Fuzzy aggregation operators were used in the fuzzy resolver. This dissertation discusses the author's work in the development of a methodology for designing a fuzzy resolver for stage three of the fault location scheme.

In the methodology, fuzzy aggregation operators were used to design the fuzzy resolver. To choose fuzzy aggregation operators to design a fuzzy resolver, commonly

used fuzzy aggregation operators were investigated, and the min, OWA, and uninorm operators were chosen as candidate operators. To take account of the accuracy of the three fault location methods, weights (important factors) were assigned to these methods. In order to incorporate these weights, transformation methods were used for each fuzzy aggregation operator to transform the outputs of the three fault location methods into effective values. After that, a fuzzy aggregation operator was used to aggregate these effective values to generate final possibility values for each line section of a feeder.

In the design process of a fuzzy resolver, the optimal weights of the three fault location methods and the optimal parameters of the OWA operator needed to be determined. In order to determine these weights and parameters, data representing many distribution systems were needed. Since field data from real distribution feeders were unavailable to this research, modeling a distribution feeder with protective devices and simulating fault cases on the feeder were feasible alternatives. The IEEE 34 node test feeder was modeled with the addition of protective devices. Load flow and short circuit analysis studies were implemented on this feeder using software WindMil to determine the protective devices' settings. The author developed a methodology for modeling TCC-based protective devices in MATLAB SimPowerSystems blockset. Faults were exhaustively simulated at all line sections to generate data. After generating data, the optimal parameters of the fuzzy resolver (the weights of the three fault location methods and the parameters of the OWA operator) needed to be determined. Genetic algorithm based methods were used to determine them. Two objectives were used in the optimization process. The first objective was to maximize the number of actual faulted sections whose possibility values are greater than or equal to a large possibility value  $p_1$ , which aimed to achieve the result that actual faulted sections had a large possibility value. The other was to maximize the number of non-faulted sections whose possibility values are less than a small possibility value  $p_2$ , which aimed to achieve the result that actual faulted sections had a large possibility value. Fuzzy resolvers were designed with respect



to a single objective function individually and with respect to two objective functions, respectively. The performance of the designed fuzzy resolvers was studied.

## 7.2 CONCLUSIONS

This dissertation discussed the work in the development of the fuzzy resolver methodology. In the fuzzy resolver methodology, fuzzy aggregation operators were used to design fuzzy resolvers. Commonly used fuzzy aggregation operators were investigated and then three of these operators, the min, OWA, and uninorm operators, were chosen based on the characteristics of the fault location problem. The IEEE 34 node test feeder was simulated to generate data that was used to design and validate the fuzzy resolver methodology. Genetic algorithm based optimization methods were used to determine the optimal parameters of fuzzy resolvers. Two objective functions were used in the optimization process. The first objective function was to maximize the number of actual faulted sections whose possibility values are greater than or equal to a large possibility value  $p_1$ , which aimed to achieve the result that actual faulted sections had a large possibility value. The other objective function was to maximize the number of non-faulted sections whose possibility values are less than a small possibility value  $p_2$ , which aimed to achieve the result that actual faulted sections had a large possibility value. In the design process, fuzzy resolvers were first designed with respect to the first objective function individually and the second objective function individually. After that, fuzzy resolvers were designed with respect to two objective functions. When fuzzy resolvers designed with respect to two objective functions, the problem to obtain the optimal parameters of the fuzzy resolver was a multi-objective optimization problem. In multi-objective problems, there may not exist a global optimum with respect to all objectives. Usually there is a set of solutions that are superior to the rest of the solutions with respect to all objectives. The solutions in this set are called Pareto-optimal solutions (or non-dominated solutions). When the fuzzy resolver was designed with respect to two objective functions, Pareto-optimal solutions were found.

After the optimal parameters of a fuzzy resolver were obtained in the design process, the number of actual faulted sections whose possibility values are greater than or equal to a large possibility value  $p_1$  and the number of non-faulted sections whose possibility values are less than a small possibility value  $p_2$  were evaluated at these optimal weights. The results indicated that fuzzy resolvers designed with respect to two objective functions had better performance than fuzzy resolvers designed with respect to a single objective function because the fuzzy resolvers designed with respect to a single objective function usually did not obtain Pareto-optimal solutions. The fuzzy resolver designed using the uninorm operator had better performance than fuzzy resolvers designed using the min operator and OWA operator because its solution was larger than the solutions of the min and OWA operators with respect to two objective functions. For the min and OWA operator, the fuzzy resolvers designed with respect to two objective functions had better performance than the fuzzy resolvers without weights because the fuzzy resolvers without weights usually did not obtain a Pareto-optimal solution. For the uninorm operator, the fuzzy resolver without weights and the fuzzy resolver designed with respect to two objective functions had the same performance.

After fuzzy resolvers were designed, the performance of the designed fuzzy resolvers was studied. In the performance studies, the  $\alpha$ -level (a specific possibility value) was used to classify potential faulted sections and non-faulted sections. The line sections with a possibility value greater than or equal to the  $\alpha$ -level were identified as potential faulted sections, while the line sections with a possibility value less than the  $\alpha$ -level were identified as non-faulted sections. Through these studies, it was found that for the min and OWA operators, the fuzzy resolvers designed with respect to two objective functions could achieve the best achievable results when the preset value  $p_1$  of the first objective function was equal to the  $\alpha$ -level. The fuzzy resolvers without weights could not achieve the best achievable results. Without the constraint of the second objective function, the fuzzy resolvers designed with respect to the first objective function usually did not

achieve the best achievable results. For the uninorm operator, the fuzzy resolver designed with respect to two objective functions, the fuzzy resolver designed with respect to the first objective function, and the fuzzy resolver without weights all achieved the best achievable results. The transformation method used by the uninorm operator tended to reduce the difference between high possibility values and low possibility values when  $w$  decreased, and no weight was equivalent to  $w=1$ . Therefore, when using weights, the difference between high possibility values and low possibility values was reduced. Therefore, the fuzzy resolver designed without weights was better than the fuzzy resolvers designed both with respect to two objective functions and with respect to the first objective function.

Based on these performance studies, some recommendations about designing desirable fuzzy resolvers were obtained. The author recommends designing a fuzzy resolver using the min operator without weights. If fuzzy resolvers are designed using the min operator and OWA operator, the author suggests the methodology for designing fuzzy resolvers with respect to two objective functions, and  $p_1$  of the first objective function should be equal to the  $\alpha$ -level.

### **7.3 FUTURE WORK**

There is still some room to improve this research work. In this dissertation, only one distribution feeder was simulated to generate fault data to design fuzzy resolvers. In order to design a good fuzzy resolver, field data from several actual feeders are needed to generalize the parameters of the fuzzy resolver. If data from several real feeders are available, the process of designing the fuzzy resolver needs to be performed with this data. In the performance study, the  $\alpha$ -level was used to identify potential faulted sections and non-faulted sections, and the author did not analyze the number of non-faulted sections whose possibility values were less than  $p_2$  of the second objective function. In the future, the analysis should be done. When modeling reclosers at the substation, only

phase overcurrent protections were modeled and ground overcurrent protections were not modeled. In the future, ground overcurrent protections need to be modeled.

## REFERENCES

- [1] A.A. Girgis, C.M. Fallon, and D.L. Lubkerman, "A fault location technique for rural distribution feeder," *IEEE Transactions on Industry Application*, vol. 29, no. 6, pp. 1170-1175, 1993.
- [2] M.M. Saha, F. Provost, and E. Rosolowski, "Fault location method for MV cable network," in *Proceedings of the Seventh International Conference on Developments in Power System Protection*, Amsterdam, Netherlands, April 2001, pp 323-326.
- [3] S. Santoso, R.C. Dugan, J. Lamoree, and A. Sundaram, "Distance estimation technique for single line-to-ground faults in a radial distribution system," in *Proceedings of IEEE Power Engineering Society Winter Meeting*, vol. 4, Singapore, January 2000, pp 2551-2555.
- [4] R. Das, M.S. Sachdev, and T.S. Sidhu, "A technique for estimating locations of shunt faults on distribution lines," in *Proceedings of IEEE Conference on Communications, Power, and Computing*, vol. 1, Manitoba, Canada, May 1995, pp 6-11.
- [5] M.S. Sachdev, R. Das, and T.S. Sidhu, "Determining locations of faults in distribution systems," in *Proceedings of the Sixth International Conference on Developments in Power System Protection*, Nottingham, UK, March 1997, pp 188-191.
- [6] R. Das, M.S. Sachdev, and T.S. Sidhu, "A fault locator for radial subtransmission and distribution lines," in *Proceedings of IEEE PES Summer Meeting*, vol. 1, Seattle, WA, July 2000, pp 443-448.
- [7] R.K. Aggarwal, Y. Aslan, and A.T. Johns, "An interactive approach to fault location on overhead distribution lines with load taps," in *Proceedings of the Sixth International Conference on Developments in Power System Protection*, Nottingham, UK, March 1997, pp 184-187.
- [8] R.K. Aggarwal, Y. Aslan, and A.T. Johns, "New concept in fault location for overhead distribution systems using superimposed components," *IEE Proceedings-*

- Generation, Transmission and Distribution*, vol. 144, no. 3, pp 309-316, May 1997.
- [9] M. Choi, S. Lee, D. Lee, and B. Jin, "A new fault location algorithm using direct circuit analysis for distribution systems," *IEEE Transactions on Power Delivery*, vol. 19, no. 1, pp 35-41, January 2004.
- [10] D. Thomas, R. Carvalho, and E. Pereira, "Fault location in distribution systems based on traveling waves," in *Proceedings of Power Technology Conference*, vol. 2, Bologna, Italy, June 2003, pp 468-472.
- [11] Z.Q. Bo, G. Waller, and M.A. Redfern, "Accurate fault location technique for distribution system using fault-generated high-frequency transient voltage signals," *IEE Proceedings- Generation, Transmission and Distribution*, vol. 146, no. 1, pp 73-79, January 1999.
- [12] A.T. Johns, L.L. Lai, M. El-Hami, and D.J. Daruvala, "New approach to directional fault location for overhead power distribution feeder," *IEE Proceedings- Generation, Transmission and Distribution*, vol. 138, no. 4, pp 351-357, July 1991.
- [13] M. El-Hami, L.L. Lai, D.J. Daruvala, and A.T. Johns, "A new travelling-wave based scheme for fault detection on overhead power distribution feeders," *IEEE Transactions on Power Delivery*, vol. 7, no. 4, pp 1825-1833, October 1992.
- [14] Y. Tang, H.F. Wang, R.K. Aggarwal, and A.T. Johns, "Fault indicator in transmission and distribution systems," in *Proceedings of Electric Utility Deregulation and Restructuring and Power Technologies*, London, UK, April 2000, pp. 238-243.
- [15] F. H. Magnago and A. Abur, "A new fault location technique for radial distribution systems based on high frequency signals," in *Proceedings of IEEE PES Summer Meeting*, vol. 1, Alberta, Canada, July 1999, pp 426-431
- [16] C. Fukui and J. Kawakami, "An expert system for fault section estimation using information from protective relays and circuit breakers," *IEEE Transactions on Power Delivery*, vol. PWRD-1, no. 4, pp. 83-90, October 1986.
- [17] F. Elckhoff, E. Handschin, and W. Hoffmann, "Knowledge based alarm handling and

- fault location in distribution networks,” *IEEE Transactions on Power Systems*, vol. 7, no. 2, pp 770-776, May 1992.
- [18] T. Kimura, S. Nishimatsu, Y. Ueki, and Y. Fukuyama, “Development of an expert system for estimating fault section in control center based on protective system simulation,” *IEEE Transactions on Power Delivery*, vol. 7, no. 1, pp. 167-172, January 1992.
- [19] Y. Liu and N.N. Schulz, “Knowledge-based system for distribution system outage locating using comprehensive information,” *IEEE Transactions on Power Systems*, vol. 17, no. 2, pp. 451-456, May 2002.
- [20] Y.Y. Hsu, F.C. Lu, Y. Chien, J.P. Liu, J.T. Lin, et al. “An expert system for locating distribution system faults,” *IEEE Transactions on Power Delivery*, vol. 6, no. 1, pp. 366-372, January 1991.
- [21] E. M. Martinez and E.F. Richards, “An expert system to assist distribution dispatchers in the location of system outages,” in *Proceedings of the 35<sup>th</sup> Annual Rural Electric Power Conference*, Dearborn, MI, April 1991, pp. A2/1-A2/5.
- [22] H. Monsef, A.M. Ranjbar, and S. Jadid, “Fuzzy rule-based expert system for power system fault diagnosis,” *IEE Proceedings-Generation, Transmission and Distribution*, vol. 144, no. 2, pp. 186-192, March 1997.
- [23] S. Kumano, N. Ito, T. Goda, Y. Uekubo, S. Kyomoto, et al. “Development of expert system for operation at substation,” *IEEE Transactions on Power Delivery*, vol. 8, no. 1, pp. 56-65, January 1993.
- [24] J. Ypsilantis, H. Lee, and C.Y. Teo, “Adaptive, rule based fault diagnostician for power distribution networks,” *IEE Proceedings-Generation, Transmission and Distribution*, vol. 139, no. 6, pp. 461-468, November 1992.
- [25] C.Y. Teo, “Automation of knowledge acquisition and representation for fault diagnosis in power distribution networks,” *Electric Power Systems Research*, vol. 27, no. 3, pp. 183-189, August 1993.

- [26] H.T. Yang, W.Y. Chang, and C.L. Huang, "A new neural networks approach to on-line fault section estimation using information of protective relays and circuit breakers," *IEEE Transactions on Power Delivery*, vol. 9, no. 1, pp. 220-230, January 1994.
- [27] H.T. Yang, W.Y. Change, and C.L. Huang, "Power system distributed on-line fault section estimation using decision tree based neural nets approach," *IEEE Transactions on Power Delivery*, vol. 10, no. 1, pp. 540-546, January 1995.
- [28] T. Bi, Y. Ni, C.M. Shen, and F.F. Wu, "An on-line distributed intelligent fault section estimation system for large-scale power networks," *Electric Power Systems Research*, vol. 62, no. 3, pp. 173-182, 2002.
- [29] T. Bi, Y. Ni, C.M. Shen, and F.F. Wu, "Efficient multiway graph partitioning method for fault section estimation in large-scale power networks," *IEE Proceedings-Generation, Transmission and Distribution*, vol. 149, no. 3, pp. 289-294, May 2002.
- [30] M.A. Al-shaher, M.M. Sabra, and A.S. Saleh, "Fault location in multi-ring distribution network using artificial neural network," *Electric Power Systems Research*, vol. 64, no. 2, pp. 87-92, February 2003.
- [31] L. Sousa Martins, J.F. Martins, V. Fernão Pires, and C.M. Alegria, "A neural space vector fault location for parallel double-circuit distribution lines," *International Journal of Electric Power and Energy Systems*, vol. 27, no. 3, pp. 225-231, March 2005.
- [32] E.A. Mohamed and N.D. Rao, "Artificial neural network based fault diagnostic system for electric power distribution feeders," *Electric Power Systems Research*, vol. 35, no. 1, pp. 1-10, October 1995.
- [33] M.T. Glinkowski and N.C. Wang, "ANNs Pinpoint underground distribution faults," *IEEE Computer Applications in Power*, vol. 8, no. 4, pp. 31-34, October 1995.
- [34] S.A. Shahrestani, J. Ypsilantis, and H. Yee, "Application of pattern recognition to identification of power system faults," *Electric Power Systems Research*, vol. 34, no.



- 3, pp. 211-215, 1995.
- [35] P. Järventausta, P. Verho, and J. Partanen, "Using fuzzy sets to model the uncertainty in the fault location process of distribution networks," *IEEE Transactions on Power Delivery*, vol. 9, no. 2, pp. 954-960, April 1994.
- [36] C.S. Chang, J.M. Chen, D. Srinivasan, F.S. Wen, and A.C. Liew, "Fuzzy logic approach in power system fault section identification," *IEE Proceedings- Generation, Transmission and Distribution*, vol. 144, no. 5, pp. 406-414, September 1997.
- [37] H.J. Cho and J.K. Park, "An expert system for fault section diagnosis of power systems using fuzzy relations," *IEEE Transactions on Power Systems*, vol. 12, no. 1, pp. 342-348, February 1997.
- [38] W. Zhong and W.H. Liu, "Application of a fuzzy set method in distribution system fault location," in *Proceedings of IEEE International Symposium on Circuits and Systems*, vol. 1, Atlanta, GA, May 1996, pp. 617-620.
- [39] F.S. Wen and C.S. Chang, "Probabilistic approach for fault-section estimation in power systems based on a refined genetic algorithm," *IEE Proceedings-Generation, Transmission and Distribution*, vol. 144, no. 2, pp. 160-168, March 1997.
- [40] S.J. Huang, "Application of immune-based optimization method for fault section estimation in a distribution system," *IEEE Transactions on Power Delivery*, vol. 17, no. 3, pp. 779-784, July 2002.
- [41] Y.C. Huang, C.M. Huang, C.C. Liao, J.F. Chen, and H.T. Yang, "A new intelligent fast Petri-Net model for fault section estimation of distribution systems," in *Proceedings of International Conference on Power System Technology*, vol. 1, Perth, Australia, December 2000, pp. 217-222.
- [42] K.L. Lo, H.S. Ng, and J. Trecat, "Power systems fault diagnosis using Petri nets," *IEE Proceedings-Generation, Transmission and Distribution*, vol. 144, no. 3, pp. 231-236, May 1997.
- [43] K.L. Lo, H.S. Ng, D.M. Grant, and J. Trecat, "Extended Petri nets models for fault

- diagnosis for substation automation,” *IEE Proceedings-Generation, Transmission and Distribution*, vol. 146, no. 3, pp. 229-234, May 1999.
- [44] P. Deepal Rodrigo, A. Pahwa, and J.E. Boyer, “Location of outages in distribution systems based on statistical hypotheses testing,” *IEEE Transactions on Power Delivery*, vol. 11, no. 1, pp. 546-551, January 1996.
- [45] C.F. Chien, S.L. Chen, and Y.S. Lin, “Using Bayesian network for fault location on distribution feeder,” *IEEE Transactions on Power Delivery*, vol. 17, no. 13, pp. 785-793, July 2002.
- [46] D. Thukaram, H.P. Khincha, L. Jenkins, and K. Visakha, “A three phase fault detection algorithm for radial distribution networks,” in *Proceedings of IEEE Region 10 Conference on Computers, Communications, Control and Power Engineering*, vol. 2, Beijing, China, October 2002, pp. 1242-1248.
- [47] W.H. Chen, C.W. Liu, and M.S. Tsai, “On-line fault diagnosis of distribution substations using hybrid cause-effect network and fuzzy rule based method,” *IEEE Transactions on Power Delivery*, vol. 15, no. 2, pp. 710-717, April 2002.
- [48] Y.C. Huang, H.T. Yang, and C.L. Huang, “A new intelligent hierarchical fault diagnosis system,” *IEEE Transactions on Power Systems*, vol. 12, no. 1, February 1997.
- [49] C. Wang, H. Nouri, and T.S. Davies, “A mathematical approach for identification of fault sections on the radial distribution systems: voltage sensor,” in *Proceedings of the 10<sup>th</sup> Mediterranean Electrotechnical Conference*, vol. 3, Lemesos, Cyprus, May 2000, pp. 882-886.
- [50] A. Newbould, L. Hu, and K. Chapman, “Cable automation for urban distribution systems,” in *Proceedings of the 7<sup>th</sup> International Conference on Development in Power System Protection*, Amsterdam, Netherlands, April 2001, pp. 319-322.
- [51] J. Zhu, D.L. Lubkerman, and A.A. Girgis, “Automated fault location and diagnosis on electric power distribution feeders,” *IEEE Transactions on Power Delivery*, vol.

12, no. 2, pp. 801-809, 1997.

- [52] S.J. Lee, M.S. Choi, S.H. Kang, B.G. Jin, D.S. Lee, et al. "An intelligent and efficient fault location and diagnosis scheme for radial distribution systems," *IEEE Transactions on Power Delivery*, vol. 19, no. 2, pp. 524-532, April 2004.
- [53] Signature Systems, "Radial fault locator answer module," [Online]. Available: <http://www.signaturesystem.com/radialanswer.html>. (Accessed April, 2005)
- [54] ABB, "RES505-C1: disturbance monitoring terminal," [Online]. Available: <http://www.abb.com>. (Accessed April, 2005)
- [55] ABB, "Inform power system monitoring PSM 505," [Online]. Available, [http://library.abb.com/GLOBAL/SCOT/scot221.nsf/VerityDisplay/55AA2F18687568CAC1256D67002A5749/\\$File/1MRB520376-Ben-PSM505.pdf](http://library.abb.com/GLOBAL/SCOT/scot221.nsf/VerityDisplay/55AA2F18687568CAC1256D67002A5749/$File/1MRB520376-Ben-PSM505.pdf). (Accessed April, 2005)
- [56] P.M. Van Oirsouw and F. Provoost, "Fault localization in an MV distribution network," Phase to Phase BV. [Online]. Available: <http://www.phasetophase.nl/pdf/faultlocalisationpaper.pdf>. (Accessed April, 2005)
- [57] SEL Inc. "Distance relay/fault locator," [Online]. Available: <http://www.selinc.com>. (Accessed April, 2005)
- [58] K. Zimmerman and David Costello, "Impedance-based fault location experience," SEL Inc. [Online]. Available at [www.selinc.com/techpprs.htm](http://www.selinc.com/techpprs.htm). (Accessed April, 2005)
- [59] E.O. Schweitzer, III, "A review of impedance-based fault locating experience," *Presented before the 14th Annual Iowa-Nebraska System Protection Seminar*. SEL Inc. [Online]. Available at [www.selinc.com/techpprs.htm](http://www.selinc.com/techpprs.htm). (Accessed April, 2005)
- [60] T. Takagi, Y. Yamakoshi, M. Yamaura, R. Kondow, and T. Matsushima, "Development of a new type fault location using the one-terminal voltage and current data," *IEEE Transactions on Power Apparatus and Systems*, vol. PAS-101, no. 8, pp. 2892-2898, August 1982.

- [61] GE, "F60 feeder management relay," [Online]. Available: <http://www.geindustrial.com>. (Accessed April, 2005)
- [62] G.C. Lampley, "Fault detection and location on electrical distribution system," in *Proceedings of 2002 IEEE Rural Electric Power Conference*, Colorado Springs, CO, May 2002, pp. B1\_1-B1\_5. (Accessed April, 2005)
- [63] G.J. Klir and Y. Bo, *Fuzzy Sets and Fuzzy Logic: Theory and Applications*. Upper Saddle River, NJ: Prentice Hall PTR, 1995.
- [64] R.R. Yager, "On mean type aggregation," *IEEE Transactions on Systems, Man, and Cybernetics - Part B: Cybernetics*, vol. 26, no. 2, pp. 209-221, April 1996.
- [65] R.R. Yager, "On ordered weighted averaging aggregation operators in multicriteria decisionmaking," *IEEE Transactions on Systems, Man, and Cybernetics*, vol. 18, no. 1, pp. 183-190, January 1988.
- [66] R.R. Yager and A. Rybalov, "Full reinforcement operators in aggregation techniques," *IEEE Transactions on Systems, Man, and Cybernetics-Part B: Cybernetics*, vol. 28, no. 6, pp. 757-769, December 1998.
- [67] W.H. Kersting, *Distribution System Modeling and Analysis*, Boca Raton, FL: CRC Press, 2002.
- [68] L.A. Zadeh, "Fuzzy sets", *Information Control*, vol. 8 (3), pp. 338-353, 1965.
- [69] K. Andoh, "A fault location approach for fuzzy fault section estimation on radial distribution feeders", M.S. thesis, Texas A&M University, College Station, 2000.
- [70] K. Manivannan, "Fuzzy logic based operated device identification in power distribution systems", M.S. thesis, Texas A&M University, College Station, 2002.
- [71] R.R. Yager, "Including importances in OWA aggregations using fuzzy system modeling," *IEEE Transactions on Fuzzy Systems*, vol. 6, no. 2, pp. 286-294, May 1998.
- [72] E. Chong and S.H. Zak, *An Introduction to Optimization*, New York: Wiley, 2001.
- [73] E. Beale, *Introduction to Optimization*, New York: Wiley, 1988.

- [74] D.E. Goldberg, *Genetic Algorithms in Search, Optimization, and Machine Learning*, New York: Addison-Wesley, 1989.
- [75] M. Gen, *Genetic Algorithms and Engineering Optimization*, New York: Wiley, 2000.
- [76] L. Davis, *Handbook of Genetic Algorithm*, New York: Van Nostrand Reinhold, 1991.
- [77] W.H. Kersting, "Radial distribution test feeders," in *Proceedings of IEEE Power Engineering Society Winter Meeting*, vol. 2, Columbus, OH, April 2001, pp. 908-912.
- [78] Hydro-Québec, TransÉnergie Technologies, *SimPowerSystems for Use with Simulink*, Natick, MA: The Mathworks Inc, February 2003.
- [79] Mathworks, *Simulink–Dynamic System Simulation for Matlab*, Natick, MA: The Mathworks Inc, November 2000.
- [80] T. Gönen, *Electric Power Distribution System Engineering*, New York: McGraw-Hill, 1986.
- [81] P.M. Anderson, *Analysis of Faulted Power Systems*, New York: Wiley-IEEE Press, 1995.
- [82] Mathworks, *Writing S-Functions*, Natick, MA: The Mathworks Inc, November 2000.
- [83] P.M. Anderson, *Power System Protection*, New York: McGraw-Hill, 1999.
- [84] Cooper Power Systems, *Overcurrent Protection for Distribution Systems–Seminar Notes and Reference Materials*, San Francisco, CA: Cooper Power Systems, May 1995.
- [85] H. Pohlheim, "GEATbx: Genetic and evolutionary algorithm toolbox for use with MATLAB documentation," [Online]. <http://www.geatbx.com/docu/algindex.html>. (Accessed May, 2004)
- [86] J.D. Shaffer, "Multiple objective optimization with vector evaluated genetic algorithms," in *Proceedings of the 1<sup>st</sup> International Conference on Genetic Algorithms*, Pittsburgh, PA, July 1985, pp. 93-100.
- [87] M.P. Fourman, "Compaction of symbolic layout using genetic algorithms," in *Proceedings of the 1<sup>st</sup> International Conference on Genetic Algorithms*, Pittsburgh,

- PA, July 1985, pp. 141-153.
- [88]H. Tamaki, H. Kita, and S. Kobayashi, "Multi-objective optimization by genetic algorithms: a review," in *Proceedings of IEEE International Conference on Evolutionary Computation*, Nagoya, Japan, May 1996, pp. 141-153.
- [89]C.M. Fonseca and P.J. Fleming, "Genetic algorithm for multiobjective optimization formulation, discussion and generalization", in *Proceedings of the 5<sup>th</sup> International Conference on Genetic Algorithms*, Urbana-Champaign, IL, June 1993, pp. 416-423.
- [90]J. Horn, N. Nafpliotis and D.E. Goldberg, "A niched Pareto genetic algorithm for multiobjective optimization," in *Proceedings of the 1<sup>st</sup> IEEE Conference on Evolutionary Computation*, Orlando, FL, June 1994, pp. 82-87.
- [91]H. Tamaki, M. Mori, M. Araki, Y. Mishima and H. Ogai, "Multi-criteria optimization by genetic algorithms: A case of scheduling in hot rolling process," in *Proceedings of the 3<sup>rd</sup> Conference of the Association of Asian-Pacific Operational Research Societies*, Fukuoka, Japan, July 1994, pp. 374-381.
- [92]J. Li, K. Butler-Purry, C. Benner, D. Russell, and R. Langari, "Selecting a fuzzy aggregation operator for the multi-criteria fault location problem", in *Proceedings of the Power Systems Conference and Exposition*, New York, NY, October 2004, pp. 1134-1140.
- [93]IEEE Distribution System Analysis Subcommittee, "Radial test feeders," [Online]. <http://ewh.ieee.org/soc/pes/dsacom/testfeeders.html>. (Accessed August, 2003)
- [94]Milsoft, *WindMil Users Guide (version 5.0)*, Abilene, TX: Milsoft Integrated Solutions, Inc., 2001.
- [95]J. Li, K. Butler-Purry, and C. Benner, "Modeling of TCC-based Protective Devices", in *Proceedings of 2003 IEEE/PES Transmission and Distribution Conference*, vol. 1, Dallas, TX, September 2003, pp. 150-156.

## APPENDIX A

### A *The IEEE 34 node test feeder*

The parameters and load flow results of the IEEE 34 node test feeder are listed in A.1-A.9. They are line segment data, overhead line configurations and their impedance and susceptance, transformer data, spot loads, distributed loads, shunt capacitors, regulator data, and load flow results. These data were downloaded from the web at <http://ewh.ieee.org/soc/pes/dsacom/testfeeders.html>.

#### A.1 Line Segment Data

Section	Node A	Node B	Length(ft.)	Config.
1	800	802	2580	300
2	802	806	1730	300
3	806	808	32230	300
4	808	810	5804	303
5	808	812	37500	300
6	812	814	29730	300
7	814	850	10	301
8	816	818	1710	302
9	816	824	10210	301
10	818	820	48150	302
11	820	822	13740	302
12	824	826	3030	303
13	824	828	840	301
14	828	830	20440	301
15	830	854	520	301
16	832	858	4900	301
17	832	888	0	XFM-1
18	834	860	2020	301
19	834	842	280	301
20	836	840	860	301
21	836	862	280	301
22	842	844	1350	301
23	844	846	3640	301
34	846	848	530	301
25	850	816	310	301
26	852	832	10	301
27	854	856	23330	303
28	854	852	36830	301
29	858	864	1620	303
30	858	834	5830	301
31	860	836	2680	301
32	862	838	4860	304
33	888	890	10560	300

## A.2 Overhead Line Configurations (Config.)

Config.	Phasing	Phase	Neutral	Spacing ID
		ACSR	ACSR	
300	B A C N	1/0	1/0	500
301	B A C N	#2 6/1	#2 6/1	500
302	A N	#4 6/1	#4 6/1	510
303	B N	#4 6/1	#4 6/1	510

## A.3 Transformer Data

	kVA	kV-high	kV-low	R - %	X - %
Substation:	2500	69 - D	24.9 -Gr. W	1	8
XFM -1	500	24.9 - Gr.W	4.16 - Gr. W	1.9	4.08

## A.4 Spot Loads

Node	Load	Ph-1	Ph-1	Ph-2	Ph-2	Ph-3	Ph-3
	Model	kW	kVAr	kW	kVAr	kW	kVAr
860	Y-PQ	20	16	20	16	20	16
840	Y-I	9	7	9	7	9	7
844	Y-Z	135	105	135	105	135	105
848	D-PQ	20	16	20	16	20	16
890	D-I	150	75	150	75	150	75
830	D-Z	10	5	10	5	25	10
Total		344	224	344	224	359	229

## A.5 Distributed Loads

Node	Node	Load	Ph-1	Ph-1	Ph-2	Ph-2	Ph-3	Ph-3
A	B	Model	kW	kVAr	kW	kVAr	kW	kVAr
802	806	Y-PQ	0	0	30	15	25	14
808	810	Y-I	0	0	16	8	0	0
818	820	Y-Z	34	17	0	0	0	0
820	822	Y-PQ	135	70	0	0	0	0
816	824	D-I	0	0	5	2	0	0
824	826	Y-I	0	0	40	20	0	0
824	828	Y-PQ	0	0	0	0	4	2
828	830	Y-PQ	7	3	0	0	0	0
854	856	Y-PQ	0	0	4	2	0	0
832	858	D-Z	7	3	2	1	6	3
858	864	Y-PQ	2	1	0	0	0	0
858	834	D-PQ	4	2	15	8	13	7
834	860	D-Z	16	8	20	10	110	55
860	836	D-PQ	30	15	10	6	42	22
836	840	D-I	18	9	22	11	0	0
862	838	Y-PQ	0	0	28	14	0	0
842	844	Y-PQ	9	5	0	0	0	0
844	846	Y-PQ	0	0	25	12	20	11
846	848	Y-PQ	0	0	23	11	0	0
Total			262	133	240	120	220	114

## A.6 Shunt Capacitors



Node	Ph-A	Ph-B	Ph-C
	kVAr	kVAr	kVAr
844	100	100	100
848	150	150	150
Total	250	250	250

## A.7 Regulator Data

Regulator ID:	1		
Line Segment:	814 - 850		
Location:	814		
Phases:	A - B -C		
Connection:	3-Ph,LG		
Monitoring Phase:	A-B-C		
Bandwidth:	2.0 volts		
PT Ratio:	120		
Primary CT Rating:	100		
Compensator Settings:	Ph-A	Ph-B	Ph-C
R - Setting:	2.7	2.7	2.7
X - Setting:	1.6	1.6	1.6
Voltage Level:	122	122	122
Regulator ID:	2		
Line Segment:	852 - 832		
Location:	852		
Phases:	A - B -C		
Connection:	3-Ph,LG		
Monitoring Phase:	A-B-C		
Bandwidth:	2.0 volts		
PT Ratio:	120		
Primary CT Rating:	100		
Compensator Settings:	Ph-A	Ph-B	Ph-C
R - Setting:	2.5	2.5	2.5
X - Setting:	1.5	1.5	1.5
Voltage Level:	124	124	124

## A.8 Impedance and Susceptance of Overhead Line Configurations

## Configuration 300:

	Z (R +jX) in ohms per mile		
1.3368+j1.3343	0.2101+j0.5779	0.2130+j0.5015	
0.2101+j0.5779	1.3238+j1.3569	0.2066+j0.4591	
0.2130+j0.5015	0.2066+j0.4591	1.3294+j1.3471	
	B in micro Siemens per mile		
5.3350	-1.5313	-0.9943	
-1.5313	5.0979	-0.6212	
-0.9943	-0.6212	4.8880	

## Configuration 301:

	Z (R +jX) in ohms per mile		
1.9300+j1.4115	0.2327+j0.6442	0.2359+j0.5691	
0.2327+j0.6442	1.9157+j1.4281	0.2288+j0.5238	
0.2359+j0.5691	0.2288+j0.5238	1.9219+j1.4209	
	B in micro Siemens per mile		
5.1207	-1.4364	-0.9402	
-1.4364	4.9055	-0.5951	
-0.9402	-0.5951	4.7154	

## Configuration 302:

	Z (R +jX) in ohms per mile		
2.7995+j1.4855	0.0000+j0.0000	0.0000+j0.0000	
0.0000+j0.0000	0.0000+j0.0000	0.0000+j0.0000	
0.0000+j0.0000	0.0000+j0.0000	0.0000+j0.0000	
	B in micro Siemens per mile		
4.2251	0.0000	0.0000	
0.0000	0.0000	0.0000	
0.0000	0.0000	0.0000	

## Configuration 303:

	Z (R +jX) in ohms per mile	
0.0000+j0.0000	0.0000+j0.0000	0.0000+j0.0000
0.0000+j0.0000	2.7995+j1.4855	0.0000+j0.0000
0.0000+j0.0000	0.0000+j0.0000	0.0000+j0.0000
	B in micro Siemens per mile	
0.0000	0.0000	0.0000
0.0000	4.2251	0.0000
0.0000	0.0000	0.0000

## Configuration 304:

	Z (R +jX) in ohms per mile	
0.0000+j0.0000	0.0000+j0.0000	0.0000+j0.0000
0.0000+j0.0000	1.9217+j1.4212	0.0000+j0.0000
0.0000+j0.0000	0.0000+j0.0000	0.0000+j0.0000
	B in micro Siemens per mile	
0.0000	0.0000	0.0000
0.0000	4.3637	0.0000
0.0000	0.0000	0.0000

### A.9 Power Flow Results

- R A D I A L F L O W S U M M A R Y - DATE: 6-24-2004 AT 16:34:11 HOURS ---  
 SUBSTATION: IEEE 34; FEEDER: IEEE 34

SYSTEM	PHASE		PHASE		PHASE		TOTAL	
INPUT	(A)		(B)		(C)			
kW :	759.136		666.663		617.072		2042.872	
kVAr :	171.727		90.137		28.394		290.258	
kVA :	778.318		672.729		617.725		2063.389	
PF :	.9754		.9910		.9989		.9901	
LOAD	(A-N)----(A-B)-		--(B-N)----(B-C)-		--(C-N)----(C-A)-		---WYE-----DELTA--	
kW :	359.9	246.4	339.3	243.3	221.8	359.0	921.0	848.8
TOT :	606.322		582.662		580.840		1769.824	
kVAr :	230.9	128.7	216.9	128.7	161.8	184.6	609.6	441.9
TOT :	359.531		345.609		346.407		1051.547	
kVA :	427.6	278.0	402.7	275.3	274.6	403.7	1104.5	957.0
TOT :	704.903		677.452		676.293		2058.647	
PF :	.8417	.8864	.8425	.8840	.8078	.8894	.8339	.8870
TOT :	.8601		.8601		.8589		.8597	
LOSSES	(A)		(B)		(C)			
kW :	114.836		80.389		77.824		273.049	
kVAr :	14.200		10.989		9.810		34.999	
kVA :	115.711		81.137		78.440		275.283	
CAPAC	(A-N)----(A-B)-		--(B-N)----(B-C)-		--(C-N)----(C-A)-		---WYE-----DELTA--	
R-kVA:	250.0	.0	250.0	.0	250.0	.0	750.0	.0
TOT :	250.000		250.000		250.000		750.000	
A-kVA:	265.7	.0	264.8	.0	265.9	.0	796.3	.0
TOT :	265.658		264.760		265.869		796.287	

--- V O L T A G E P R O F I L E ---- DATE: 6-24-2004 AT 16:34:18 HOURS ----  
 SUBSTATION: IEEE 34; FEEDER: IEEE 34

```

-----
NODE |  MAG      ANGLE |  MAG      ANGLE |  MAG      ANGLE |mi.to SR
-----
      |  _____ A-N _____ |  _____ B-N _____ |  _____ C-N _____ |
800 |  1.0500 at   .00 |  1.0500 at -120.00 |  1.0500 at  120.00 |   .000
802 |  1.0475 at  -.05 |  1.0484 at -120.07 |  1.0484 at  119.95 |   .489
806 |  1.0457 at  -.08 |  1.0474 at -120.11 |  1.0474 at  119.92 |   .816
808 |  1.0136 at  -.75 |  1.0296 at -120.95 |  1.0289 at  119.30 |  6.920
810 |                    |  1.0294 at -120.95 |                    |  8.020
812 |  .9763 at -1.57 |  1.0100 at -121.92 |  1.0069 at  118.59 |  14.023
814 |  .9467 at -2.26 |  .9945 at -122.70 |  .9893 at  118.01 |  19.653
RG10 |  1.0177 at -2.26 |  1.0255 at -122.70 |  1.0203 at  118.01 |  19.654
850 |  1.0176 at -2.26 |  1.0255 at -122.70 |  1.0203 at  118.01 |  19.655
816 |  1.0172 at -2.26 |  1.0253 at -122.71 |  1.0200 at  118.01 |  19.714
818 |  1.0163 at -2.27 |                    |                    |  20.038
820 |  .9926 at -2.32 |                    |                    |  29.157
822 |  .9895 at -2.33 |                    |                    |  31.760
824 |  1.0082 at -2.37 |  1.0158 at -122.94 |  1.0116 at  117.76 |  21.648
826 |                    |  1.0156 at -122.94 |                    |  22.222
828 |  1.0074 at -2.38 |  1.0151 at -122.95 |  1.0109 at  117.75 |  21.807
830 |  .9894 at -2.63 |  .9982 at -123.39 |  .9938 at  117.25 |  25.678
854 |  .9890 at -2.64 |  .9978 at -123.40 |  .9934 at  117.24 |  25.777
852 |  .9581 at -3.11 |  .9680 at -124.18 |  .9637 at  116.33 |  32.752
RG11 |  1.0359 at -3.11 |  1.0345 at -124.18 |  1.0360 at  116.33 |  32.752
832 |  1.0359 at -3.11 |  1.0345 at -124.18 |  1.0360 at  116.33 |  32.754
858 |  1.0336 at -3.17 |  1.0322 at -124.28 |  1.0338 at  116.22 |  33.682
834 |  1.0309 at -3.24 |  1.0295 at -124.39 |  1.0313 at  116.09 |  34.786
842 |  1.0309 at -3.25 |  1.0294 at -124.39 |  1.0313 at  116.09 |  34.839
844 |  1.0307 at -3.27 |  1.0291 at -124.42 |  1.0311 at  116.06 |  35.095
846 |  1.0309 at -3.32 |  1.0291 at -124.46 |  1.0313 at  116.01 |  35.784
848 |  1.0310 at -3.32 |  1.0291 at -124.47 |  1.0314 at  116.00 |  35.885
860 |  1.0305 at -3.24 |  1.0291 at -124.39 |  1.0310 at  116.09 |  35.169
836 |  1.0303 at -3.23 |  1.0287 at -124.39 |  1.0308 at  116.09 |  35.677
840 |  1.0303 at -3.23 |  1.0287 at -124.39 |  1.0308 at  116.09 |  35.839
862 |  1.0303 at -3.23 |  1.0287 at -124.39 |  1.0308 at  116.09 |  35.730
838 |                    |  1.0285 at -124.39 |                    |  36.650
864 |  1.0336 at -3.17 |                    |                    |  33.989
XF10 |  .9997 at -4.63 |  .9983 at -125.73 |  1.0000 at  114.82 |  32.754
888 |  .9996 at -4.64 |  .9983 at -125.73 |  1.0000 at  114.82 |  32.754
-----

```

890 | .9167 at -5.19 | .9235 at -126.78 | .9177 at 113.98 | 34.754  
 856 | | .9977 at -123.41 | | 30.195

#### A.10 Settings of Protective Devices

The settings of each protective device are listed in the following table. It lists the start node and end node of the line section where a protective device locates, protective device's types and ratings, and recloser's operation curves and reclosing times.

Start Node	End Node	Type	Rating	Curves	Settings
800	802	Recloser	50H	[Fast Slow Slow]	[1.0 1.0]
808	810	Fuse	2T		
816	822	Fuse	15T		
824	826	Fuse	5QA		
854	856	Fuse	1T		
832	888	Fuse	12T		
858	864	Fuse	1T		
834	842	Fuse	20K		
836	862	Fuse	3T		

## VITA

Jun Li was born in Xi'an, People's Republic of China. He received his Bachelor of Engineering degree and Master of Engineering degree in electrical engineering in 1993 and 1996 from Xi'an Jiaotong University in China. He received his Ph.D. degree in electrical engineering at Texas A&M University in December 2005. He was a research assistant in the Power System Automation Laboratory at Texas A&M University.

He is a student member of IEEE and the honor society of Phi Kappa Phi. He can be reached at [aggiejunli@yahoo.com](mailto:aggiejunli@yahoo.com). His permanent address is no. 334 You Yi East Road, Xi'an, 710054, People's Republic of China.